Isothermal amplification of nucleic acids and homogeneous assays for proteins

by

Michael S. Reid

A thesis submitted in partial fulfillment of the requirements for the degree of

Doctor of Philosophy

Department of Chemistry
University of Alberta

Abstract

The detection of specific proteins and deoxyribonucleic acid (DNA) can be used for disease diagnostics, pathogen identification, and the study of biological processes. Many proteins and nucleic acids occur at low concentrations, making their detection challenging. The detection of trace-level DNA is aided by several isothermal and exponential amplification technologies that have been developed; there are no equivalent strategies for protein detection. The major goal of my research is to expand the use of isothermal and exponential amplification of DNA to facilitate the detection of proteins. Four protein detection strategies and improvements to an existing DNA amplification technique have been designed and developed in this thesis.

I developed a homogeneous protein detection strategy with an amplified signal by incorporating isothermal amplification of DNA. I use binding induced DNA assembly (BINDA) to activate a linear amplification of DNA by enzymatic nicking and strand displacement. To increase the sensitivity of the assay, I added the exponential amplification reaction (EXPAR) to the design. The exponentially amplified signal generated by EXPAR increases the amount of DNA generated. However, the incorporation of EXPAR increased the background amplification. Therefore, I modified the design to occur at higher temperature for a reduced background amplification. The modified design had a binding phase at 37 °C to allow for antibody–target binding, followed by amplification occurring at 55 °C, which is the optimum temperature of EXPAR.

While EXPAR is a well-used technique, it is limited by the occurrence of background amplification. Exponential amplification in EXPAR is achieved by a

feedback mechanism that generates additional target sequences. Consequently, background amplification generates the same amplification products as target specific amplification products; therefore, background amplification is indistinguishable from target-specific amplification. I devised several methods to test the mechanisms that contribute to the triggering of background amplification. Blocking mechanisms that prevent nonspecific hybridization at the 3′-end of EXPAR templates as well as the entire length of the template showed reduction of background amplification. By designing these blocking strategies, I was able to reduce background amplification in EXPAR, resulting in an improved detection limit by 3 orders of magnitude.

Next, I used loop mediated isothermal amplification (LAMP) as a signal amplifier for protein detection. LAMP is a well-used DNA amplification technique capable of detecting single copies of DNA. This strategy used BINDA to trigger the ligation of DNA probes; the ligated product served as the target molecule for LAMP. Control reactions also were designed to evaluate critical reaction components. This design is isothermal, exponential, and procedurally simple, only requiring addition of the reagents in a single step.

The techniques described in this thesis may be applied to the detection of a wide range of proteins, provided suitable affinity ligands are available. Furthermore, because of the isothermal and homogeneous nature of these techniques, they may be adapted to point-of-care diagnostics. Due to the two binding probes used in these strategies, they are well suited for the study of protein–protein interactions.

Preface

This thesis is original work by Michael Reid. Components of Chapter 1 have been published as **Reid, M.S.**, Le, X.C., Zhang, H. Exponential isothermal amplification of nucleic acids and assays for proteins, cells, small molecules, and enzyme activities, Angewandte Chemie International Edition. DOI 10.1002/ange.201712217. I was responsible for manuscript composition. X.C. Le and H. Zhang were involved with manuscript composition and editing.

Chapter 3 has been submitted to Analytical Chemistry for publication as "**Reid, M.S.**, Paliwoda, R.E., Zhang, H, Le, X.C. Reduction of background generated from template-template hybridizations in the Exponential Amplification Reaction." I was responsible for the data collection and analysis, concept formation, as well as manuscript composition. Paliwoda, R.E. aided with manuscript editing. Zhang, H. was involved with concept formation and manuscript composition. Le, X.C. was the supervisory author and was involved with concept formation and manuscript composition.

Acknowledgements

First, I would like to thank my supervisor, Dr. Chris Le, for all of his support and guidance throughout my time in his lab. Chris has a unique ability to guide his students with leading questions and suggestions that train us to think critically and become better researchers. He has taught me so much on how to conduct research: from developing new projects and designing small lab experiments to effectively communicating the work that was done. Chris allows his students the freedom to explore and develop diverse projects of their own interest, while always being available to provide guidance and feedback. Chris is always encouraging and seeking out opportunities for his students to present their work. He has given me so much useful feedback on how to become a better communicator, whether it be writing or presenting my work. I feel very fortunate to have a supervisor who cares for and supports his students, not only in their academic endeavours but also in their professional and personal lives. Additionally, I would like to thank Hongquan Zhang for his many suggestions and help in problem solving.

I would also like to thank my supervisory committee, Dr. Charles Lucy and Dr. Michael Weinfeld, as well as my examining committee, Dr. Maria DeRosa, Dr. Hongquan Zhang, Dr. Leluo Guan, and Dr. Michael Serpe. You have provided me with much assistance and advice, which is greatly appreciated.

I also appreciate the support received from Katerina Carastathis, Anita Weiler, and Dianne Sergy. Your help with all the logistical aspects of graduate school relieves an enormous amount of stress; I can't imagine how the AET and Chemistry departments would run without you. Thank you to Dr. Anna Jordan for your kind assistance and encouragement.

Thank you to all the students and postdoctoral fellows in the AET division that I share the lab with. It has been wonderful to work in a place where help is so readily offered. Thank you to Feng Li, Zhixin Wang, and Ashley Newbigging for your training, valuable insight, and discussions on my projects. A special thanks to Yanwen Lin, Rebecca Paliwoda, and Aleksandra Popowich for going through each step of graduate school together. It will be exciting to see where our careers take us.

I would like to thank my whole family for their continued support in all aspects of my life. To my parents, you taught me so much growing up that has served me well as I have progressed in my career, and become a husband and father.

I would also like to thank my entire in-law family. Your support in moving and living in Alberta and in completing this degree has been much appreciated.

Thanks to Sadie and Lincoln, my two children; your laughs, screams, and overall wildness are a joy to experience. Spending time with you always provides me a nice break from the challenges of my work.

Finally, I would like to thank my wife, Cindy, for her tremendous amount of help and understanding throughout this process. I would not have been able to complete this work without your loving patience and support.

Table of Contents

List of Tables

List of Figures

List of Abbreviations

3-PLA	Triple-binder proximity ligation assay
A	Adenine
APS	Ammonium persulfate
AuNP	Gold nanoparticle
BINDA	Binding-induced DNA assembly
BI–LAMP	Binding-induced loop-mediated isothermal amplification
BIP	Backward inner primer
BISDA	Binding-induced strand displacement amplification
BISDA–EXPAR	Binding induced strand displacement amplification–exponential amplification reaction
C	Cytosine
cDNA	Complementary DNA
DMSO	Dimethyl sulfoxide
DNA	Deoxyribonucleic acid
dNTPs	Deoxynucleotide triphosphates
ds-cDNA	Double stranded complementary DNA
dsDNA	Double stranded DNA

ELISA	Enzyme linked immunosorbent assay
E-RCA	Exponential rolling circle amplification
E-SDA	Exponential strand displacement amplification
EXPAR	Exponential amplification reaction
FIP	Forward inner primer
G	Guanine
hCG	Human chorionic gonadotropin
HDA	Helicase dependent amplification
HRP	Horseradish peroxidase
HRCA	Hyperbranched rolling circle amplification
iPCR	Immuno polymerase chain reaction
Klenow LF	Klenow large fragment
LAMP	Loop-mediated isothermal amplification
LOD	Limit of detection
MB	Magnetic bead
miRNA	microRNA
NASBA	Nucleic acid sequence-based amplification
NEase	Nicking endonuclease

PAGE	Polyacrylamide gel electrophoresis
PBS	Phosphate buffered saline
PCR	Polymerase chain reaction
PDGF-BB	Prostate specific growth factor-BB
PG-RCA	Primer generation rolling circle amplification
PLA	Proximity ligation assay
PNA	Peptide nucleic acid
POC	Point-of-care
PSA	Prostate specific antigen
RNA	Ribonucleic acid
RNase	Ribonuclease
RCA	Rolling circle amplification
ROX	ROX reference dye
RPA	Recombinase polymerase amplification
RT–PCR	Real time polymerase chain reaction
SG	SYBR Green I
SNP	Single nucleotide polymorphism
SSB	Single stranded binding protein

ss-cDNA	Single stranded complementary DNA
ssDNA	Single stranded DNA
ssRNA	Single stranded RNA
T	Thymine
TBE	Tris-borate-EDTA
TEMED	1, 2-bis(dimethylamino)ethane
T_m	Melting temperature
TMA	Transcription-mediated amplification
XT	EXPAR template

Chapter 1: Introduction

1.1 Proteins and Nucleic Acids

Nucleic acids and proteins are fundamental building blocks of all organisms. Their many biological functions include the storage, translation, and regulation of genetic information, catalyzing reactions, immune response, transport of small molecules, cell signalling, and mechanical support.[1,2] While this list is not comprehensive, it demonstrates the vast utility of nucleic acids and proteins in biological systems. The widespread roles of nucleic acids and proteins in biological systems and our ability to analyse them are of great importance. The detection of these biomolecules in complex sample matrices, such as cells or serum, requires high analytical specificity and sensitivity.

Improving detection methods for proteins and nucleic acids facilitates better understanding of their structure and function, as well as factors that may alter function and structure. Detection parameters, such as specificity and sensitivity, are critical to improve to support new biological research barriers. For instance, in recent years there has been increased interest in single cell analysis.[3–7] However, single cell analysis requires more sensitive detection techniques compared to bulk cell analysis.

Beyond the study of normal biological functions, detection of both nucleic acids and proteins can be used for disease diagnosis. Changes from normal concentration or altered structure of biomolecules can be used to diagnose, prognose, or monitor a disease; these molecules often are referred to as biomarkers.[8–10] Improvements of detection parameters, such as analysis time, procedural complexity, and cost, enable increased output in clinical laboratories and are more suitable to resource limited settings, such as point-of-care (POC).[11–17] An excellent example of POC diagnostics is the human pregnancy test. It

offers a low cost, fast, and simple method that someone with no training can perform. This is possible partially due to the high concentration of the human chorionic gonadotropin (hCG) hormone. However, many biomarkers occur at low concentrations that are more difficult to detect in complicated matrices than hCG.[10,18–20] Improved detection methods will facilitate POC detection of low concentration biomarkers as well as the identification of new biomarkers.

Many detection techniques have been developed to address a wide range of applications in molecular diagnostics and imaging.[21,22] This Chapter will provide the background on emerging trends in new assay development for nucleic acids and proteins. Since many applications require ultrasensitive assays, the focus will be on exponential signal amplification techniques with isothermal and homogenous formats.

1.1.1 Functional DNA

Just as organisms use nucleic acids and proteins as building blocks, this same class of molecules can be used as tools to develop novel assays. Synthetically designed deoxyribonucleic acid (DNA) can be used in assays for target recognition, signal transduction, signal amplification, or structural support.[23] Likewise, proteins commonly are used for target recognition and signal amplification in biomarker assays.

DNA is a biopolymer made of four different nucleotide subunits that are determined by the nitrogenous bases they contain: adenine (A), thymine (T), cytosine (C), and guanine (G). DNA nanotechnology is the use of non-biological DNA for developing useful technology. In particular, precise Watson-Crick base-pairing between A-T and C-G nucleotides enables prediction of how synthetically designed DNA strands will interact with one another.[24] This has led to the creation of intricate two- and three-dimensional

DNA structures, such as lattice structures, nanotubes, and other shapes, which can be employed for useful detection strategies.[25] Beyond the formation of static structures, DNA can be designed to generate dynamic systems, such as switchable DNA structures, DNA motors, or DNA logic gates.[23] This precise control of DNA has been used widely for signal generation in biomolecule detection. Nucleic acid sequences that mimic the action of protein antibodies also have been developed.[26–28] These nucleic acids are called aptamers and can bind noncovalently to specific target molecules in a similar manner to antibodies.[29] Compared to antibodies, aptamers have better stability, are cheaper to produce, and allow more controlled functionalization.[30] The ability to predict interactions between DNA strands precisely, combined with DNAs high chemical stability and low cost to manufacture, make it an ideal molecule to build new assay designs with.

1.2 Nucleic Acid Amplification

1.2.1 Polymerase chain reaction

Chemically amplifying nucleic acids in test tubes has improved detection of nucleic acids remarkably. This is evident in the vast utilization of polymerase chain reaction (PCR) in research and clinical laboratories over the past 30 years.[31–34] PCR amplifies nucleic acid targets exponentially, achieving amplification of over 10^7-fold within 1 or 2 h. Each cycle of PCR involves: denaturation of double-stranded DNA (dsDNA) to yield two single-stranded DNA (ssDNA) templates; annealing of a primer to each ssDNA template; and extension/elongation catalyzed by a DNA polymerase. Thus, PCR reaction temperatures are changed repeatedly from a high temperature (e.g. 94–98 °C) for denaturation to a lower temperature (e.g. 50–65 °C) for annealing and enzymatic extension/elongation (e.g. 72 °C). Such thermal cycling requires appropriate equipment to achieve fast and accurate

control of temperature, which may be challenging at point-of-care and resource-limited settings. Real-time PCR (RT-PCR) is used for quantification of DNA, where fluorescent probes are used to monitor amplification after each temperature cycle. High concentrations of DNA generate a detectable fluorescence signal faster than lower concentrations, therefore, a threshold fluorescence signal is set, and the number of temperature cycles required to exceed the threshold value is used for quantification.

1.2.2 Isothermal exponential amplification of nucleic acids

Several techniques that generate exponentially amplified DNA and do not require thermal cycling have been developed.[13,22,35] Some commonly used isothermal exponential amplification techniques include nucleic acid sequence based amplification (NASBA),[36–40] helicase dependent amplification (HDA),[41–44] recombinase polymerase amplification (RPA),[45–51] exponential strand displacement amplification (E-SDA),[52–54] exponential rolling circle amplification (E-RCA),[55–59] exponential amplification reaction (EXPAR),[60] and loop-mediated isothermal amplification (LAMP).[61–69] All of these exponential DNA amplification techniques require the generation of a ssDNA template from a dsDNA amplicon to enable template-guided DNA elongation in each amplification cycle. Unlike PCR, that uses a high temperature to denature dsDNA into ssDNA, isothermal amplification techniques use a separate enzyme or the strand displacement activity of particular polymerases to generate ssDNA from dsDNA. For example, the techniques of HDA, RPA, and NASBA use helicase, recombinase, and RNase H, respectively, to unravel dsDNA or a DNA-RNA hybrid. Instead of using these additional enzymes, the techniques of E-SDA, E-RCA, LAMP, and EXPAR make use of the strand displacement activity of the polymerase to displace a DNA strand from dsDNA. The techniques in the

latter group are promising for point-of-care testing and on-site analysis because they require fewer enzymes and/or proteins in the amplification process.

1.2.3 Nucleic acid sequence-based amplification

Nucleic acid sequence-based amplification was developed first in 1991 for the detection of RNA, but it is capable of detecting RNA and DNA with comparable sensitivity to RT-PCR.[36,70] Figure 1.1 shows a schematic illustration of NASBA from either a ssRNA target or a dsDNA target. The reaction is triggered by the binding of an RNA target to a DNA forward primer. Then, the primer is extended along the target by reverse transcriptase, which generates a complementary DNA (cDNA) strand. After extension, the RNA target strand is digested by RNAase H, which leaves a single stranded cDNA (ss-cDNA). Double stranded cDNA (ds-cDNA) is generated from the binding and extension of a reverse primer. The ds-cDNA contains a promoter sequence for T7 RNA polymerase, which generates many copies of ssRNA that are the reverse complement sequence to the original RNA target. This antisense strand continues amplification by binding to the reverse primer and undergoing extension, digestion, and transcription reactions to produce many copies of the original RNA sequence. These continued cycles of generating target and antisense RNA can achieve 10^9-fold amplification in 1–2 h at 41 °C. A benefit of NASBA is that the amplified product is ssRNA, which can be adapted easily to various detection schemes without the need for denaturation. NASBA has been used for pathogen detection in food, environmental, and clinical samples.[71] Self-sustained sequence replication and transcription-mediated amplification (TMA) are two other amplification techniques with the same principles as NASBA.[37] TMA takes advantage of a reverse transcriptase that has inherent RNAse H activity so that only two enzymes are required.[72]

1.2.4 Helicase dependent amplification

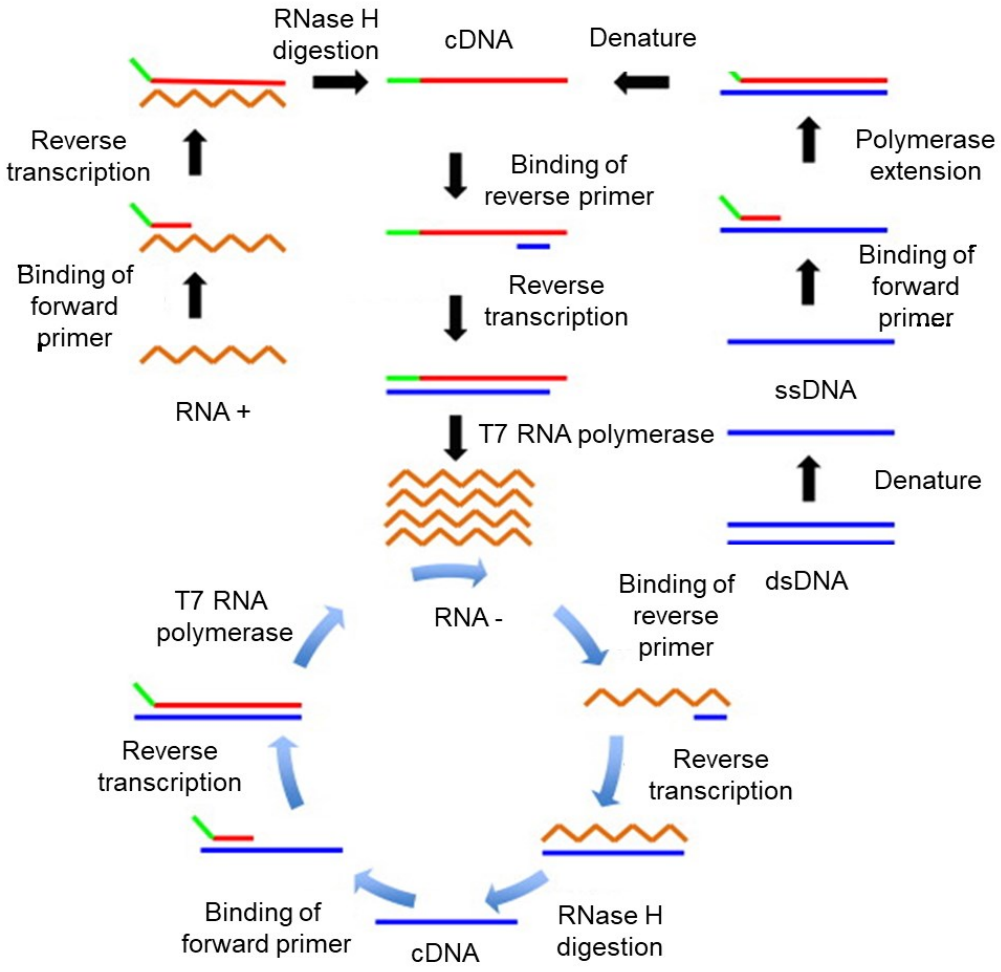

Figure 1.1 Mechanisms of nucleic acid sequence-based amplification (NASBA) from an RNA target (left) or a DNA target (right). Reprinted and modified with permission.[73] Copyright 2014 Elsevier.

Helicase dependent amplification was developed in 2004 by Vincent *et al.* and is capable of 10^7-fold amplification at 37 °C or 65 °C in 0.5–2 h.[41] HDA mimics natural DNA replication by using helicase to open dsDNA and allow primer binding. In principle, HDA

operates in a similar manner to PCR, but instead of using temperature to separate dsDNA, HDA uses helicase to separate dsDNA target (Figure 1.2). After separation, single stranded binding protein (SSB) binds to and stabilizes the ssDNA strands, preventing them from reforming dsDNA; this allows primers to bind to the ssDNA. Then, the primers are extended by polymerase, generating two new dsDNA substrates that can be amplified further. The main benefit of HDA compared to other exponential isothermal amplification techniques is the ability to amplify DNA targets that are many kilobases long. The development of thermostable proteins and the fusing of the helicase to the polymerase have improved the specificity and reaction speed of HDA in applications such as the detection of pathogens and single nucleotide polymorphisms (SNP).[42,43,74,75]

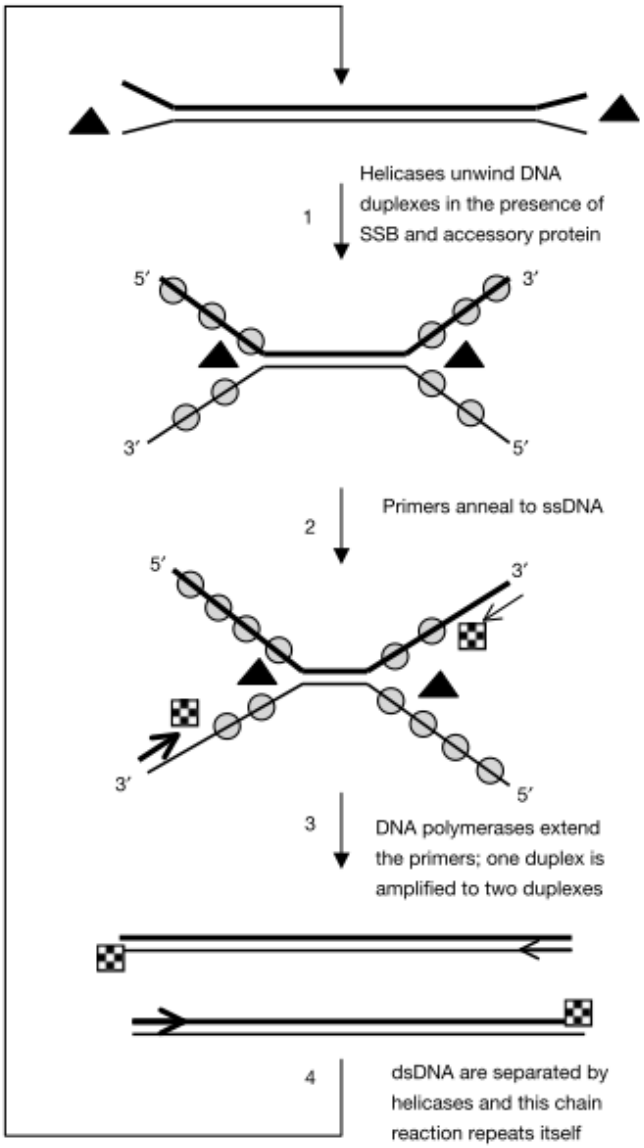

Figure 1.2 Mechanisms of helicase dependent amplification (HDA). Helicase and accessory proteins unwind DNA to allow primer binding. After extension of primers two new dsDNA templates are generated and undergo subsequence rounds of amplification. Reprinted and modified with permission.[41] Copyright 2004 John Wiley and Sons.

1.2.5 Recombinase polymerase amplification

Recombinase polymerase amplification was developed in 2006 by Piepenburg *et al.* and is capable of 10^7-fold amplification at 37 °C in 40 min.[45] Similarly to HDA, RPA uses a specific protein (recombinase) to enable the binding of primers to the dsDNA target. A recombinase-primer complex scans the dsDNA target for the complementary sequence of the primer and facilitates strand exchange, which results in a primer-target duplex (Figure 1.3). Single stranded DNA binding proteins are used to stabilize the ssDNA region generated by the strand exchange. Then, the primers are extended by polymerase, which generates a copy of the original dsDNA target and a displaced ssDNA copy of the target. The dsDNA copy undergoes another round of amplification, and the displaced ssDNA copy is bound by the next primer and continues to amplify. RPA has been used to detect single copies of a DNA target from pathogens and viruses.[76,77]

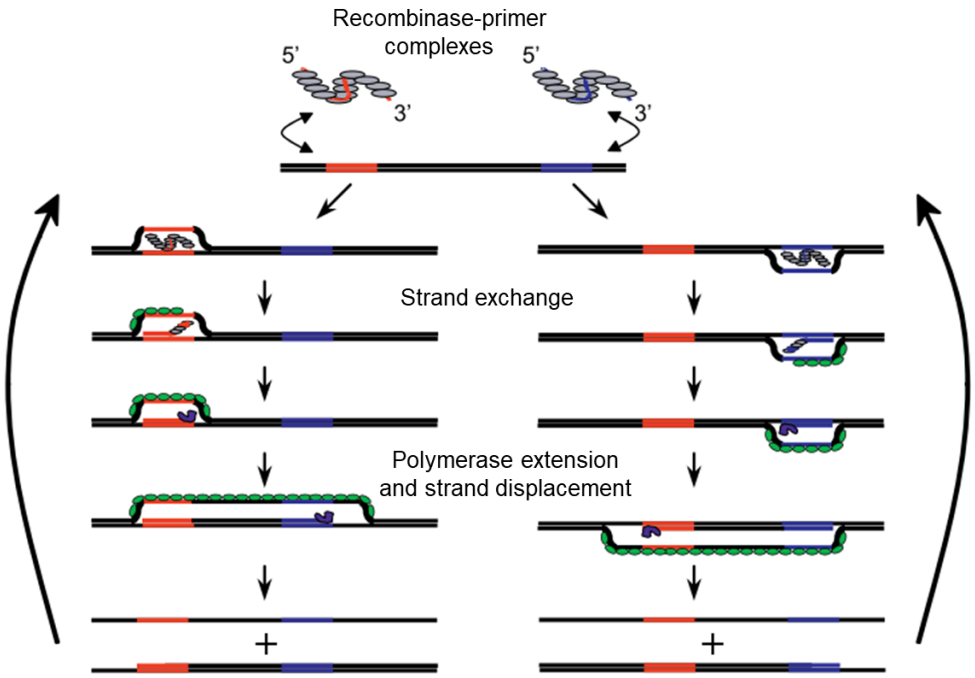

Figure 1.3 Mechanism of recombinase polymerase amplification (RPA). Recombinase proteins that have bound primers scan dsDNA until the complementary sequence of the primer is found. Recombinase then facilitates strand exchange between the dsDNA and primer. Polymerase then extends bound primers which generates a new dsDNA template and a displaced ssDNA that undergo further amplification. Reprinted and modified with permission (open access).[45]

1.2.6 Exponential strand displacement amplification

Exponential strand displacement amplification was developed first in 1992 by Walker *et al.*[52,53] E-SDA is capable of 10^7-fold amplification in 2 h at 37 °C. E-SDA uses two enzymes, a polymerase and a nicking endonuclease (NEase), which are combined with

two primers. Each primer contains both a target recognition sequence and a recognition sequence for the NEase used. Figure 1.4 shows the reaction scheme for E-SDA. Initially, heat denaturation is required to separate the dsDNA target to allow binding by the two primers, S1 and S2. Following binding by primers, DNA polymerase extends the 3′-ends of both the primer and target strands. This extension generates the NEase recognition site and NEase cleaves the phosphate backbone of one DNA strand on each primer–target duplex. This generates a nicked site, which is extended by a DNA polymerase that lacks a 5′→3′ exonuclease. Extension of the nicked site by polymerase results in the displacement of the downstream oligo. The reaction is designed so that the displaced oligo from the S1-T1 duplex binds to S2 for further amplification. Likewise, the displaced oligo from S2-T2 is amplified further by S1. This feedback loop between displaced strands and primers results in exponential amplification. E-SDA has been used for the detection of *Chlamydia trachomatis* and *Neisseria gonorrhoeae* in a clinical setting.[78–82]

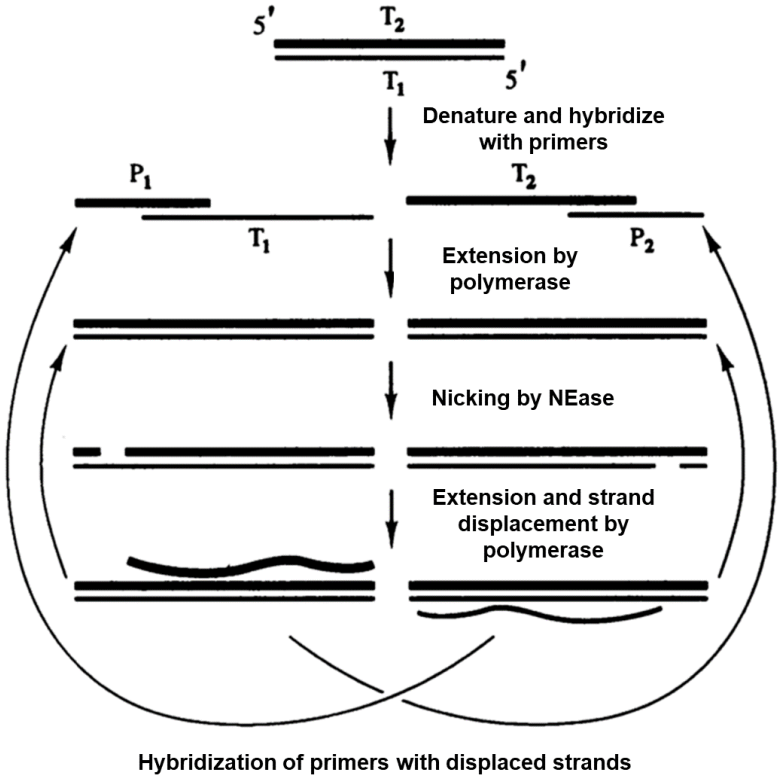

Figure 1.4 Illustration of exponential strand displacement amplification (E-SDA). Primers are extended by polymerase to generate NEase recognitions sites. After cleavage, polymerase extends from the nicked site and displaces the downstream DNA. The displaced DNA is then bound by either S1 or S2 primers to start the next round of amplification. The initial DNA-primer duplex continues nicking and strand displacement amplification. Reprinted and modified with permission.[53] Copyright 1992 Oxford University Press.

1.2.7 Exponential rolling circle amplification

Rolling circle amplification (RCA) was developed in 1995 and is capable of 10^9-fold amplification in 90 min.[55,83–85] RCA uses a single polymerase with strand displacement

activity to amplify a primer around a circular DNA template. As the polymerase elongates the primer around the circular template, it displaces the initial primer region and the previously synthesized strand. This linear amplification results in a long ssDNA that contains hundreds of repeated sequences complementary to the circular DNA template.

Several variations of RCA have been developed to increase the amplification speed and yield by introducing exponential amplification components. Each type of E-RCA incorporates additional amplification after generation of the linearly amplified ssDNA. Figure 1.5 shows three exponential variants of RCA. Figure 1.5A illustrates hyberbranched RCA (HRCA) that uses a series of additional primers for exponential amplification. The extra primers bind to the ssDNA RCA product and are extended by polymerase. Extension of HRCA primers displaces the downstream primers, allowing binding by additional primers. This cycle of primer binding, extension, and strand displacement continues to generate the hyperbranched product. Figure 1.5B shows the mechanism of circle-to-circle amplification, where a restriction enzyme is used to cleave the long RCA product to generate many short ssDNA strands. Then, the short ssDNA strands are ligated to generate a second circular template that undergoes RCA with a second primer. Figure 1.5C shows the mechanisms of primer generation RCA (PG-RCA), which is a NEase assisted RCA reaction. A second circular template that contains a NEase recognition sequence binds to the long RCA product. A NEase cleaves the original RCA product that is bound to the second circular template; each cleavage site then acts as a primer, which then is extended along the second template via RCA. The long ssDNA product is simple to adapt to different detection schemes and has been used to detect nucleic acids, proteins, cells, and small molecules.[58,59]

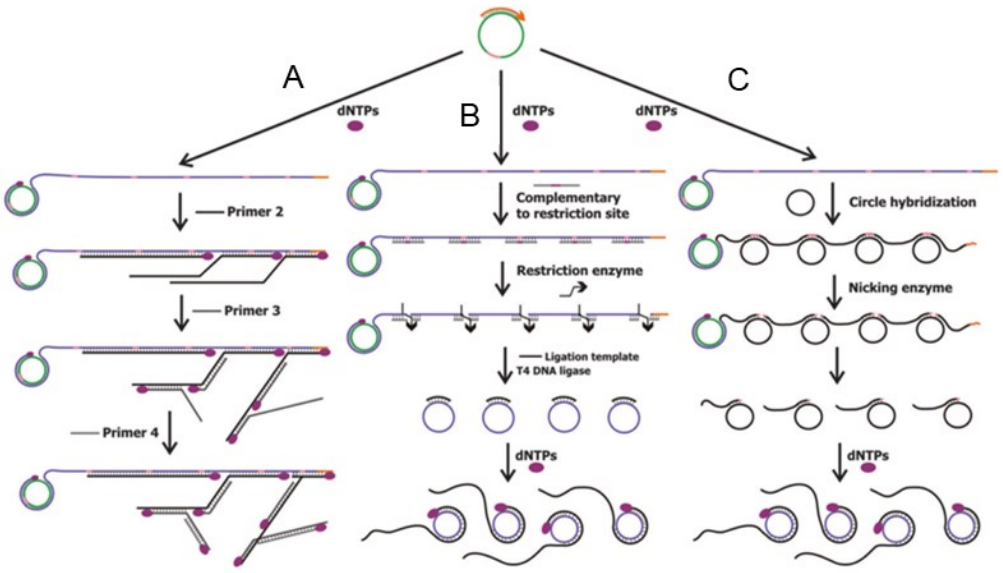

Figure 1.5 Three exponential variants of rolling circle amplification (E-RCA). (A) Hyper-branched RCA. (B) Circle-to-circle amplification. (C) primer generation RCA. Reprinted and modified with permission.[58] Copyright 2014 Royal Society of Chemistry.

1.2.8 Exponential amplification reaction

The exponential amplification reaction was developed in 2003 by Galas and co-workers and is capable of 10^8-fold amplification in less than 30 min at 55 °C.[60] EXPAR uses a DNA template and two enzymatic reactions to achieve exponential amplification of a target sequence (Figure 1.6). The EXPAR template is designed to contain two repeat regions that are complementary to a trigger sequence and separated by a short NEase recognition sequence. This type of template commonly is referred to as a X′-X′ template, where X′ is the complement of the trigger sequence and [-] is the NEase recognition sequence. The trigger sequence is a short DNA or RNA strand that can either be the target itself, such as a microRNA (miRNA), or must be generated from larger targets, such as

from a genomic DNA. Once hybridized to the template, the trigger DNA is extended along the template by a DNA polymerase with strand displacement activity. After extension, the dsDNA contains the NEase recognition sequence and NEase can cleave the extended trigger DNA strand, generating a nicked site. DNA polymerase can extend the 3′-end of the nicked site, which simultaneously displaces the newly synthesized strand. Since the template contains two X′ regions, the displaced DNA strand has the same sequence as the trigger DNA. The displaced strand then hybridizes with another template molecule, initiating new amplification, while amplification of the target DNA from the initial trigger-template complex continues. Thus, each reaction cycle produces two copies of the trigger DNA from a single target molecule, achieving exponential amplification.

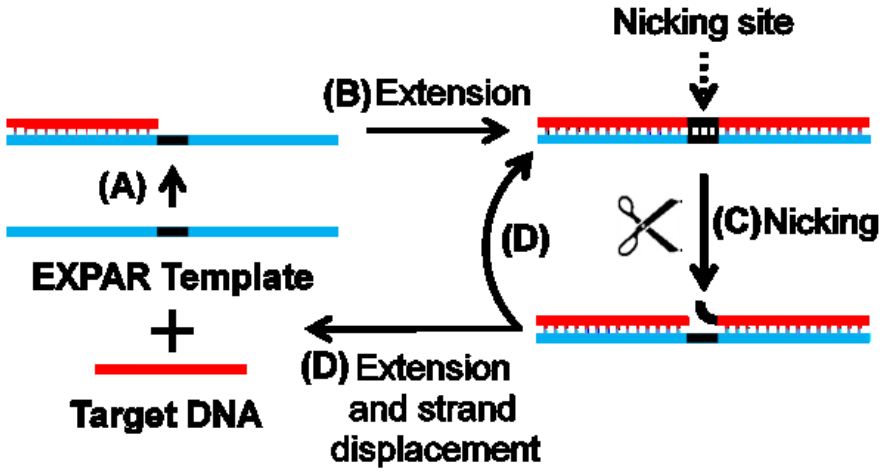

Figure 1.6 Schematic illustration of the exponential amplification reaction (EXPAR). (A) Annealing between a short DNA target and a EXPAR template. (B) Polymerase extends the target DNA along the EXPAR template to generate a NEase recognition site. (C) NEase generates a nicked site on the original target DNA strand. (D)

Polymerase extends from the nicked site, which displaces the previously synthesized strand and regenerates the NEase recognition site.

1.2.9 Loop mediated isothermal amplification

Loop-mediated isothermal amplification was developed in 2000 by Notomi *et al.* and is capable of 10^9-fold amplification in 1 h at 65 °C.[63] LAMP uses 4 primers to amplify the target DNA: a forward inner primer (FIP); a backward inner primer (BIP); and two outer primers (F3 and B3). Figure 1.7 schematically illustrates the LAMP reaction. The reaction occurs in two phases: the dumbbell structure generating step; and the cycling amplification step. After the target dsDNA is heat denatured, FIP and F3 both bind to the target and are extended by DNA polymerase. Since F3 binds the target upstream of FIP, the extension of F3 displaces the extended FIP sequence. FIP is designed so that after strand displacement, the 5′-end forms a DNA hairpin loop. The displaced sequence then is bound by BIP and B3, which are both extended by polymerase. Since B3 binds upstream of BIP, the extension of B3 displaces the extended BIP sequence. This second displaced sequence forms DNA hairpins on both the 5′ and 3′-ends, forming a dumbbell shape. This structure is the sequence required for the cycling amplification stage. Since the 3′-end is in a hairpin structure, it is extended by polymerase, which changes the dumbbell shape into a single hairpin loop with a long double stranded stem region. FIP then binds the hairpin loop and is extended along the large stem region of the hairpin loop. The ssDNA that was displaced by the extension of FIP forms a hairpin, which is then extended by polymerase and displaces the previously extended FIP. This process continues with FIP and BIP continuously priming the hairpin loops and generating many long concatemers.

LAMP has been used widely for the detection of nucleic acids, single nucleotide polymorphisms (SNPs), and pathogens.[61,86,87]

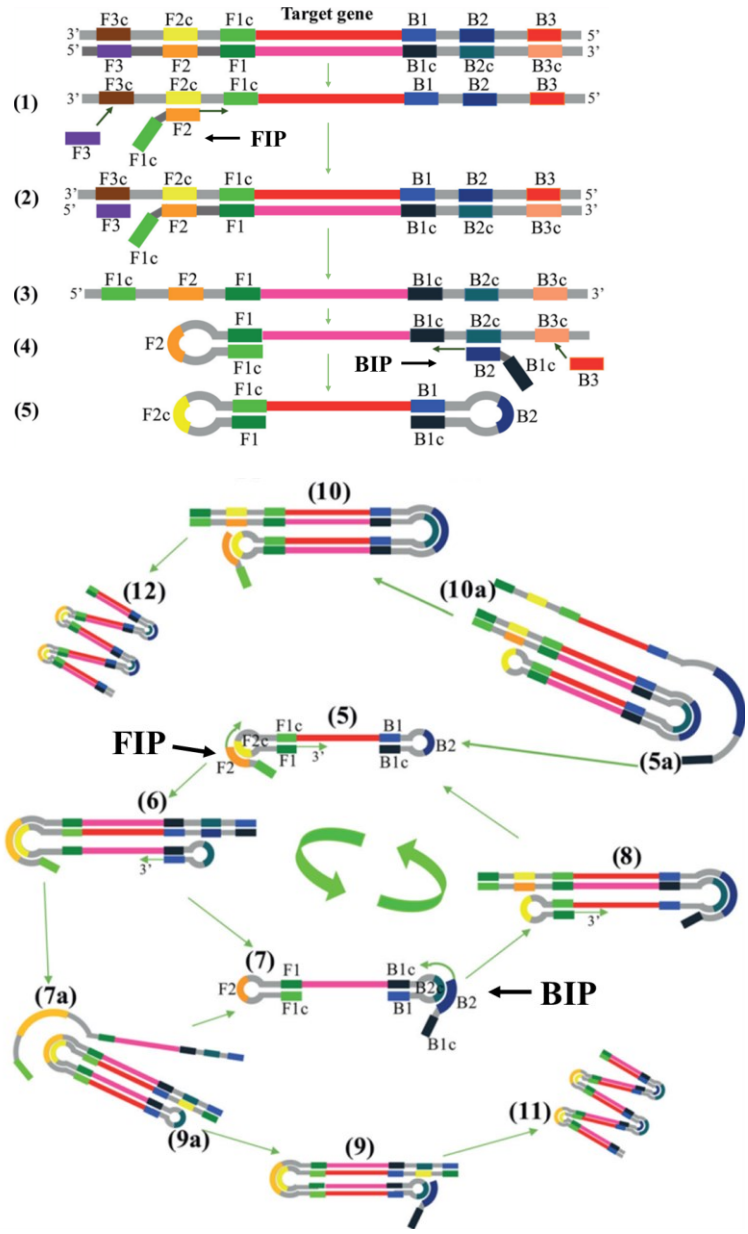

Figure 1.7 Schematic illustration of the mechanisms of loop mediated isothermal amplification (LAMP). Steps 1–5 show the generation of the dumbbell structure using two forward (F3 and FIP) and two backward (B3 and BIP) primers. Steps 5–12 show the cycling phase that generates long concatemers for exponential amplification, using FIP and BIP primers. Reprinted with modifications with permission.[88] Copyright 2017 Springer.

1.3 Protein Detection

1.3.1 Conventional immunoassays

Proteins can be measured directly using the absorption of ultraviolet light at both 280 nm and 205 nm. Amino acids containing aromatic rings absorb light at 280 nm and the C–N peptide bond absorbs light at 205 nm. Several colorimetric detection methods also can be used to detect proteins, such as the Bradford assay that uses Coomassie Blue dye, and the Lowry or bicinchoninic acid assays that use the biuret reaction to produce color. These methods are well established, but they only detect high concentrations of total protein.

To achieve more sensitive detection of specific proteins, affinity-based methods that use specific recognition elements, such as aptamers or antibodies, have been coupled with signal amplification mechanisms. The enzyme linked immunosorbent assay (ELISA) is a widely used protein detection method, both in clinical and research settings.[89,90] There are several different types of ELISA, but the most common ELISA technique uses a sandwich format in a 96 well plate.[91–93] In a sandwich ELISA, the first step is to add the sample to a well, which allows binding of the target protein by the capture antibody that is anchored to the well surface. After target capture, a washing buffer is used to remove the sample matrix from the well. This is followed by the addition of a biotinylated primary antibody that binds to the surface bound targets. This generates a sandwich complex consisting of the target protein bound between the capture antibody and the primary antibody. After incubation with the primary antibody, another washing step is performed to remove unbound primary antibodies. Following the second washing step, a streptavidin–enzyme conjugate is added; it binds to the biotinylated primary antibody. A final washing step removes unbound streptavidin–enzyme conjugates. The streptavidin–enzyme conjugate

performs two functions. First, it recognizes the primary antibody, which represents the amount of target protein captured. Second, streptavidin is conjugated to a signal producing enzyme, typically horseradish peroxidase (HRP). The final step is addition of a substrate that HRP uses to produce an amplified signal for quantification of the target.

ELISA has several advantages compared to nonspecific protein detection methods, resulting in its widespread used. The use of an enzyme to amplify the detection signal improves detection limits compared to non-amplified methods. Since the assay usually is performed in a 96-well plate, automated systems can be used, which facilitate high throughput. The multiple washing steps reduce both matrix effects and the incidence of background signal due to nonspecific antibody binding or nonspecific adsorption of reaction components on the plastic wells.

While ELISA is a well-established technique, there are several characteristics that can be improved upon. Even though HRP generates an amplified signal, the amplification is much less compared to the amplification achieved in the nucleic acid amplification techniques described in Section 1.2. Because of this, the limits of detection (LOD) achieved in ELISA assays are much higher than LODs achieved in amplified nucleic acid detection. Furthermore, with multiple washing steps, ELISA is time consuming and labour intensive. Several new strategies achieve homogenous protein detection and do not require any washing or separation steps, which decreases analysis time and simplifies procedures.

The detection of low abundance proteins represents a significant challenge since proteins cannot be amplified simply in the same manner as nucleic acids. This challenge has led to the development of protein assays that use nucleic acid amplification to generate

an amplified signal. These assays take advantage of well established nucleic acid amplification technologies to achieve highly sensitive detection of proteins.

The first technology adapting this strategy was immuno-PCR (iPCR).[94,95] iPCR operates in a similar format as ELISA but uses an antibody-DNA conjugate instead of a streptavidin–enzyme conjugate. Sandwich format iPCR uses a capture and primary antibody to bind the protein of interest, followed by the binding of the detection antibody that is labelled with a surrogate DNA. After all washing steps are completed, RT-PCR is used to detect the antibody-linked surrogate DNA. iPCR is capable of ultralow protein detection, but it requires extensive washing steps and precise temperature control for thermocycling.

Several methods similar to iPCR have been developed that incorporate isothermal nucleic acid amplification in place of RT-PCR. These techniques are advantageous because they do not require precise temperature control for thermocycling. Isothermally amplified immuno techniques include immuno-RCA, immuno-NASBA, and immuno-LAMP.[96–100] While these techniques negate the use of a thermocycler, they still require extensive washing steps to remove unbound antibody-DNA conjugates.

1.3.2 Homogenous immunoassays

Homogeneous protein assays are desirable because the lack of washing steps results in faster and simpler procedures. Typically, homogenous techniques do not require the immobilization of reaction components on a surface, which can lead to faster binding processes in a solution compared to a solid phase. Reduced handling steps also minimize the potential for user contamination, which can lead to false positives. Because

homogeneous assays only require the delivery of assay reagents, they may be used *in situ*, *in vitro,* or *in vivo*.

In heterogenous assays, amplified detection of specific proteins requires two components: affinity binding of the target and an amplification component. ELISA uses an enzyme and a substrate to achieve an amplified signal, while iPCR exponentially amplifies DNA to achieve an amplified signal. These techniques use washing steps to remove unbound affinity ligands and prevent signal generation in the absence of the target. Homogeneous assays require an alternative strategy to prevent signal generation in the absence the target. This is achieved by designing a mechanism that triggers amplification only when the target has been bound by the affinity ligand(s). Therefore, homogenous protein assays require three components: affinity binding of the target, an amplification activation mechanism, and an amplification component.

1.3.3 Binding-induced DNA assembly

To achieve homogenous detection of protein targets, our group developed the binding-induced DNA assembly (BINDA).[101,102] BINDA uses binding of a target molecule by affinity ligands to trigger the assembly of DNA motifs that can be used for detection. Two probes (Figure 1.8), each consisting of an affinity ligand-DNA conjugate, are used for target binding. Affinity ligands commonly used are antibodies or aptamers. The conjugated DNA contains a spacer region, typically a poly-T sequence, and a short complementary region between the two probes. The complementary region is short (5–7 bases) so that in the absence of the target, the probes remain separate. However, binding

of the target by both probes brings the complementary regions into close proximity, enabling them to assemble (Figure 1.9).

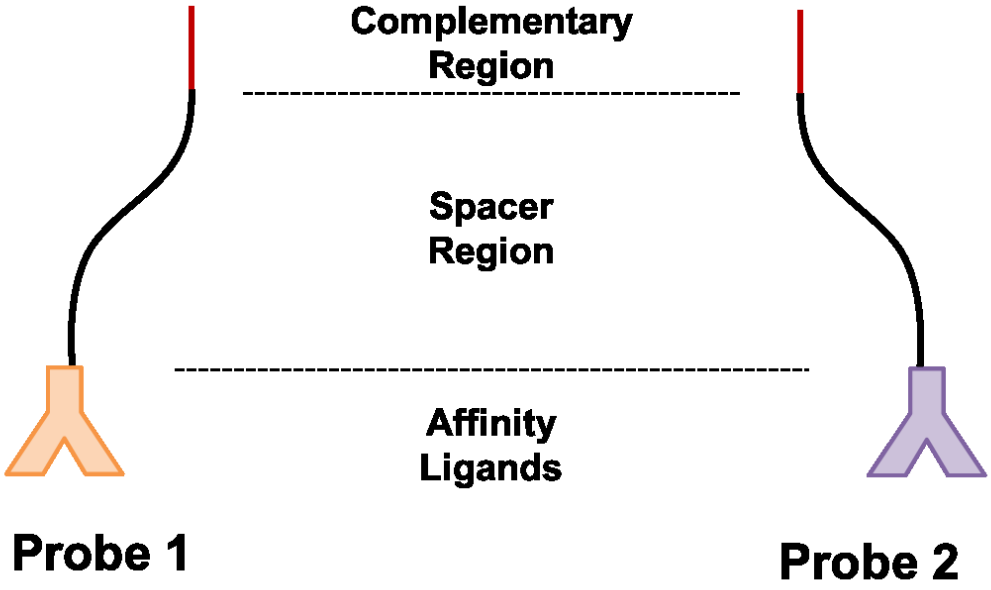

Figure 1.8 Illustration of the DNA-affinity ligand probes required for binding induced DNA assembly (BINDA). The black line represents a ssDNA poly-T sequence and the red line represents a short complementary region between probes. The inverted Y shapes represent antibodies.

Assembly between probes is enabled because both probes are anchored to the same target molecule, which increases their effective local concentration (Figure 1.9). The increased local concentration increases the stability of the short complementary region, similar to a DNA hairpin loop (Figure 1.10). The melting temperature (T_m) is used to estimate the stability between two DNA strands. The T_m of two complementary strands is defined as the temperature at which the two strands will be 50 % hybridized. Two short complementary DNA strands with a low T_m will not hybridize to form dsDNA. If those

same sequences are linked on the same DNA strand, they will hybridize to form a hairpin structure, where the two complementary strands form the stem and an arbitrary spacer sequence forms a loop; this is a well-known DNA structure. The increased stability of the stem region in a DNA hairpin is similar to the increased stability of target bound probes in BINDA. However, in BINDA the loop of a DNA hairpin is replaced by a loop consisting of the spacer regions on each probe and the target bound affinity ligands.

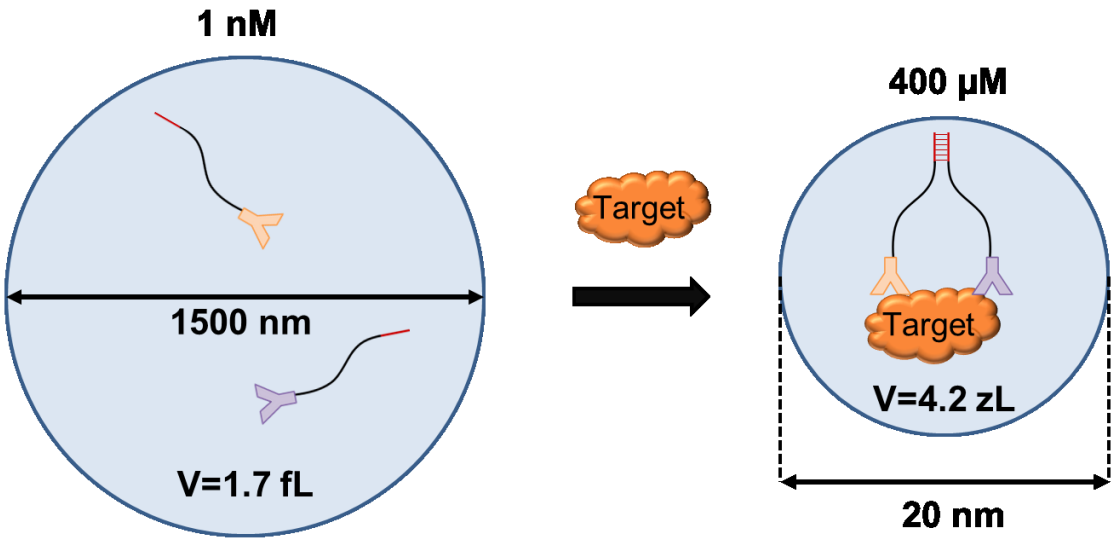

Figure 1.9 Illustration of the increased local concentration of target bound probes in BINDA. The close proximity of two probes bound to a single target increases the stability of their complementary region. Binding of two probes to a single target increases their local concentration by 4×10^5 fold.

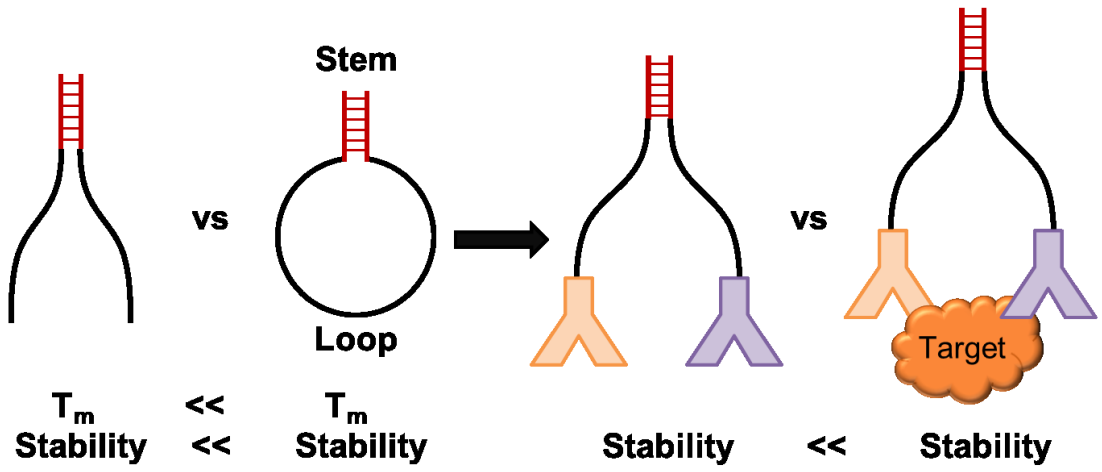

Figure 1.10 Comparison of a DNA hairpin to target bound probes in BINDA. The loop created by two target bound probes closely resembles the DNA loop in a DNA hairpin structure.

BINDA was applied first to the detection of platelet derived growth factor (PDGF-BB) and prostate specific antigen (PSA) with yoctomole detection limits.[101] The amplified signal was generated from RT-PCR. Several addition detection strategies for BINDA have been developed, including the activation of fluorescent dyes,[103–107] activation of DNAzyme amplification,[107] generation of fluorescent silver nanoclusters,[108] electrochemical signals,[109] and fluorescence resonance energy transfer.[110–114] Applications of BINDA include triggering toehold mediated strand displacement networks,[106] detecting antibody-antigen binding,[112–114] controlling molecular translators and DNA nanomotors,[103,105,107] and cell imaging.[115]

1.3.4 Proximity ligation assays

The proximity ligation assay (PLA) was developed first in 2002 by Landegren and coworkers.[116] PLA uses a similar concept to BINDA, where target binding events result

in the assembly of DNA strands (Figure 1.11). Two affinity ligand-DNA probes are used to bind the target. After target binding, an additional connector DNA hybridizes to the DNA motifs on each probe. The connector oligo places the 5′-end of one DNA motif next to the 3′-end of the other DNA motif. This orientation serves as the template for a ligase to join the two strands together, generating a new DNA strand that can be used for detection.

The first application of PLA used RT-PCR to amplify the ligated DNA product exponentially to detect as low as 24 000 molecules of cytokine platelet derived growth factor (PDGF-BB).[116] The authors also designed a solid phase format that used washing steps to remove unbound probes. The solid phase format achieved a low femtomolar detection limit of PDGF-BB.[116] The same group developed a triple-binder proximity ligation assay (3-PLA) that used an affinity ligand-DNA conjugate in place of the connector oligo.[117] 3-PLA improves the detection limit of PLA; however, the requirement of three simultaneous binding events on a single target may limit the applicability of 3-PLA. The connector oligo in PLA typically has the same number of complementary bases with each probe. Kim *et al.* discovered that using an asymmetric connector oligo improved the dynamic range of PLA by two orders of magnitude and increased sensitivity by a factor of 1.6.[118]

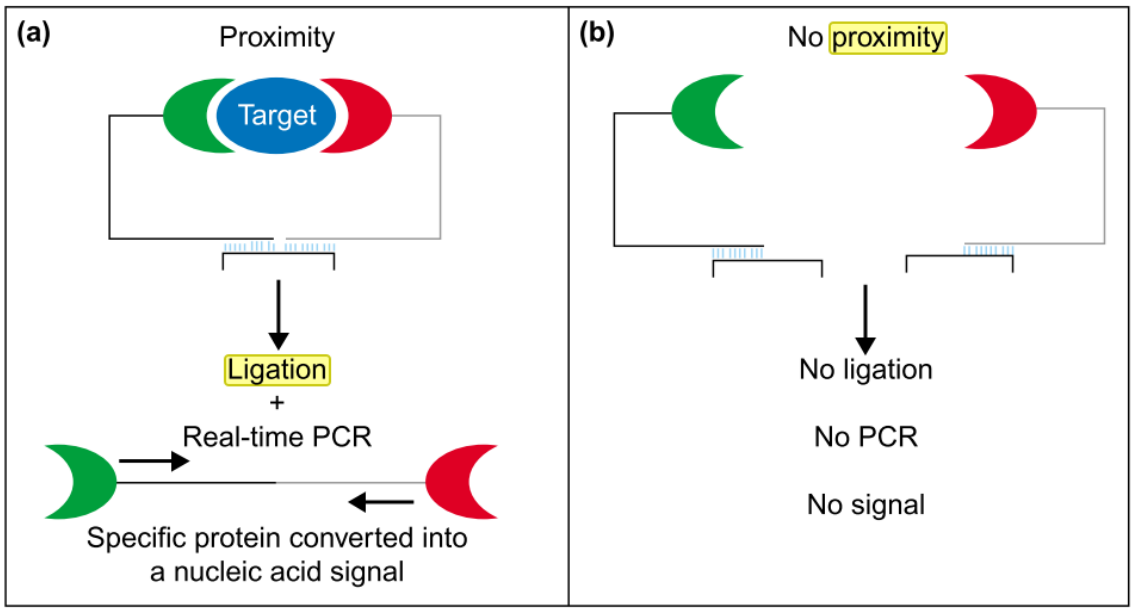

Figure 1.11 Principle of the proximity ligation assay (PLA). (a) When two probes bind to the same target, they are in close proximity. A connector oligo hybridizes to both probes, and triggers ligation between the two DNA probes. The newly ligated DNA is detected by RT-PCR. (b) In the absence of a target, probes are unable to be ligated together. Reprinted with permission.[119] Copyright 2003 Elsevier.

In situ PLA is a variant of PLA that uses RCA to generate an amplified detection signal.[57] *In situ* PLA uses two connector oligos that are ligated together to generate the circular template required for RCA (Figure 1.12). After ligation, one of the affinity ligand-DNA conjugate probes serves as the primer to be amplified around the circular RCA template. RCA generates a long concatameric repeat of the RCA template sequence that is anchored to the protein target. *In situ* PLA has been adapted widely for the imaging of fixed cells using fluorescence microscopy. In principle, *in situ* PLA can be performed without any washing steps, but for low abundance proteins, washing steps are used. PLA

has been used for several applications, including the detection of proteins and pathogens,[120–122] the study of protein–protein interactions and posttranslational modifications,[57,123–126] and biomarker development.[127–129]

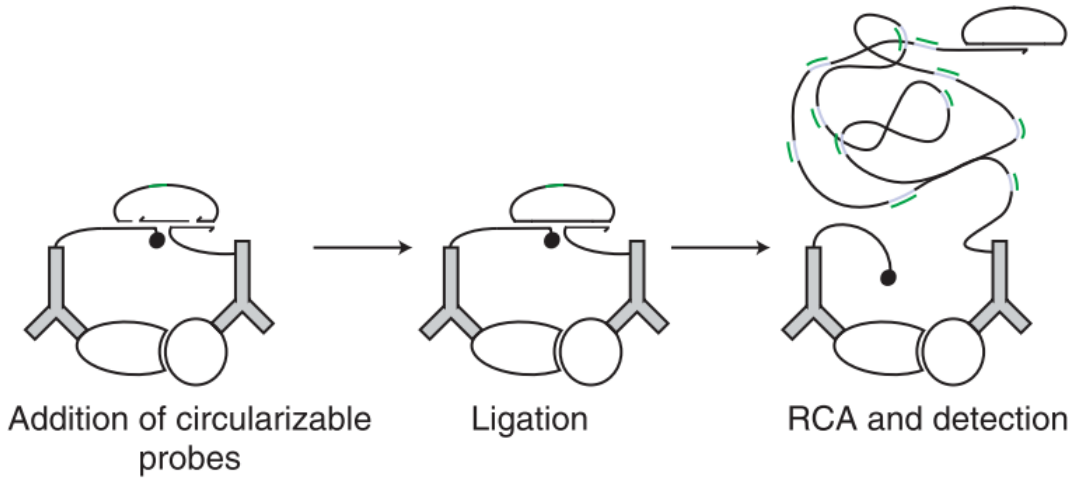

Figure 1.12 Schematic illustration of in situ PLA. Binding of two probes to the target allows circularization of two connector oligos, which triggers subsequent RCA. Reprinted with permission.[57] Copyright 2006 Springer Nature.

1.4 Thesis Objectives

The specific detection of low abundance proteins remains challenging. Complicated sample matrices require affinity-based methods for specific detection. However, many commonly used methods, such as ELISA, have insufficient signal amplification for ultra-low concentrations of protein target. In contrast, there are many technologies capable of detecting <10 copies of a DNA target. These DNA detection methods are homogenous, isothermal, rapid, and generate high amounts of amplification products. Since proteins have no comparable way of being amplified, converting protein detection into a DNA amplification provides an alternate way to detect low concentration proteins.

Using DNA amplification for protein detection in a homogenous format requires a transduction event to trigger amplification. PLA and BINDA are two techniques capable of triggering DNA amplification from a protein target in a homogenous format. PLA commonly uses PCR, which requires thermocycling. *In situ* PLA typically uses washing steps and fluorescence microscopy, making it a heterogeneous format. While fluorescence microscopy facilitates low detection limits, it requires trained personnel, more complicated sample preparation, and is not applicable to a POC setting. BINDA has been used to trigger several DNA amplification systems, including PCR and toehold mediated strand displacement networks, but it has not been coupled with isothermal and exponential DNA amplification. The use of isothermal and exponential DNA amplification with BINDA based target recognition can improve detection limits compared to non-enzymatic amplification systems.

My initial work focused on developing binding induced enzymatic strand displacement networks for the detection of proteins. Three designs were tested and

optimized. In this work, EXPAR was used for signal amplification, but I discovered that EXPAR has an inherently high background signal. Next, I investigated the cause of the high background signal in EXPAR and designed strategies to slow the onset of the background amplification to improve the detection limit of EXPAR. Although I was able to decrease the background in EXPAR, the methods used were not compatible with my original designs. I then developed an improved BINDA system that takes advantage of LAMP's powerful amplification of DNA for protein detection. The designs developed in this thesis are all homogenous, rapid, and incorporate isothermal amplification.

Chapter 2 The primary goal of this Chapter is the development of a BINDA system for protein detection that incorporates both linear and exponential enzymatic strand displacement amplification of DNA. First, a linear amplification system was designed and experimentally optimized. Building upon the linear amplification system, exponential amplification was added by incorporating EXPAR. The addition of EXPAR added a high background, so a modified BINDA system incorporating EXPAR was designed to have amplification occur at a higher temperature to reduce background.

Chapter 3. The primary objective of this Chapter investigates the cause of the inherently high background in EXPAR. Two general strategies were used to test the triggering mechanism of background amplification. The blocking strategies used to prevent background amplification provided evidence of the triggering mechanism of background amplification. Using a single stranded binding protein to reduce background amplification resulted in three orders of magnitude improvement to the EXPAR detection limit.

Chapter 4 The goal of this Chapter was to design and optimize a BINDA system that incorporates LAMP for the detection of proteins. Important reaction and design parameters were optimized. Several control experiments were used to assess the performance of different design components. This is the first reported use of LAMP for homogenous protein detection.

Chapter 5 This chapter summarizes all research conclusions and discusses future research directions of the work detailed in this thesis.

Chapter 2: Binding Induced Enzymatic Strand Displacement Amplification Reactions for Protein Detection

2.1 Introduction

Over the past 20 years, remarkable advances have been made in the homogenous detection of proteins, particularly in the development of BINDA and PLA techniques.[101,110,116] Both techniques translate protein binding by affinity ligands into unique DNA structures. PLA uses ligase to join two or more strands from target bound DNA-affinity ligand conjugates; this generates a new DNA strand that is commonly amplified by PCR or by RCA.[57,116,128,130,131] BINDA uses two DNA-affinity ligand conjugate probes that assemble via a short complementary region between DNA motifs when bound to a single target. The assembly between probes in BINDA can be amplified by PCR, trigger toehold mediated strand displacement networks, or trigger amplification via DNA motors.[101,103–106,115] However, combining these protein recognition techniques with isothermal amplification of DNA to enable detection of ultralow concentrations of proteins in solution remains challenging. Both PLA and BINDA can achieve ultralow detection when PCR is used for signal amplification. The use of PCR requires temperature cycling making PCR less suitable for POC and resource limited settings compared to isothermal techniques. *In situ* PLA can achieve ultralow detection limits but are typically used to detect surface bound proteins on fixed cells with fluorescence microscopy. This requires trained personnel, is not amenable to POC setting, and does not allow for high throughput.

The primary objective of this chapter is to use the principles of BINDA to design a binding induced strand displacement amplification (BISDA) technique that uses isothermal enzymatic strand displacement amplification for protein detection. The second

objective is to develop two additional strategies that build upon the linear amplification of BISDA and incorporate exponential amplification by using EXPAR. Each strategy uses isothermal amplification with a homogenous format that results in a simple procedure. These properties are desirable for POC settings and amenable to high throughput since the procedure only requires the addition of reagents followed by the monitoring of fluorescence.

The BISDA strategy is illustrated in Figure 2.1. BISDA is designed to have target recognition and signal amplification components. Upon binding of the target by both the template probe (**PT**) and primer probe (**PR**), the complementary region between the two probes assembles to form a dsDNA region. The probes are designed so that after assembly, **PR** acts as a primer that can be extended by polymerase along **PT**. After extension, the dsDNA recognition sequence of NEase is generated, which allows the NEase to cleave the phosphate backbone of the extended **PR** strand. This generates a nicked site that can be extended by polymerase. The second extension by polymerase displaces the previously extended strand, generating a single stranded trigger DNA (**T**) and regenerating the NEase recognition site. The cycle of polymerase extension/strand displacement and nicking by NEase continues to achieve linear amplification of **T**. The increasing amount of **T** generated with each cycle generates a fluorescence signal by activating a toehold mediated strand displacement beacon (**FQ**). The beacon was constructed of a fluorophore strand (**F**) that is fully complementary to **T-28** and a quencher strand (**Q**) that has same sequence as **T-28** with eight bases shorter on the 5′-end. The amount of fluorescence generated is then directly related to the amount of target present.

EXPAR was incorporated into the BISDA system to achieve an exponentially amplified signal (Figure 2.2). The **T** oligo amplified in BISDA is designed to act as the trigger DNA in EXPAR. Two modifications are required to incorporate EXPAR with BISDA: the addition of an EXPAR template (**XT**) and the use of SYBR Green I (SG) instead of **FQ**. **XT** is designed to have the same NEase recognition sequence used in BISDA so that the same NEase and polymerase function with both BISDA and EXPAR components. SG is used to lower the cost of the assay and facilitate simpler sample preparation.

The final strategy uses BISDA and EXPAR, but the EXPAR component occurs at 55 °C, where EXPAR is typically operated at (Figure 2.3). A short (10 min) extension phase at 37 °C is used, followed by exponential amplification (EXPAR) at 55 °C, to incorporate the higher temperature amplification. The higher temperature has two main advantages: faster amplification speed and lower occurrence of nonspecific DNA interactions. The faster amplification is achieved because polymerase enzymes with higher optimum operating temperatures typically have increased speed. Decrease of nonspecific DNA interactions occurs because higher temperatures destabilize them.

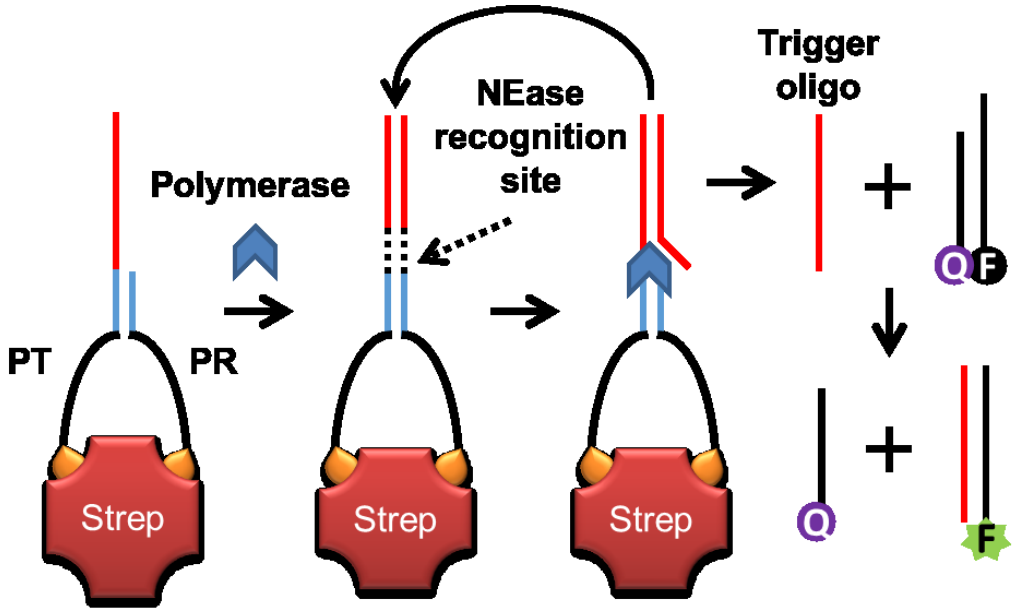

Figure 2.1 Schematic illustration of binding induced strand displacement amplification (BISDA). The short complementary region (blue) between **PT** and **PR** anneal when bound to the same streptavidin target molecule. After annealing, **PR** is extended by polymerase. After extension, NEase cleaves the backbone of the extended **PR** strand at the recognition site (black dots) that was previously generated. Polymerase then extends from the nick site and displaces the previously synthesized strand. The bound probes continue to undergo nicking and strand displacement to generate many copies of trigger DNA (**T**) which generate fluorescence by activating a toehold mediated strand displacement beacon (**FQ**).

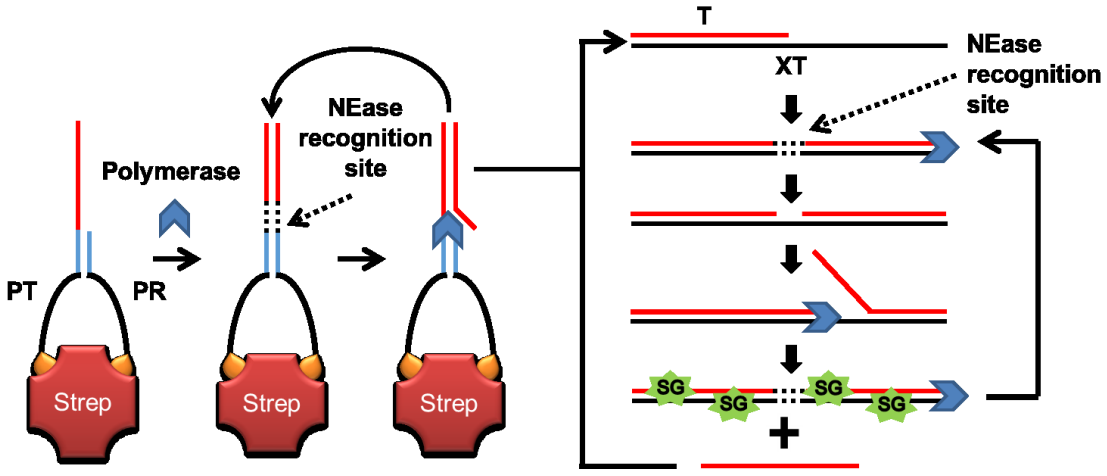

Figure 2.2 Schematic illustration of BISDA incoporating EXPAR. The reaction is triggered in the same way as in BISDA (Figure 2.1); however, **T** is amplified further by EXPAR. **T** anneals to **XT**, followed by extension of **T** along **XT** by polymerase. This extension generates the NEase recognition site, which is then cleaved by NEase, generating a nick site. Polymerase extends from the nick site and displaces the previously extended strand. The displaced strand has the same sequence as **T** and can anneal to another **XT** molecule to undergo amplification. The original template continues to undergo strand displacement amplification, generating increasing amounts of **T**; thus, each cycle generates two strands of **T** for exponential amplification. The signal is generated by SYBR Green I (SG) binding to ds**XT**.

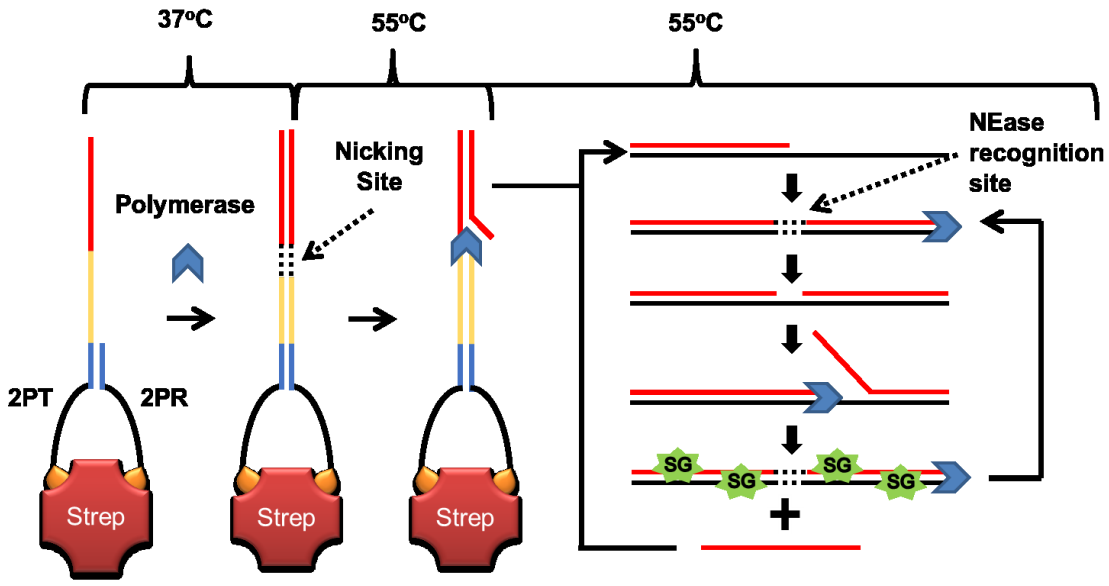

Figure 2.3 Schematic illustrations of 2-stage BISDA incorporating EXPAR. An initial binding and extension phase occurs at 37 °C, similar to standard BISDA. **2PT** has a stabilization region (yellow) to stabilize the hybridization between probes when the temperature is increased to 55 °C. The NEase is inactive at 37 °C; therefore, no nicking occurs until the temperature is increase to 55 °C. After the temperature is increased to 55 °C, the NEase becomes active, and the reaction proceeds in the same manner as BISDA–EXPAR (Figure 2.2) but at a higher temperature.

2.2 Experimental

2.2.1 Materials and reagents

All oligonucleotides were synthesized, labelled, and purified by Integrated DNA Technologies (Coralville, IA). DNA sequences and modification are listed in Tables 2.1, 2.2, 2.3. Klenow (3′→5′ exo-) polymerase, Klenow large fragment polymerase, Bst 2.0 polymerase, Nt.BbvCI NEase, Cutsmart buffer, and NEBuffer 3.1 were from New England Biolabs (Whitby, ON, Canada). SYBR Green I (10 000X), SYBR Gold (10

000X), deoxynucleotide triphosphates (10 mM mix), and ROX reference dye (ROX) were from Life Technologies (Burlington, ON, Canada). Ammonium persulfate (APS) and 40% 19:1 acrylamide:bisacrylamide used for polyacrylamide gel electrophoresis (PAGE) were from BioRad (Mississauga, ON, Canada). 1, 2-bis(dimethylamino)ethane (TEMED), Tris-borate-EDTA (TBE) buffer, and DNA gel loading dye were from Fisher Scientific (Nepean, ON, Canada). Recombinant human ErbB2/Her2 Fc Chimera and biotinylated polyclonal anti human ErbB2/Her2 goat IgG were from R&D Systems (Minneapolis, MN). All experiments used nanopure H_2O (>18MΩ), purified by an Ultrapure Milli-Q water system.

Table 2.1 DNA sequences and modifications for BISDA

DNA Name	**Sequence**
Template Probe (**PT**)	5′-C GCT TGA ACG CTG TGC TAG ATG TGC TGA GGA TAG GAT GGT TTT TTT TTT-**Biotin**-3′
6 base Primer Probe (**PR6**)	5′-**Biotin** -TTT TTT TTT TTT TTT CTA TCC-3′
7 base Primer Probe (**PR7**)	5′-**Biotin** -TTT TTT TTT TTT TTT CTA TCC T-3′
8 base Primer Probe (**PR8**)	5′-**Biotin** -TTT TTT TTT TTT TTT TC CTA TCC-3′
F	5′-**FAM**-C GCT TGA ACG CTG TGC TAG ATG TGC TGA-3′
Q	5′-T CTA GCA CAG CGT TCA AGC G–**Iowa Black**-3′
Blocker 8 (**B-8**)	5′-TTT CAT CCT AT TTT-3′
Blocker 9 (**B-9**)	5′-TTT CCA TCC TAT TTT-3′

Blocker 10 (**B-10**)	5′-TTT ACC ATC CTA T TTT-3′
Blocker 11 (**B-11**)	5′-TTT ACC ATC CTA TC TTT-3′
The blue colored regions highlight the complementary sequence between template and primer probes. Underlined regions contain either the full or partial NEase recognition sequence.	

Table 2.2 DNA sequences and modifications for the 37 °C EXPAR

DNA Name	**Sequence**
EXPAR Template 28 (**XT-28**)	5′- C GCT TGA ACG CTG TGC TAG ATG TGC TGA GGT C GCT TGA ACG CTG TGC TAG ATG TGC TGA–**SpC3**-3′
EXPAR Template 19 (**XT-19**)	5′- TAG GTG AAC GTG GAG CTG AGG GCT AGG TGA ACG TGG AGC TGA -**Phos**-3′
EXPAR Template 15 (**XT-15**)	5′-GGT TTT A TTT GCT GAG GTT TTA T TTG CTG A-**Phos**-3′
EXPAR Template 11 (**XT-11**)	5′-GGT TTT GCT GAG GTT TTG CTG A-**Phos**-3′
EXPAR Template 8 (**XT-8**)	5′-GGT GCT GAG GTG CTG A-**Phos**-3′
Trigger 28 (**T-28**)	5′-TCA GCA CAT CTA GCA CAG CGT TCA AGC G-3′
Trigger 19 (**T-19**)	5′- TCA GCT CCA CGT TCA CCT A-3′
Trigger 15 (**T-15**)	5′-T CAG CAA A TAA AAC C-3′
Trigger 11 (**T-11**)	5′-TCA GCA AAA CC-3′
Trigger 8 (**T-8**)	5′-TCA GCA CC-3′

Table 2.3 DNA sequences and modifications for the 2-stage BISDA–EXPAR

DNA Name	**Sequence**
2-stage Template Probe (**2PT**)	5′-AAC TAT ACA ACC TAC TAC CTC ACT CAG ACT CCT CTC GAA CAC TTT TTT TTT TTT TTT TTT TTT TTT T-**Biotin**-3′
2-stage Primer Probe 7 (**2PR7**)	5′-**Biotin**-TTT TTT TTT TTT TTT TTT TTT TTT AGT GTT C
2-stage Primer Probe 6(**2PR6**)	5′-**Biotin**-TTT TTT TTT TTT TTT TTT TTT TTT GT GTT C
EXPAR Template 55 (**XT-55**)	5′-AAC TAT ACA ACC TAC TAC CTC ATT CAG ACT CAA ACT ATA CAA CCT ACT ACC TCA A-**Phos**-3′
Trigger 55 (**T-55**)	5′-T GAG GTA GTA GGT TGT ATA GTT-3′
The red colored regions highlight the complementary sequence between template and primer probes	

2.2.2 Preparation of the toehold-mediated strand displacement beacon

A toehold-mediated strand displacement beacon (**FQ**) was used to detect **T-28**. The beacon was constructed of a fluorophore strand (**F**) that is fully complementary to **T-28** and a quencher strand (**Q**) that has same sequence as **T-28** with eight bases shorter on the 5′-end. **F** and **Q** were received lyophilized, subsequently dissolved in nanopure water to

50 μM and 100 μM, respectively, and stored at -20 °C. To prepare **FQ**, **F** and **Q** were diluted to 5 μM and 10 μM, respectively, in 1X Cutsmart buffer (50 mM Potassium Acetate, 20 mM Tris-Acetate, 10 mM Magnesium Acetate, 100 μg/mL BSA, pH 7.9) by mixing 20 μL of 50 μM **F**, 20 μL of 100 μM **Q**, 20 μL of 10X Cutsmart buffer, and 140 μL nanopure water. The 5 μM **FQ** solution was annealed by heating to 90 °C for 5 min, followed by cooling to 25 °C over 1.5 hours. The ratio of **F** to **Q** was kept at 1:2 to minimize background fluorescence.

2.2.3 Binding induced DNA probes

The template probes (**PT**, **2PT**) and primer probes (**PR6**, **PR7**, **PR8**, **2PR6**, **2PR7**) used to detect streptavidin in all three designs consist of binding induced DNA assembly complementary regions, a poly-T spacer region, and biotin labels on the 5′ and 3′ ends of primer probes and template probes, respectively. For the analysis of streptavidin, template probes and primer probes were used directly and biotin serves as the affinity ligand for streptavidin recognition. Probes used for the detection of Her2 protein were constructed by linking biotinylated polyclonal anti human ErbB2/Her2 goat IgG to **PT** or **PR6** via streptavidin in solutions of 1X phosphate buffered saline (PBS). 25 μL of 2 μM streptavidin was mixed with 25 μL of 2 μM **PT** or **PR6** and incubated at 37 °C for 30 min, followed by 25 °C for 30 min. The resulting mixture was added to 50 μL of 1 μM biotinylated Her2 antibody and incubated at 25 °C for 30 min. Then, this mixture was diluted to 200 nM Her2-Probe conjugate by adding 150 μL of 1 mM biotin and stored at 4°C. Excess biotin was used to block the vacant biotin binding locations on streptavidin; this prevents any free **PT** or **PR6** from linking to the same streptavidin molecule and triggering background amplification.

2.2.4 BISDA procedure

The procedures for detecting streptavidin and human epidermal growth factor receptor 2 (Her2) using BISDA are similar and therefore described together. The procedure consists of making two master mixes and adding them to a target or a blank that contains only buffer. The two master mixes were a reagent mix and an enzyme mix. The reagent mix contained deoxynucleotide triphosphates (dNTPs), **FQ**, **PT**, **PR6; PR7; or PR8**, and Cutsmart buffer. The enzyme mix contained Nt.BbvCI, Klenow (exo-), and Cutsmart buffer. For the analysis of Her2, the reagent mix contained Probe-Her2 antibody conjugates and was added to either Her2 or a blank buffer and incubated for 20 min at room temperature to allow for complete binding of antibody probes before addition of the enzyme and reagent mixes. For the analysis of streptavidin, the enzyme mix was added immediately following the addition of reagent mix because the binding between biotin and streptavidin is rapid and does not require an incubation phase. After both mixes were added to the sample, the resulting 100 µL solution was transferred to a black 96 well microplate and placed in a preheated multi-mode DX880 microplate reader (Beckman Coulter). Fluorescence was monitored at 37 °C with excitation/emission set at 485/515 nm to detect **F**. The final concentrations of reagents, unless otherwise noted, were 5 nM of each probe, 0.25 mM dNTPs, 1X Cutsmart buffer, 100 nM **FQ**, 0.2 U/µL Nt.BbvCI, 0.1 U/ µL Klenow (exo-), and varying amounts of streptavidin or Her2.

2.2.5 EXPAR procedure

The procedure for EXPAR uses a reagent mix and an enzyme mix that are both added to the target or blank. The reagent mix consists of dNTPs, SG, ROX, **XT-28**; **XT-19**; **XT-15**; **XT-11**; or **XT-8**, and Cutsmart buffer. The enzyme mix contained Nt.BbvCI, Klenow

(exo-) or Klenow LF, and Cutsmart buffer. After the reagent mix and enzyme mix were prepared and added to **T-28**, **T-19**, **T-15**, **T-11**, **T-8**, or the blank, the resulting 100 µL reaction solutions were transferred to a black 96 well plate. The plate was placed in a preheated multi-mode DX880 microplate reader. Fluorescence was monitored at 37 °C with excitation/emission set at 485/515 nm to detect SG and 535/595 nm to detect ROX as a reference dye. Final concentrations of reagents, unless otherwise noted, were 0.25 mM dNTPs, 1X Cutsmart buffer, 1X SG, 125 nM ROX, 100 nM **XT-28**, 0.2 U/µL Nt.BbvCI, 0.1 U/ µL Klenow (exo-), and varying concentrations of **T-28**.

EXPAR products were visualized on a 12 % native polyacrylamide gel. The gel was made by combining 4.5 mL of 40 % 19:1 acrylamide/bisacrylamide, 3 mL of 5X TBE buffer, 7.5 mL nanopure water, 15 µL TEMED, and 93 µL of 10 % APS. EXPAR reactions were incubated for 30 min with higher concentrations of reagents so that the products could be visualized. The final reaction concentrations of EXPAR reagents were 2 µM **XT-28**, 2.5 mM dNTPs, 1X Cutsmart buffer, 0.5 U/µL Klenow LF or Klenow (exo-), 1 U/µL Nt.BbvCI, and varying amounts of **T-28**. After incubation for 30 min, 10 µL of each EXPAR reaction was mixed with 2 µL of 6X DNA gel loading dye and then loaded onto the PAGE gel. The PAGE gel was run for 1 h at 120 V, followed by staining with SYBR gold and imaged by an ImageQuant 350 (IQ 350) digital imaging system (GE Healthcare).

2.2.6 BISDA incorporating EXPAR

The procedure for BISDA–EXPAR follows a similar protocol as BISDA. The reagent mix consists of dNTPs, SG, ROX, **PT**, **PR6**, **XT-28**, and Cutsmart buffer. The enzyme mix contained Nt.BbvCI, Klenow (exo-), and Cutsmart buffer. Reagent and enzyme mixes

were added to streptavidin or a blank, and the final 100 µL reaction solution was transferred to a black 96 well plate. The plate was placed in a preheated multi-mode DX880 microplate reader, and fluorescence was monitored at 37 °C with excitation/emission set at 485/515 nm to detect SG and 535/595 nm to detect ROX reference dye. The final concentrations of reagents, unless otherwise noted, were 5 nM of each probe, 0.25 mM dNTPs, 1X Cutsmart buffer, 1X SG, 125 nM ROX, 100 nM **XT-28**, 0.2 U/µL Nt.BbvCI, 0.1 U/ µL Klenow (exo-), and varying amounts of streptavidin.

2.2.7 BISDA and EXPAR conducted in two-stages

In a typical 2-stage BISDA–EXPAR reaction, a probe mix and a master mix were prepared and added to either a streptavidin target or a blank containing only buffer. The probe mix contained **2PT** and **2PR6** or **2PR7**. The master mix contained dNTPs, SG, ROX, NEBuffer 3.1 (100 mM NaCl, 50 mM Tris-HCl, 8-10 mM $MgCl_2$, 100 µg/mL BSA, pH 7.9, 7.4), **XT-55**, Nt.BstNBI, and Bst 2.0. To initiate the reaction, 4 µL of probe mix were added to 2 µL streptavidin or blank buffer, followed by addition of 14 µL of the mastermix. The resulting reaction solutions were transferred to an Applied Biosystems StepOnePlus real-time PCR system. The reaction was held at 37 °C for 10 min, to allow extension of either **2PR6** or **2PR7**, followed by increasing the temperature to 55 °C and monitoring the fluorescence using the FAM dye filter to measure SG and the ROX dye filter to measure ROX. The final concentrations of reagents, unless otherwise noted, were 100 pM of each probe, 0.25 mM dNTPs, 1X NEB3.1 buffer, 1X SG, 125 nM ROX, 100 nM **XT-28**, 0.5 U/µL Nt.BstNBI, 0.4 U/ µL Bst 2.0, and varying amounts of streptavidin.

2.3 Results and Discussion

2.3.1 Design of probes for the construction of Binding induced strand displacement amplification (BISDA)

PT and **PR** probes were purchased with biotin labels on their 3′ and 5′-ends, respectively. This allows **PT** and **PR** to be used directly for the detection of streptavidin, where biotin serves as the affinity ligand. The use of biotin labelling also allows simple construction of probes for different target proteins by linking **PT** and **PR** to antibodies. Streptavidin can bind four different biotin molecules, which allows use of streptavidin as a linking molecule to join DNA motifs to affinity ligands for other proteins.

The 3′-end of **PR** was designed to have a short (6–8 nucleotide) complementary region to **PT**. This region is short enough that in the absence of target, the two probes exist as ssDNA probes. In the presence of a target, when both probes bind to a single target molecule, they are brought into close proximity, which promotes hybridization between the 3′-end of **PR** and the middle of **PT.** IDTs Oligoanalyzer 3.1 software was used to estimate the stability between probes when they are free in solutions or bound to a target. To estimate the stability of free probe hybridization, the T_m of the 6–8 base sequence was used. A hairpin sequence was used to estimate the stability between two target bound probes. The hairpin consisted of the complementary region between **PT** and **PR** on the 5′ and 3′-ends, respectively, separated by a 100-T sequence. The 100-T sequence is used to mimic the spacing between target bound probes. By using estimated melting temperatures, the complementary sequence was designed to maximize the difference in stability between bound and unbound probes.

Since **PT** and **PR** also are used when BISDA is combined with EXPAR, it was important to minimize any nonspecific interactions between **PT**, **PR**, and **XT**. Avoiding any complementarity between the 3′-end of **PR** and **XT** is critically important because **XT** is present in solution at high concentration. Hybridization between the 3′-end of **PR** and **XT** would result in extension of **PR** by polymerase and trigger EXPAR, which would result in high background signals.

2.3.2 Detection of streptavidin using BISDA

The ability of the BISDA system to amplify **T** linearly was tested using streptavidin as the target and a toehold mediated strand displacement beacon (**FQ**) to detect **T**. Streptavidin was chosen to test the feasibility of our strategy due to the strong binding affinity between biotin and streptavidin ($K_d = 10^{-14}$ M). The strong and rapid binding between biotin and streptavidin enabled evaluation of reaction parameters, such as complementary region length, probe concentration, and the use of blockers, without being limited by weak affinity ligand-target binding. **FQ** was used to detect **T** because it only produces a signal when **T** is present, unlike nonspecific DNA fluorescent dyes. Nonspecific DNA dyes, such as SYBR dyes, generate fluorescence from any DNA sequence. Since the BISDA system contains two DNA probes at high concentrations relative to the target, a nonspecific DNA dye would generate a high background fluorescence.

Figure 2.4 shows a typical amplification profile of a streptavidin target and blank reactions for BISDA. When 1 nM streptavidin is present, an increase of fluorescence signal is observed. The increased signal is due to the increase of displaced **T-28,** which undergoes toehold mediated strand displacement to activate **FQ**. When no streptavidin is present, no **T-28** is generated to activate **FQ,** and the fluorescence remains constant at the baseline level.

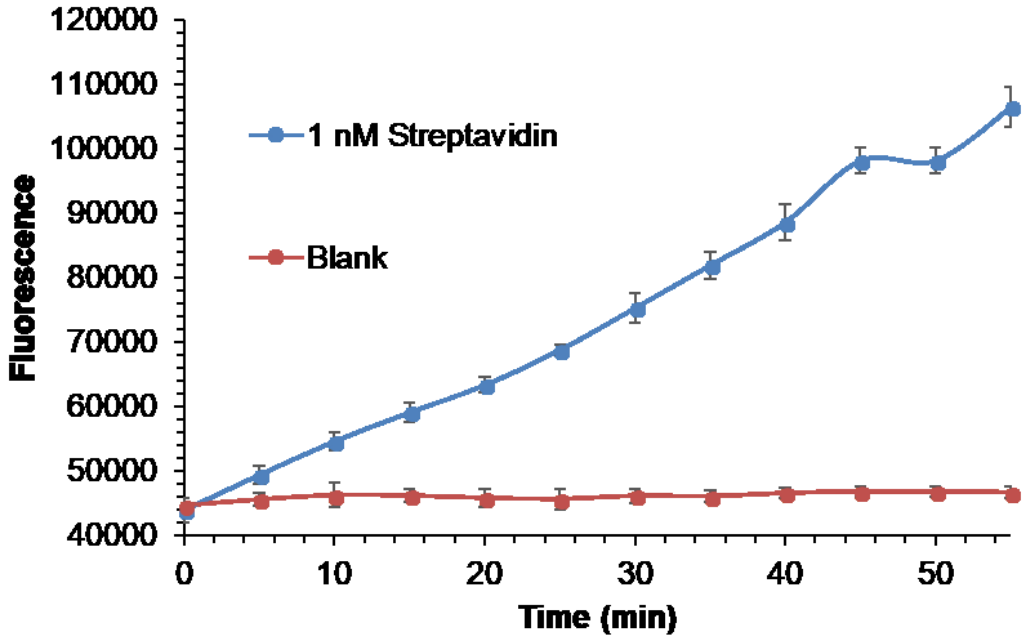

Figure 2.4 Amplification profile of BISDA. Fluorescence increases in the presence of streptavidin by the continual generation of **T-28**, which activates the **FQ** toehold strand displacement beacon. Data shown is the mean ± standard deviation of triplicate experiments.

The length and G-C content of the complementary region between **PT** and **PR** was designed to achieve the largest ΔT_m between free and target bound probes. Achieving little or no hybridization between free probes is critical to ensure a low background signal. Conversely, achieving a high percentage of bound probes that hybridized together is required to achieve a high signal. Figure 2.5 shows fluorescence after 40 min reaction time using 6, 7, and 8 nucleotide complementary regions between **PT** and **PR**. Comparing the target and blank fluorescence signals, a 6 base and 7 base complementary regions show similar results. However, when the complementary region is increased to 8 bases, both the target and background fluorescence signals greatly increase, indicating target independent hybridization between probes that triggers amplification. This shows the critical importance of having an appropriate complementary region between probes to ensure signal generation while limiting background. **PR6**, which has a 6 base complementary region with **PT**, was used for all further experiments because it showed comparable target fluorescence as the 7 base length but, in principle, should minimize target independent hybridization.

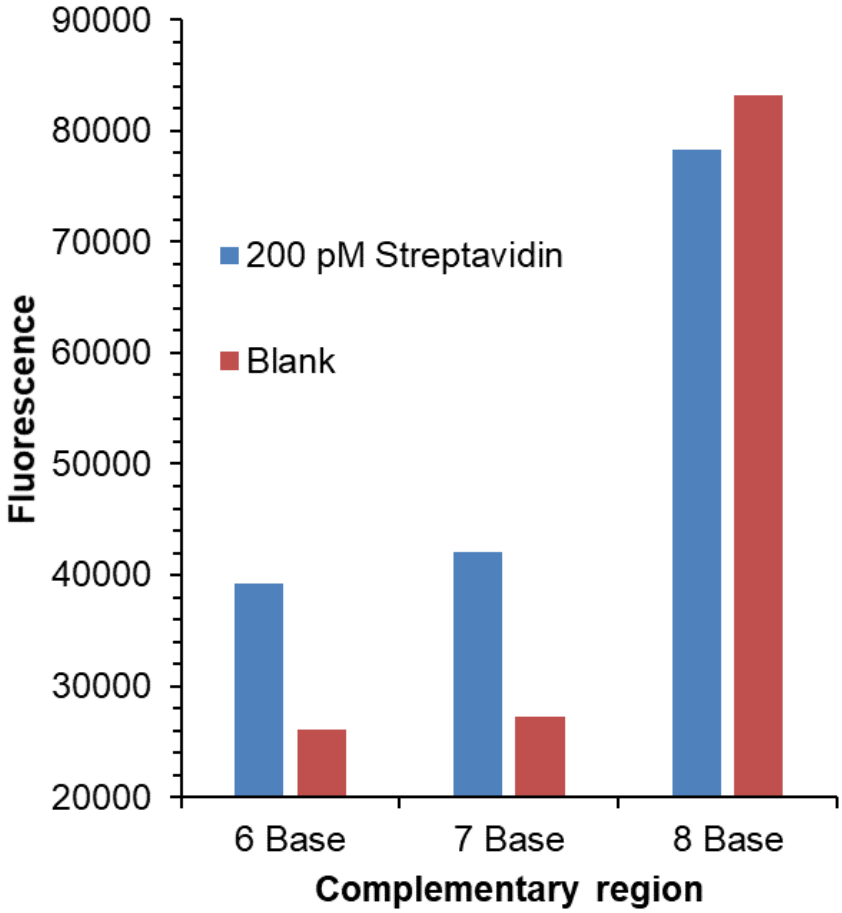

Figure 2.5 Effect of the length of the complementary region between **PT** and **PR**. Each reaction was incubated at 37 °C for 40 min, and the fluorescence signal was measured for 200 pM target and blank reactions. Six Base corresponds to the use of **PT** and **PR6**, 7 Base used **PT** and **PR7**, and 8 Base used **PT** and **PR8**. Data shown is the mean of duplicate experiments.

The system must generate higher amounts of **T** with increasing streptavidin concentrations to be quantitative. Figure 2.6 shows the fluorescence signals from 1–500 pM streptavidin after 40 min of incubation at 37 °C. The increased fluorescence signal as the concentration of streptavidin is increased confirms that the assay produces increasing

amounts of **T** relative to the target and is suitable for quantitation. As low as 1 pM streptavidin generates a higher signal than the blank. The ability to generate higher amounts of ssDNA trigger with increasing streptavidin concentrations in BISDA is required for quantitation using BISDA and also ensures the possibility for quantitation when EXPAR is incorporated into the system.

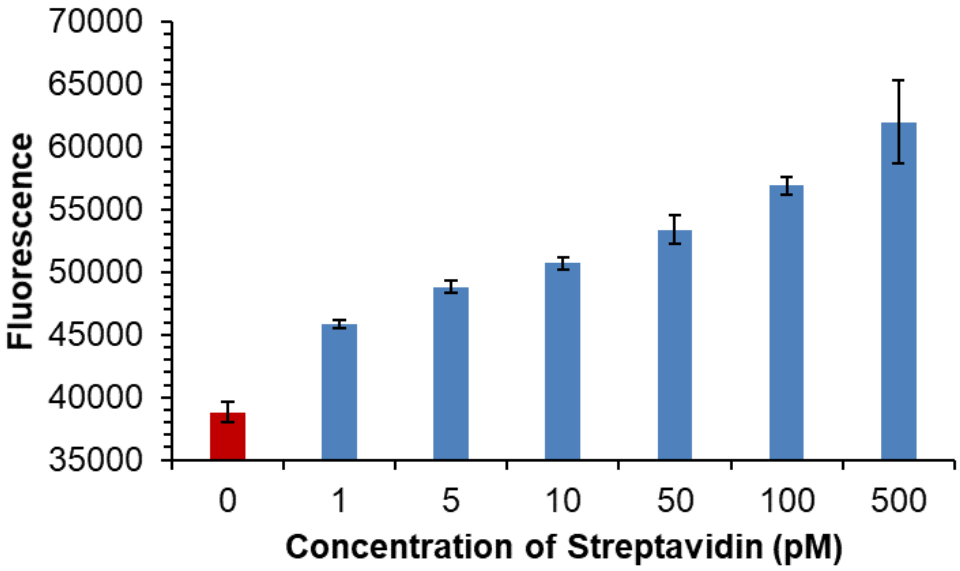

Figure 2.6 Fluorescence response of BISDA to varying concentrations of streptavidin. Data shown is the mean ± standard deviation of triplicate experiments.

2.3.3 Detection of Her2 using BISDA

Her2, a breast cancer transmembrane protein biomarker, was used to test the feasibility of BISDA further: specifically, the ability to trigger BISDA using antibody probes. To detect molecules other than streptavidin, affinity ligands for the desired target must be conjugated to **PT** and **PR**. Polyclonal Her2 antibodies were used as affinity ligands to detect Her2 in a buffered system. It is important to note that either 2 monoclonal

antibodies that bind different epitopes or polyclonal antibodies must be used to ensure that both probes are able to bind to a single Her2 molecule.

It is common to link biotinylated affinity ligands to biotinylated DNA probes through streptavidin. By mixing a 1:1:1 ratio of biotinylated DNA to streptavidin to biotinylated antibody (Ab), construction of **PT** linked Ab and **PR6** linked Ab is achieved. Excess biotin is added to block unoccupied streptavidin binding sites. This prevents any free **PT** or **PR** from binding to the same streptavidin molecule and generating a background.

Antibodies have lower binding affinities (K_d ~10^{-9}) compared to streptavidin-biotin ($K_d = 10^{-14}$), therefore, a higher concentration of antibody probes may be required to achieve more complete binding of a target. The principle of BINDA is based on the increased stability between probes bound to the same target molecule, which increases their local concentration. High probe concentrations lead to strong target binding and a correspondingly higher target specific signal. However, this may also lead to a high background signal from target independent hybridization between probes. Low probe concentration will reduce target independent hybridization between probes but may also decrease target triggered signal. The optimum probe concentration will maximize target triggered probe hybridization while limiting target independent probe hybridization.

Figure 2.7 shows the detection of Her2 using BISDA with Her2 probe concentrations ranging from 2 to 8 nM. As the concentration of probes increases, both target and blank signals increase; this is consistent with BINDA principles. Two nM probes showed little target specific signal, while 8 nM probes had very high background.

Four and six nM probes have similar differences between target and background signals. A probe concentration of 5 nM was chosen for further experiments

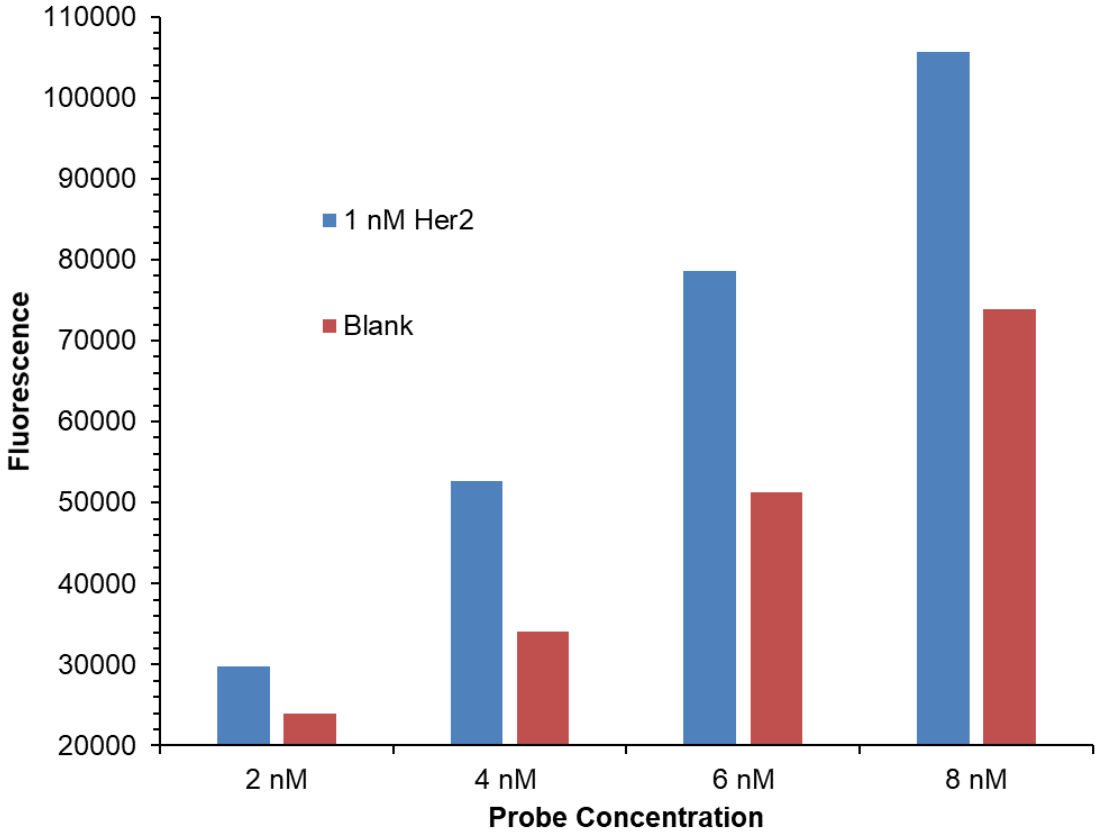

Figure 2.7 Effect of probe concentration on detecting Her2 with BISDA. Each concentration of probes corresponds to a concentration of **PT** linked antibody and **PR6** linked antibody. Data shown is the mean of duplicate experiments.

Although probe concentrations and probe complementary length have been optimized for BISDA, a background signal persists. To address this issue, blocking oligos were designed (illustrated in Figure 2.8). The blocker forms a duplex with the complementary region on **PT**, preventing weak hybridization between **PT** and **PR** when

probes are free in solution. Upon target binding, the increased stability between **PT** and **PR6** displaces the blocker oligo and allows for normal hybridization between **PT** and **PR6.** The sequence is short so that it can be displaced easily by target triggered hybridization between probes. A high concentration of blocker is used relative to the probes, which increases its stability with **PT** and the corresponding blocking efficiency.

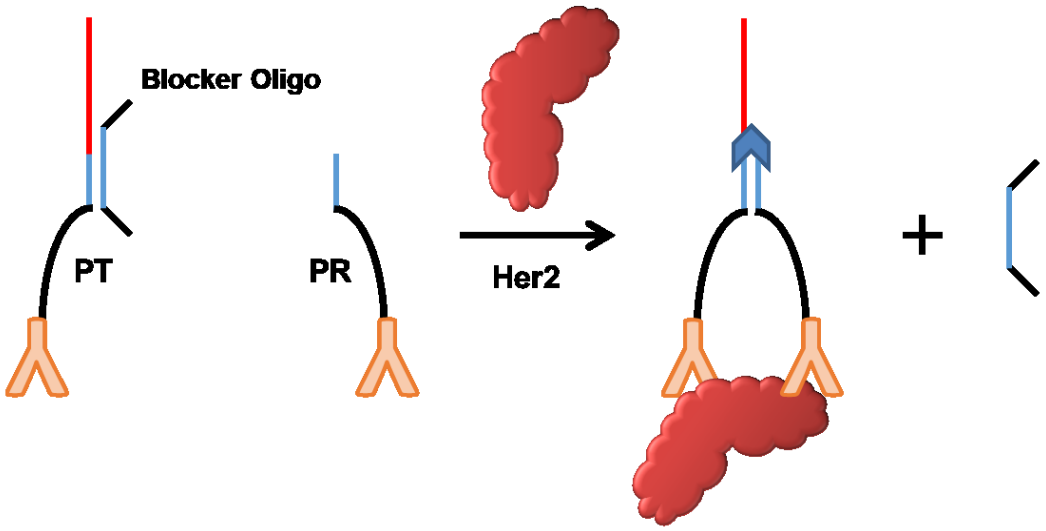

Figure 2.8 Schematic illustration of a blocking oligo. When probes are free in solution the blocking oligo anneals to the complementary region of **PT.** Upon target binding by both probes, the complementary region of **PR** displaces the blocking oligo and the reaction proceeds.

The blocker is designed to achieve a stable enough hybridization to prevent nonspecific interaction between probes but weak enough to be displaced when probes are bound to the target. Four blocking sequences were designed from 8 to 11 bases. Each blocker DNA has a 3-T sequence on each end. This prevents extension by polymerase as well as facilitates displacement by **PR6** when both probes are target bound.

Figure 2.9 shows that as the length of the blocker increases, both the target triggered and background signals decrease. The 8 base-blocker shows some decrease in background signal while maintaining high target triggered amplification. This demonstrates how a blocker can be used effectively to improve signal to background.

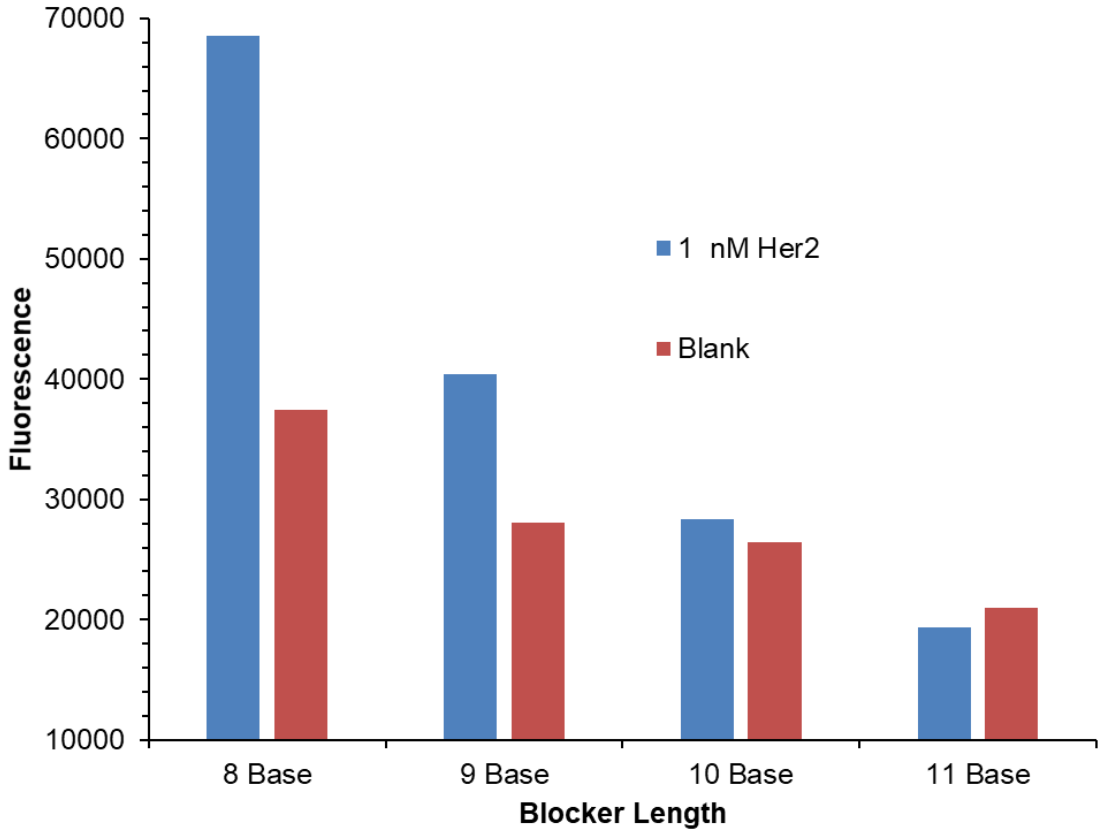

Figure 2.9 Effect of the length of blocking oligo in BISDA. Blocker lengths of 8, 9, 10, and 11 correspond to blocker sequences **B-8**, **B-9**, **B-10**, and **B-11**, respectively. Data shown is the mean of duplicate experiments.

2.3.4 Exponential amplification reaction (EXPAR)

Incorporation of exponential amplification can facilitate ultrasensitive detection of proteins.[116,132] Exponential amplification can enable much lower amounts of target to be

detected because it yields higher amounts of amplification products compared to linear amplification. Since displaced **T-28** from BISDA was designed to be the trigger oligo for EXPAR, incorporating exponential amplification with BISDA only requires the addition of **XT-28**. However, since EXPAR typically occurs at 55 °C, the ability of EXPAR to operate at 37 °C was tested before combining with BISDA.

Figure 2.10 shows two native PAGE images of EXPAR products after reacting for 30 min. Both Klenow LF and Klenow (exo-) were evaluated as the polymerase in EXPAR at 37 °C. Lane 5 in Figure 2.10A shows that Klenow LF can extend **T-28** along **XT-28**; however, it shows no excess trigger generated, indicating that Klenow LF has slow strand displacement activity. Figure 2.10B uses Klenow (exo-), which lacks the 3′→5′ exonuclease region found on the large fragment version of Klenow polymerase. Lanes 2-8 of Figure 2.10B show EXPAR products using Klenow (exo-) as polymerase with **T-28** starting concentrations from 2 pM to 1 μM. Not only is Klenow (exo-) able to extend **T-28** along the EXPAR template, but it also produces excess trigger, indicating that it has high strand displacement activity. Lane 1 shows the EXPAR reaction with a 200 nM starting trigger without NEase. The products are a mixture of fully extended template and single stranded template, indicating that the initial trigger oligos are extended along the template, but in the absence of NEase no additional triggers are generated to be amplified by other templates.

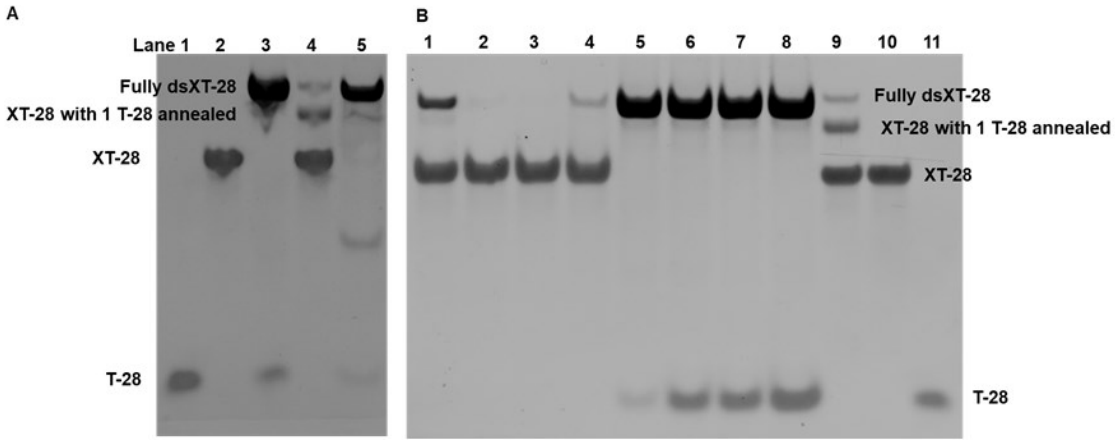

Figure 2.10 Native PAGE images of EXPAR products. (A) Lane 1 contained 2 μM **T-28**. Lane 2 contained 2 μM **XT-28**. Lane 3 contained 4 μM **T-28** and 2 μM **XT-28**. Lane 4 contained 200 nM **T-28** and 2 μM **XT-28**. Lane 5 contained 200 nM **T-28**, 2 μM **XT-28**, Klenow LF, and Nt.BbvCI. (B) Lane 1 contained 200 nM **T-28**, 2 μM **XT-28**, and Klenow (exo-). Lanes 2-8 contained EXPAR reactions using 2 μM **XT-28**, Klenow (exo-), and Nt.BbvCI and varying **T-28** concentrations. Lane 2 contained 2 pM **T-28**. Lane 3 contained 20 pM **T-28**. Lane 4 contained 200 pM **T-28**. Lane 5 contained 2 nM **T-28**. Lane 6 contained 20 nM **T-28**. Lane 7 contained 200 nM **T-28**. Lane 8 contained 1 μM **T-28**. Lane 9 contained 200 nM **T-28** and 2 μM **XT-28**. Lane 10 contained 2 μM **XT-28**. Lane 11 contained 1 μM **T-28**.

The amplified product detected in EXPAR is a double-stranded EXPAR template. The signal is generated using SYBR Green I (SG), which has increased fluorescence after binding to dsDNA.[133]. Similar to RT-PCR, high concentrations of trigger DNA generate a detectable fluorescence signal faster than lower concentrations. Therefore, a threshold fluorescence signal is set, and the time required to exceed the threshold value is used for

quantification. Figure 2.11 shows a typical EXPAR amplification profile for 100 pM of **T-28**, 200 nM positive control, reagent blank, and a negative control. 200 nM **T-28** is used as a positive control to generate fully ds**XT-28** and produces the maximum fluorescence signal. The negative control occurs in the absence of NEase and polymerase and shows baseline fluorescence with no amplification. The blank reaction contains no **T-28**, but background amplification occurs. Background amplification is common in EXPAR.

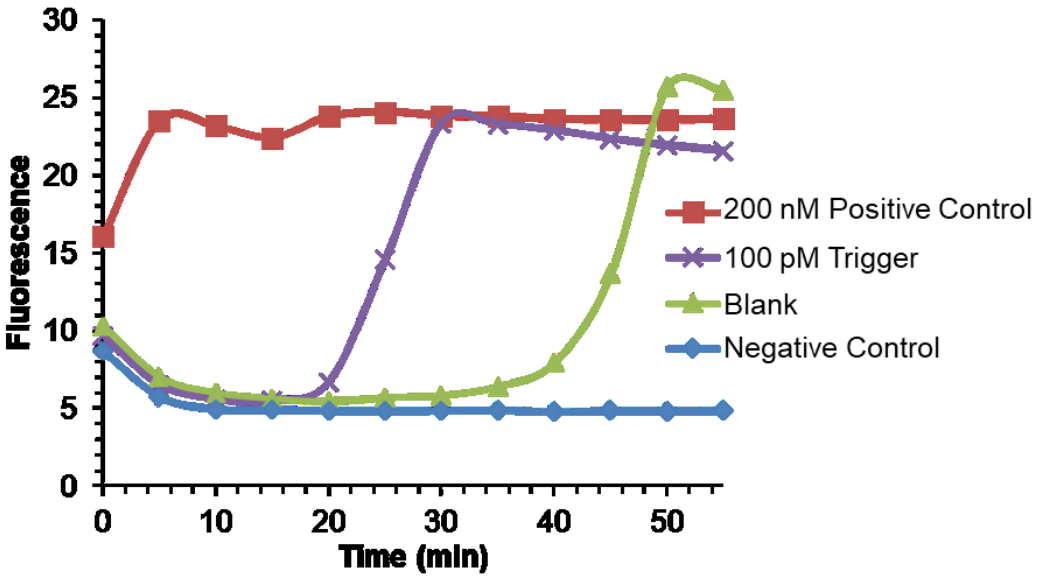

Figure 2.11 Real-time fluorescence monitoring of EXPAR reactions. The positive control uses 200 nM **T-28** and 100 nM **XT-28**. This produces a reaction where all templates are fully dsDNA, which yields the maximum fluorescence signal. The negative control (N.C.) lacks Klenow (exo-) and Nt.BbvCI; this represents the baseline fluorescence. Data shown is the mean of duplicate experiments.

Several reaction conditions were investigated in EXPAR to achieve the highest difference between target triggered amplification and background amplification. The length of trigger sequence in EXPAR can affect the amplification speed and the rate of background amplification. Ideally, the trigger sequence has a T_m that is near the reaction temperature.[60] This allows the trigger sequence to hybridize with EXPAR templates and be extended by polymerase but also to dissociate readily and be extended along additional templates. With normal EXPAR temperatures (~55 °C), this usually results in an approximately 20 nucleotide trigger. The amplified **T-28** sequence from BISDA is 28 nucleotides long: this length was chosen to be able to activate **FQ**. Five EXPAR templates and their corresponding trigger sequences were tested to determine the optimum length of trigger sequence in EXPAR.

Figure 2.12 shows the amplification profiles of each trigger sequence and the corresponding EXPAR template. Even though the T_m between **XT-28** and **T-28** is much higher than the reaction temperature, the strand displacement activity of Klenow (exo-) allows fast target specific amplification and shows the slowest background amplification of all lengths tested.

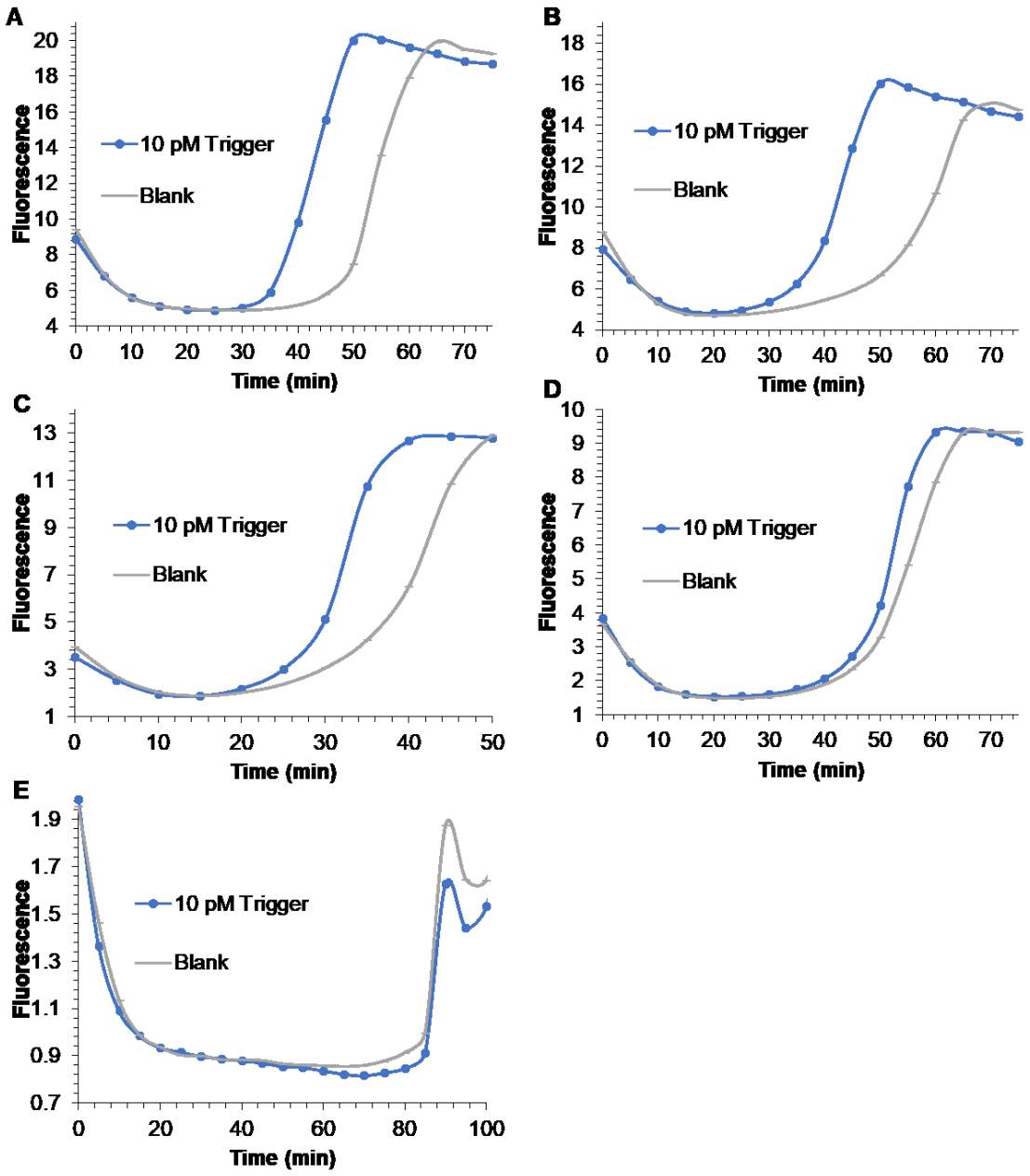

Figure 2.12 Evaluation of the trigger DNA length in EXPAR. Each solution contained the same reaction conditions but with varying trigger lengths and the corresponding EXPAR template. (A) **T-28** and **XT-28** (B) **T-19** and **XT-19** (C) **T-15** and **XT-15** (D) **T-11** and **XT-11** (E) **T-8** and **XT-8**. Data shown is the mean of duplicate experiments.

The concentration of EXPAR template can also affect amplification in EXPAR. Figure 2.13 shows parallel reactions with varying concentrations of **XT-28**. Higher concentrations of template resulted in faster amplification. This may be due to increased duplex stability with a higher concentration of DNA, which increases background amplification. Nonspecific background amplification seen in blank reactions occurs not only in blank reactions but also in target specific reactions. The time that background amplification occurs acts as a baseline, and target specific amplification is adding to background amplification. It is then reasonable that increasing template concentrations would increase reaction speed of both the blank and target specific amplification. A 100 nM template was chosen as the optimum concentration because amplification occurred in under 1 h and showed a larger difference between target triggered and blank amplification signals compared to a higher concentration of template.

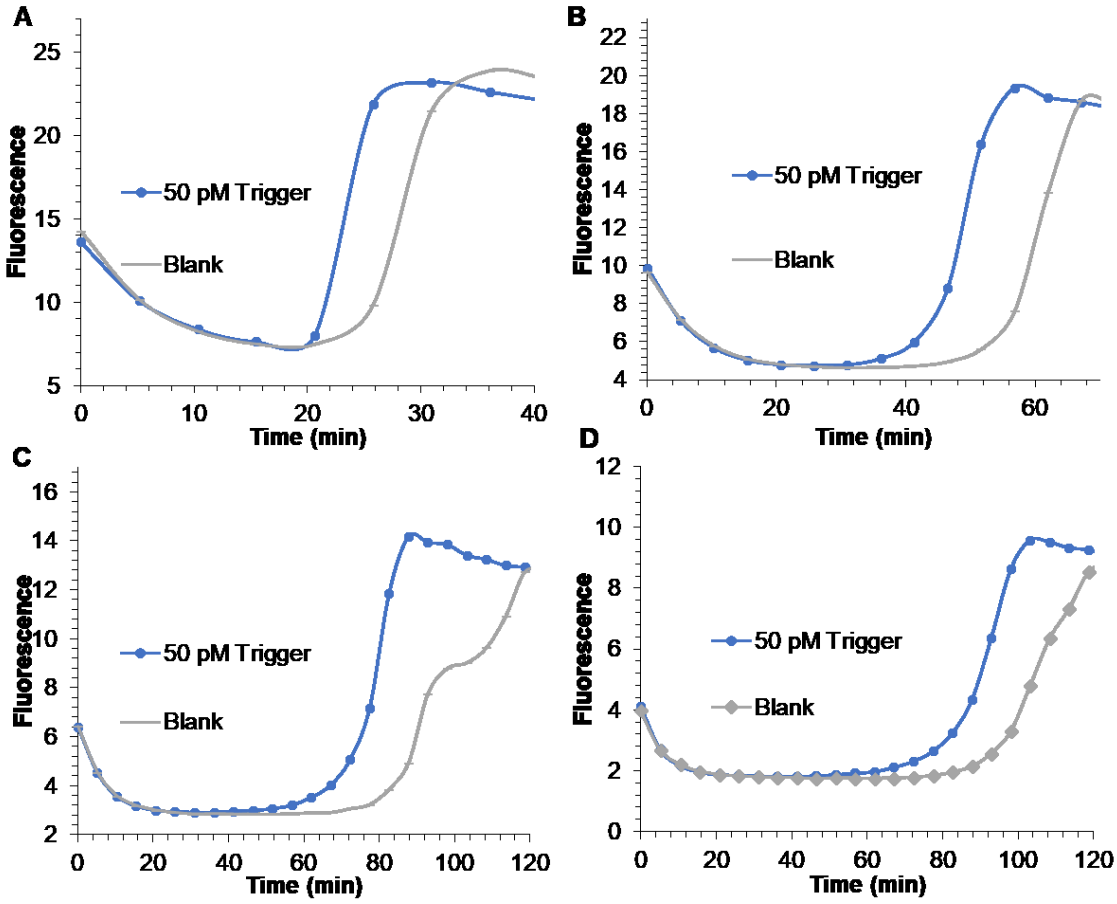

Figure 2.13 Effect of EXPAR template concentration on the signal and blank signals in EXPAR. Increasing concentrations of **XT-28** were used in parallel to determine the optimum concentration. (A) 200 nM **XT-28** (B) 100 nM **XT-28** (C) 50 nM **XT-28** (D) 25 nM **XT-28**. Data shown is the mean of duplicate experiments.

2.3.5 BISDA incorporating EXPAR

After confirming EXPAR functions at 37 °C, I combined EXPAR with BISDA. The NEase concentration was optimized first, using 500 pM streptavidin for the target signal. Sufficient NEase is required to generate nicked sites at a similar speed as polymerase

generates NEase recognitions sites. However, as Figure 2.14 shows, higher NEase concentrations increase background amplification. 0.2 U/µL Nt.BbvCI was chosen as the optimum concentration due to target specific amplification under 1 h and lower background signal compared to higher concentrations of NEase.

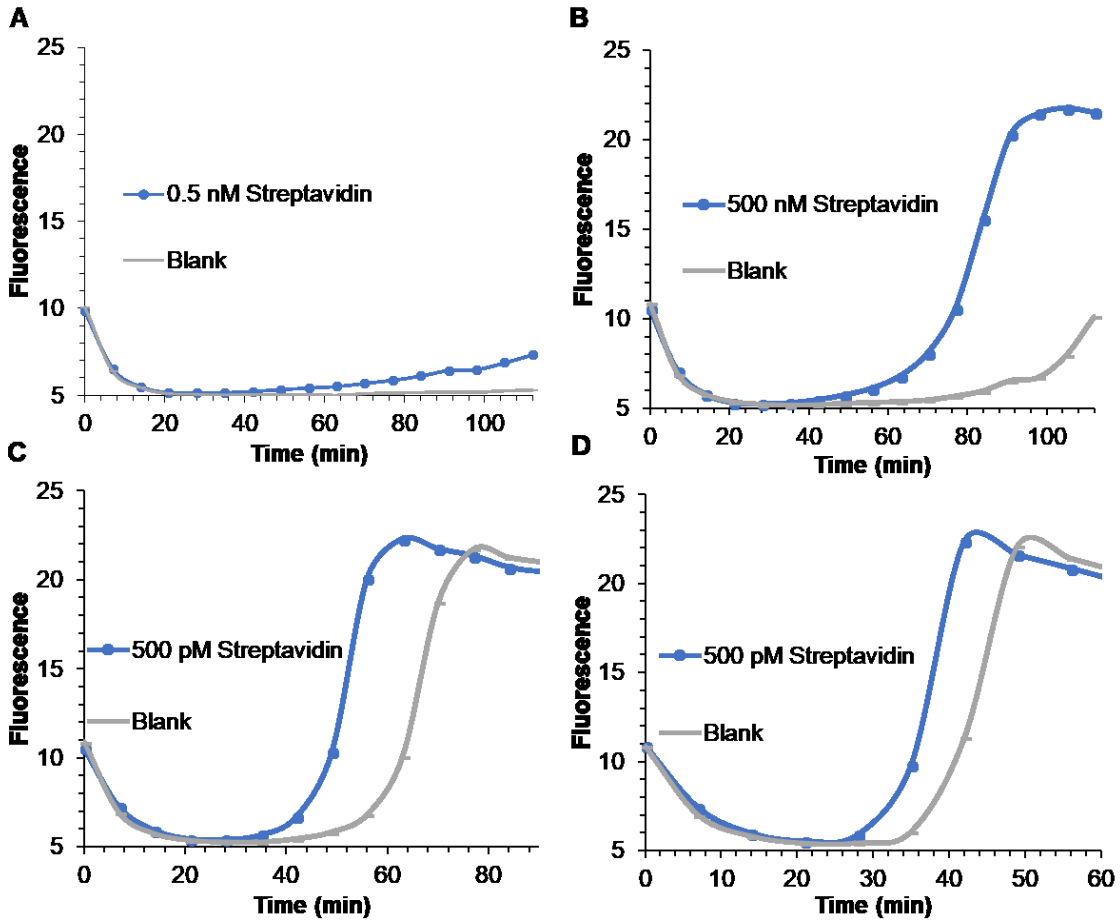

Figure 2.14 Effect of NEase concentration on the signal and blank reactions in BISDA–EXPAR. (A) 0.05 U/µL Nt.BbvCI (B) 0.1 U/µL Nt.BbvCI (C) 0.2 U/µL Nt.BbvCI (D) 0.4 U/µL Nt.BbvCI. Data shown is the mean of duplicate experiments.

The concentration of polymerase also was optimized by comparing concentrations from 0.05 U/µL to 0.2 U/µL. In Figure 2.15, the lowest background signal was achieved with 0.05 U/µL Klenow (exo-) and had comparable target specific signals to higher concentrations, therefore, 0.05 U/µL Klenow (exo-) was chosen as the optimum concentration.

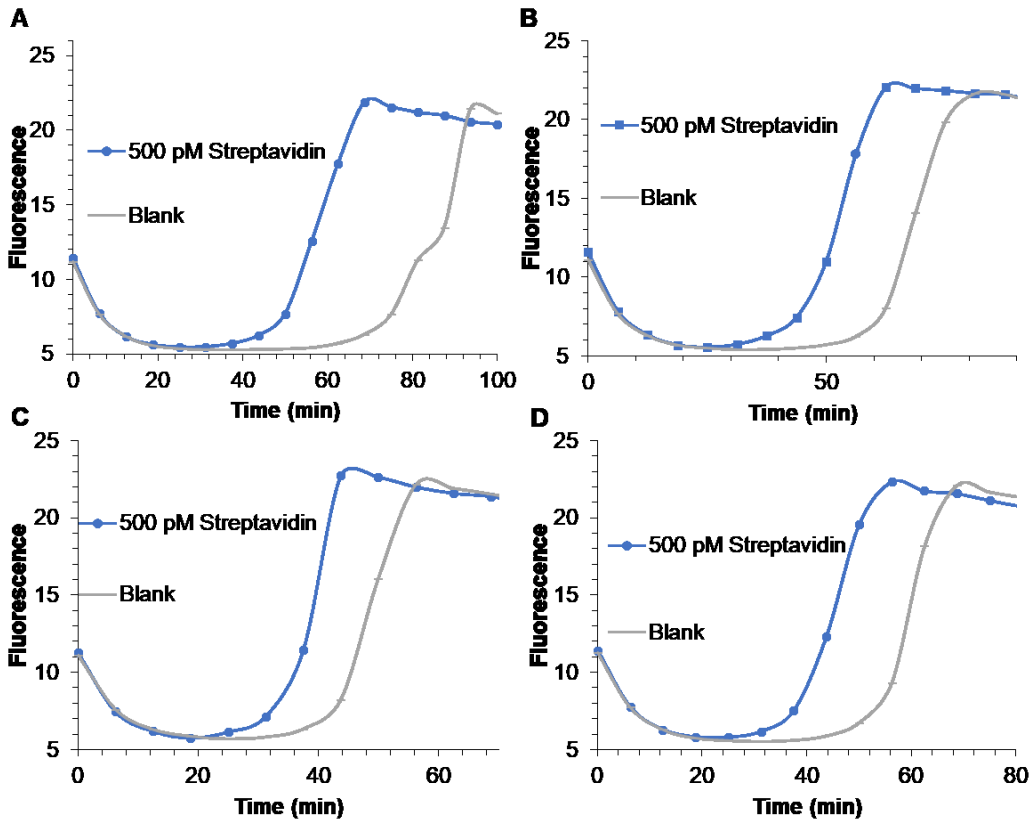

Figure 2.15 Effect of polymerase concentration on the signal and blank reactions in BISDA–EXPAR. (A) 0.05 U/µL Klenow (exo-) (B) 0.1 U/µL Klenow (exo-) (C) 0.2 U/µL Klenow (exo-) (D) 0.4 U/µL Klenow (exo-). Data shown is the mean of duplicate experiments.

Although the reaction parameters of BISDA and EXPAR were optimized both separately and together, background amplification remained high in BISDA–EXPAR. In principle, exponential amplification should improve the sensitivity and corresponding detection limits in BISDA–EXPAR. However, compared to BISDA, where 1 pM streptavidin could be detected, BISDA–EXPAR was unable to distinguish the 100 pM streptavidin from the blank (Figure 2.16). Although EXPAR does achieve exponential amplification, the high level of background that it introduces limits the overall BISDA–EXPAR reaction.

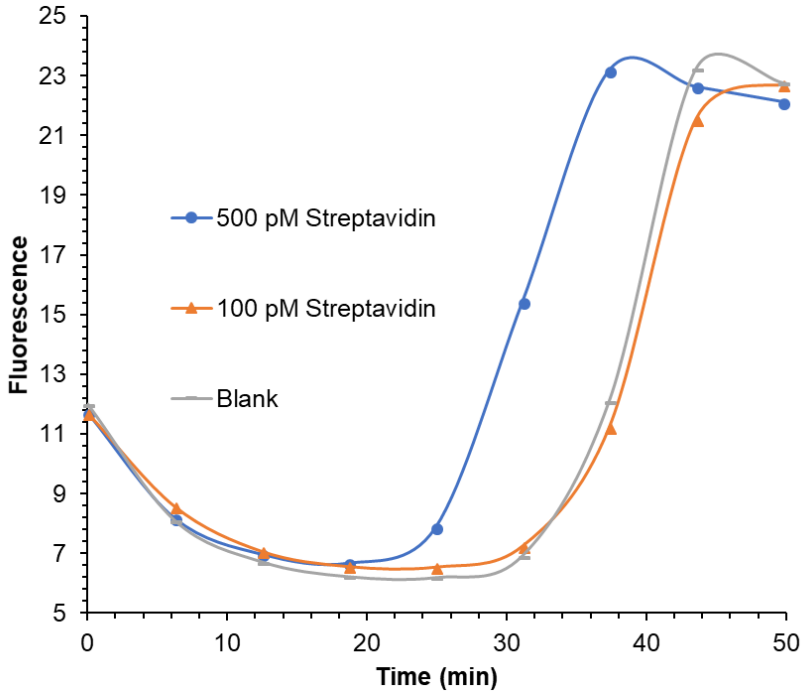

Figure 2.16 Signal response of BISDA–EXPAR with 500 pM and 100 pM streptavidin. Data shown is the mean of duplicate experiments.

Figure 2.17 shows the signal response of EXPAR from 10 pM to 1 nM of **T-28**. Operating at 37 °C, EXPAR can only detect 10 pM or higher of trigger DNA. I anticipated that the BISDA–EXPAR assay would have higher sensitivity than EXPAR alone since each target protein generates more than one trigger DNA to be amplified by EXPAR. However, the results show that coupling EXPAR with BISDA increases the detection limit of the system. This could be attributed to the extra probe DNA strands generating nonspecific amplification with EXPAR templates. This EXPAR system operates at a much lower temperature than EXPAR traditionally is used at, which required alternate polymerase and NEase enzymes that may not be as efficient as their higher temperature equivalents. Also, at lower temperatures, weak DNA–DNA interactions occur more frequently than at higher temperatures, which could lead to background amplification.

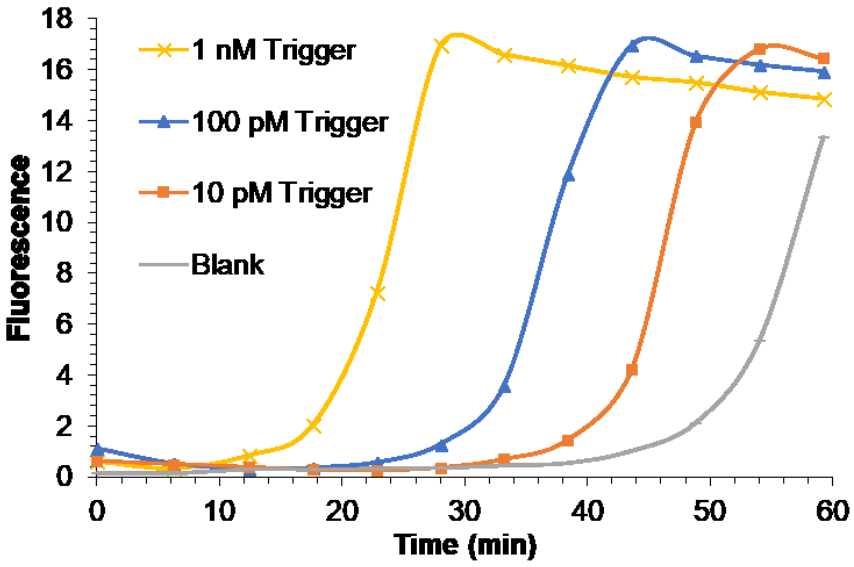

Figure 2.17 Signal response of EXPAR with varying **T-28** concentrations. Data shown is the mean of duplicate experiments.

2.3.6 Two-stage reaction combining BISDA with EXPAR

To improve the detection limit of the combined BISDA–EXPAR system I designed a modified strategy where an initial target binding and probe extension phase occurs at 37 °C, followed by nicking, strand displacement, and EXPAR at 55 °C. The goal of this 2-stage system is to incorporate protein binding at 37 °C, the optimum temperature for many antibodies, but make use of improved EXPAR performance at 55 °C. This design requires the polymerase to operate at both 37 °C and 55 °C. I take advantage of Bst 2.0 polymerase, which exhibits activity at a broad range of temperatures: its optimum temperature is 60 °C; however, it remains 10–15% active at 37 °C. This allows Bst 2.0 to extend target bound probes at 37 °C and have activity at 55 °C for strand displacement and EXPAR.

In BISDA and BISDA–EXPAR, amplification occurs at 37 °C, where the short complementary region between probes is sufficient to keep bound probes together in a duplex form as the reaction cycles. In 2-stage BISDA–EXPAR probe binding occurs at 37 °C and amplification at 55 °C. The probes need to be constructed so that even if affinity ligands release the target protein at 55 °C, probes that were initially bound to target molecules remain hybridized together. Also, even if affinity ligands remain bound to the target at 55 °C, the increase in temperature could cause the probes to separate, which would stop the linear amplification component.

Probe **2PT** (Figure 2.3) is designed similar to **PT** but includes an extra stabilizing sequence between the probe complementary region and the NEase recognition sequence. This added region stabilizes the duplex formed between the probes after extension of **2PR** by polymerase at 37 °C. After extension by polymerase there are 42 bases complementary between probes. Increasing the reaction temperature to 55 °C allows nicking to occur,

leaving a 20 base complementary length between **2PT** and **2PR**. After initial extension at 37 °C, 2-stage BISDA–EXPAR proceeds in the same manner as BISDA–EXPAR but at an elevated temperature of 55 °C.

The effect that the length of the complementary region between **2PR** and **2PT** had on amplification was investigated. Based on previous results from Section 2.3.1, only 6 and 7 base lengths were used since 8 bases produced a very high background. Figure 2.18 shows that 6 and 7 base complementary regions have similar target triggered signals. However, the 7 base length complementary region has a higher background signal than the 6 base length; therefore, a 6 base complementary region was used for further experiments.

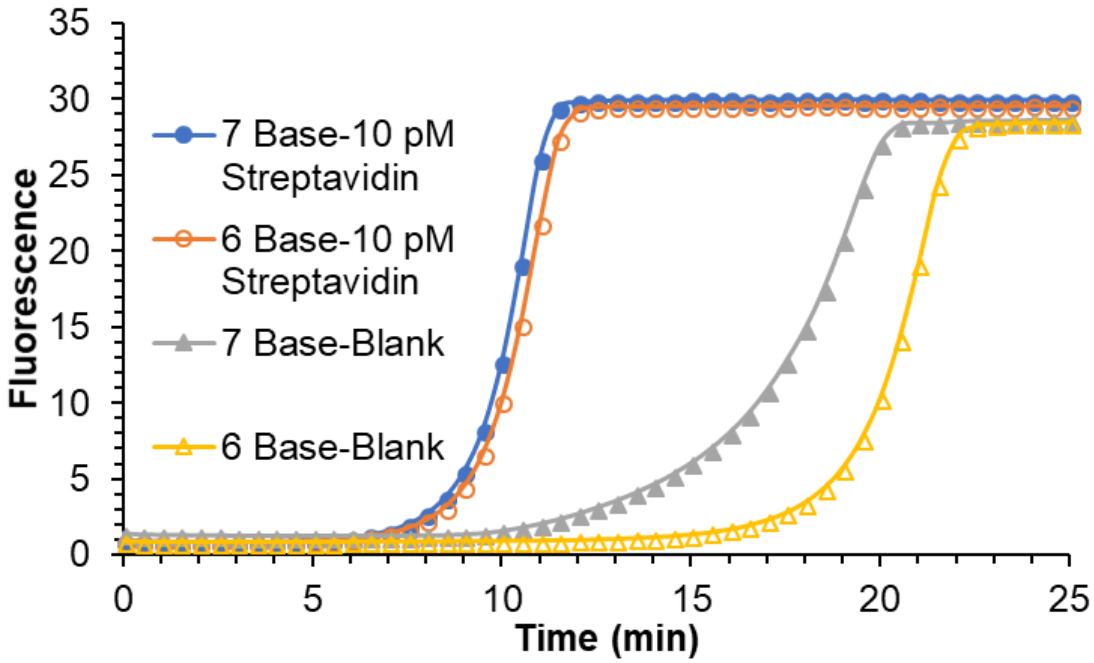

Figure 2.18 Comparison of a 6 and 7 base complementary length between probes in 2-stage BISDSA–EXPAR. 6 Base uses **2PT** and **2PR6** probes and 7 Base uses **2PT** and **2PR7** probes. Data shown is the mean of triplicate experiments.

Next, the effect of probe concentration on amplification was investigated. Figure 2.19 shows probe concentrations ranging from 500 to 50 pM. In this range of probe concentrations, there was little effect on target specific or background amplification. One hundred pM probes were used for further experiments because, in principle, a lower concentration of probes leads to a lower background amplification. A 50 pM probe concentration was not chosen because for two probes to be able to bind a single target molecule simultaneously, the probe concentration must be in excess; 50 pM probes would limit the dynamic range of the assay to <50 pM target.

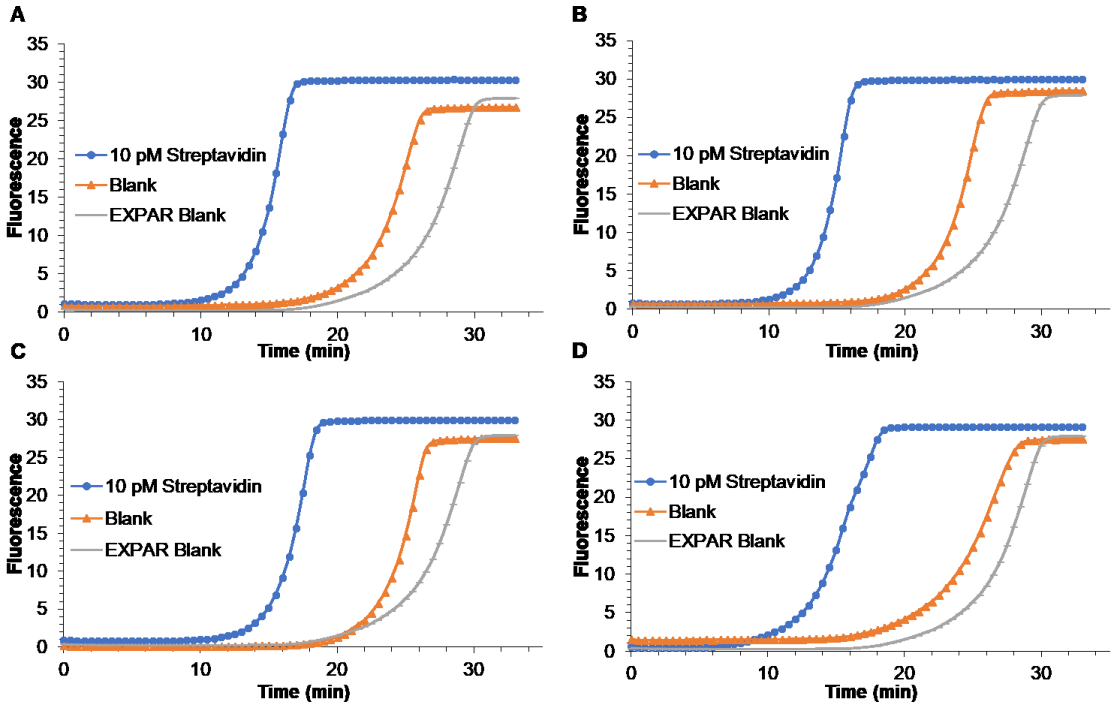

Figure 2.19 Effect of probe concentration on amplification in 2-stage BISDA–EXPAR. Blank reactions contain no streptavidin. EXPAR blanks contain no streptavidin and no probes, only EXPAR templates. (A) 500 pM probes. (B) 250 pM probes. (C) 100 pM probes. (D) 50 pM probes. Data shown is the mean of triplicate experiments.

The concentration of EXPAR template also was investigated (Figure 2.20). Similar to findings in Section 2.3.2, a lower concentration of **XT-55** reduced nonspecific amplification. Twenty-five nM **XT-55** was used for further experiments because it showed lower background amplification compared to higher concentrations. Twenty-five nM **XT-55** showed a small decrease in target-specific amplification speed compared to 100 nM and 50 nM XT, but lowering the concentration of **XT-55** to 10 nM slowed the target specific amplification by several minutes.

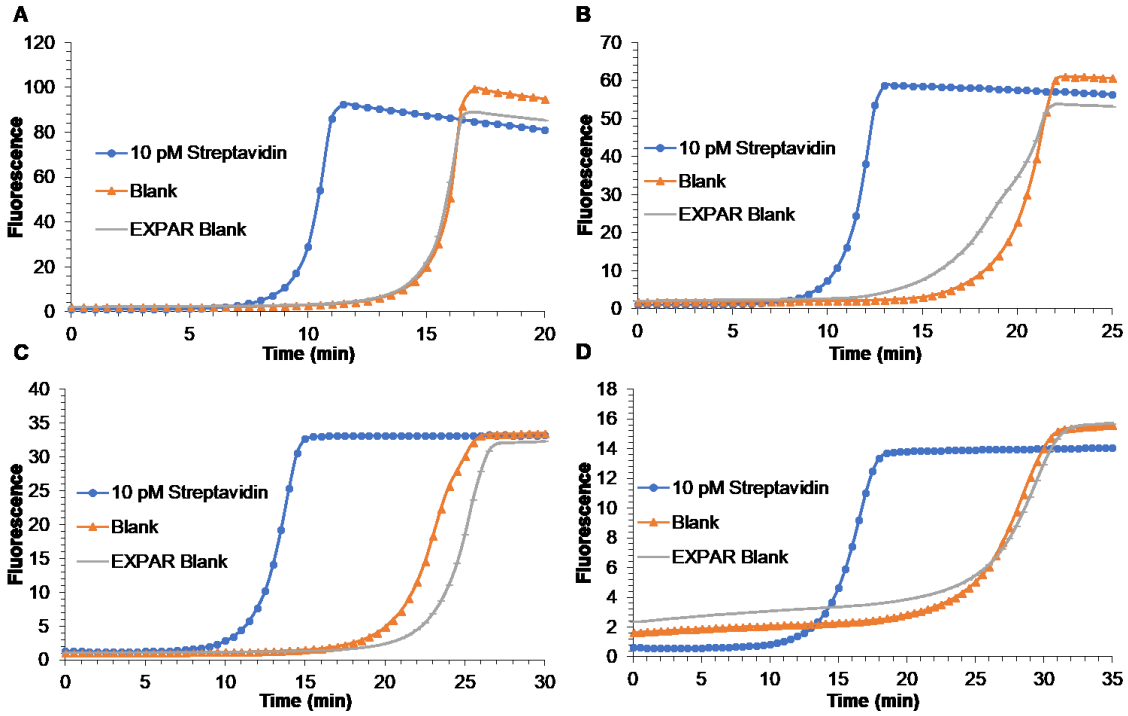

Figure 2.20 Effect of EXPAR template concentration in 2-stage BISDA–EXPAR. 100 pM probes were used. Blank reactions contain no streptavidin. EXPAR blanks contain no streptavidin and no probes. (A) 100 nM **XT-55**. (B) 50 nM **XT-55**. (C) 25 nM **XT-55**. (D) 10 nM **XT-55**. Data shown is the mean of triplicate experiments.

Magnesium ion concentration is another critical paramer because it affects the stability of DNA hybridization and is used as the cofactor by polymerase and NEase. Higher concentrations of Mg^{2+} will stabilize the complementary region between probes and lead to faster enzyme kinetics, while lower concentrations of Mg^{2+} will reduce background by destabilizing nonspecific probe hybridization. Figure 2.21 shows the amplification profiles of 2-stage BISDA–EXPAR with four different Mg^{2+} concentrations. The lower concentrations of Mg^{2+} show slower amplification speed but a greater difference between target specific amplification and nonspecific background amplification. Therefore, 4 mM Mg^{2+} was chosen as the optimum Mg^{2+} concentration because of slower background amplification.

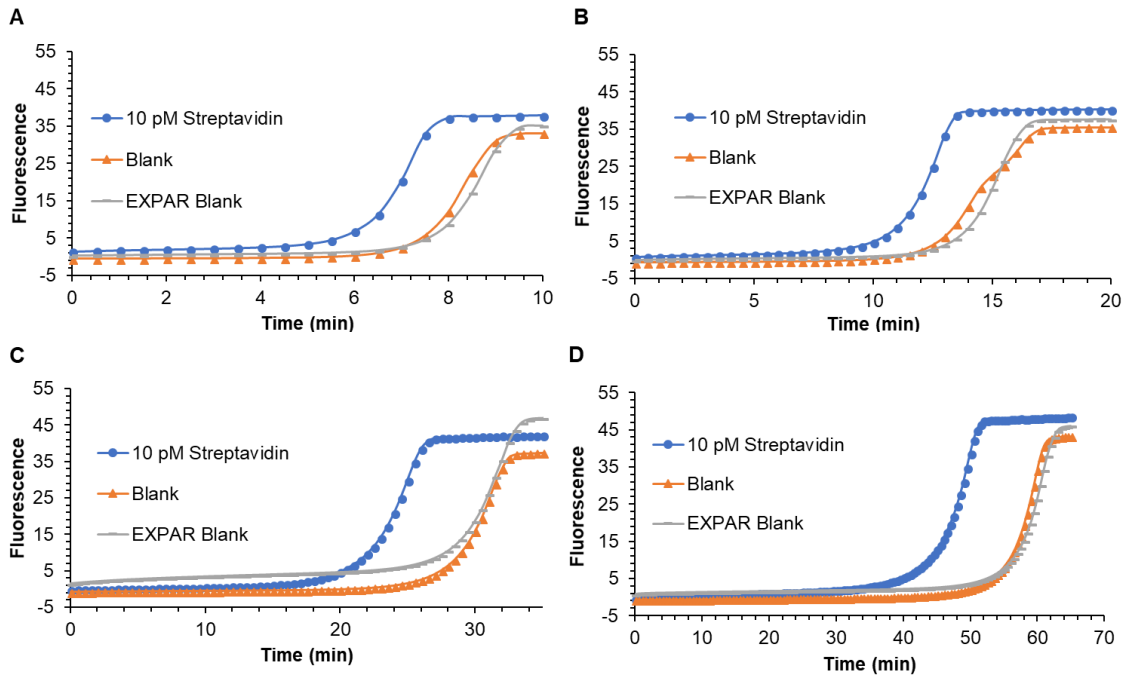

Figure 2.21 Effect of Mg2+ concentration on amplification in 2-stage BISDA–EXPAR. Blank reactions contain no streptavidin. EXPAR blanks contain no streptavidin and no probes. (A) 10 mM Mg^{2+} (B) 8 mM Mg^{2+} (C) 6 mM Mg^{2+} (D) 4 mM Mg^{2+}. Data shown is the mean of triplicate experiments.

To estimate the current performance of the system I ran several concentrations of streptavidin with the optimized conditions. Figure 2.22 shows the amplification profiles triggered by streptavidin concentrations from 1 pM to 1 nM. The blank reaction has a comparable signal with 1 pM of streptavidin. Also, the 100 pM streptavidin curve is faster than the 1 nM curve. This is reasonable since only 100 pM of each probe is used, so the reaction with 1 nM streptavidin contains many streptavidin molecules with only 1 bound probe, which generates no signal.

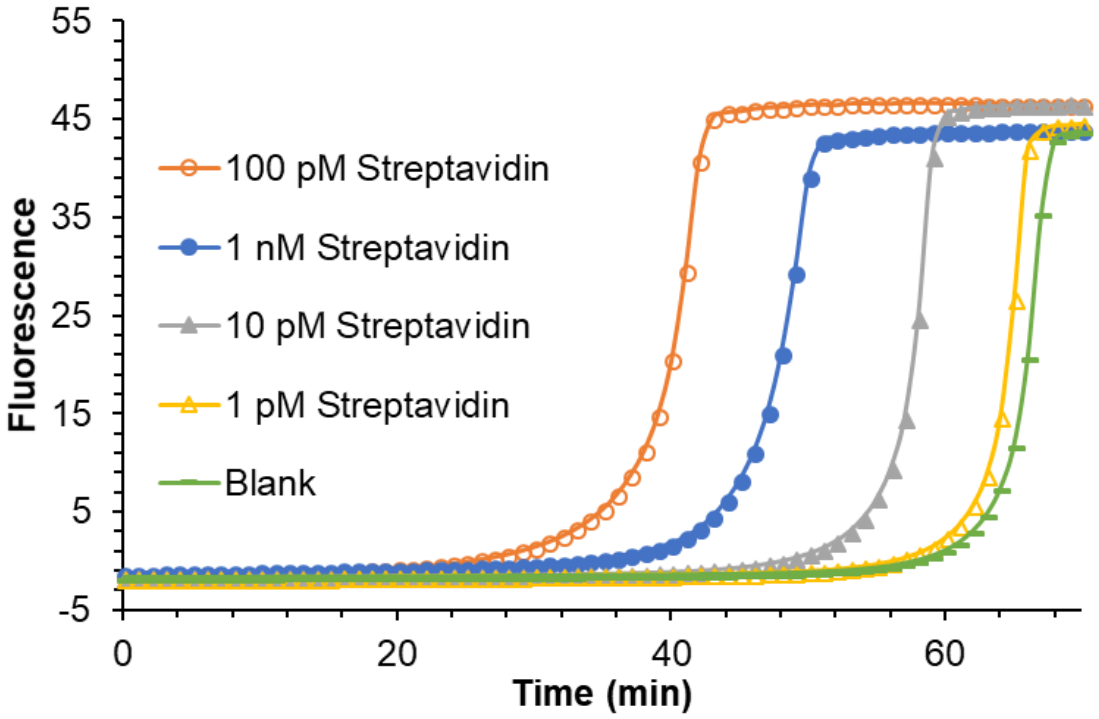

Figure 2.22 Signal response in 2-stage BISDA–EXPAR to varying concentrations of streptavidin target (1 nM–1 pM and blank). Data shown is the mean of triplicate experiments.

2.4 Conclusions

Three protein assays based on enzymatic strand displacement amplification networks have been developed. Each design uses protein recognition by affinity ligands to trigger amplification of a DNA sequence. The first linear BISDA system is capable of detecting as low as 1 pM of target streptavidin and has the potential to be used for the detection of other protein targets by changing the affinity ligands, shown by the detection of Her2. The second system, BISDA–EXPAR, used two amplification systems working in tandem to achieve exponential amplification of DNA from a streptavidin target. The feasibility of BISDA–EXPAR has been demonstrated, but with the current optimizations, the detection limits are high (>10 pM) due to the intrinsically high background amplification from the EXPAR reaction. The third amplification system is 2-stage BISDA–EXPAR that utilizes the unique ability of Bst 2.0 polymerase to be active at a wide range of temperatures. This allows an initial hybridization and extension phase to occur at 37 °C, followed by an increase to 55 °C for amplification to occur. Two-stage BISDA–EXPAR also is limited by a high EXPAR background. In principle, if the background signal from EXPAR is reduced, both systems using EXPAR would be capable of sub-pM detection limits due to the increased amplification compared to the linear BISDA system. All designs have the potential to be used in resource limited settings as the procedure is simple, and a simple heating block and fluorescence reader are the only equipment required.

Chapter 3: Investigations into Background from Template–Template Interactions in the Exponential Amplification Reaction of DNA

3.1 Introduction

Exponential amplification of nucleic acids is a powerful strategy for signal amplification in new assays that enables the detection of pathogens, genetic markers, microRNAs, and many other biological targets.[22,134,135] Recently, Exponential Amplification Reaction (EXPAR) has seen increased usage in both direct nucleic acid detection and as a signal amplifier in new assay designs.[60,136,137] EXPAR has been adapted for the detection of a wide range of targets, such as miRNA,[138–146] DNA,[147–150] proteins,[151–155] enzyme activity,[156] and metals.[157] The EXPAR procedure is simple, requiring only the mixing of all reagents in a single vial (or plate well), and allowing the reaction to take place at a constant temperature, typically 55–60 °C.

EXPAR displays high amplification efficiency (10^6–10^8) in a short time (<30 min), which makes it appealing for generating an amplified signal. EXPAR uses a DNA template and two enzymatic reactions to achieve exponential amplification of a target sequence (Figure 3.1). The EXPAR template is designed to contain repeat regions (X′-X′) that are complementary to the target sequence (X) and separated by a short nicking enzyme (NEase) recognition sequence. Once hybridized to the template, the target DNA is extended along the template by a DNA polymerase. After extension, the NEase cleaves the extended target DNA strand, generating a nick. DNA polymerase can extend the 3′-end of the nicked site, which simultaneously displaces the newly synthesized strand. The displaced strand then hybridizes with another template molecule, initiating new amplification, while amplification of the target DNA from the initial target–template

complex continues. Thus, each reaction cycle produces two copies of the target DNA from a single target molecule, achieving exponential amplification.

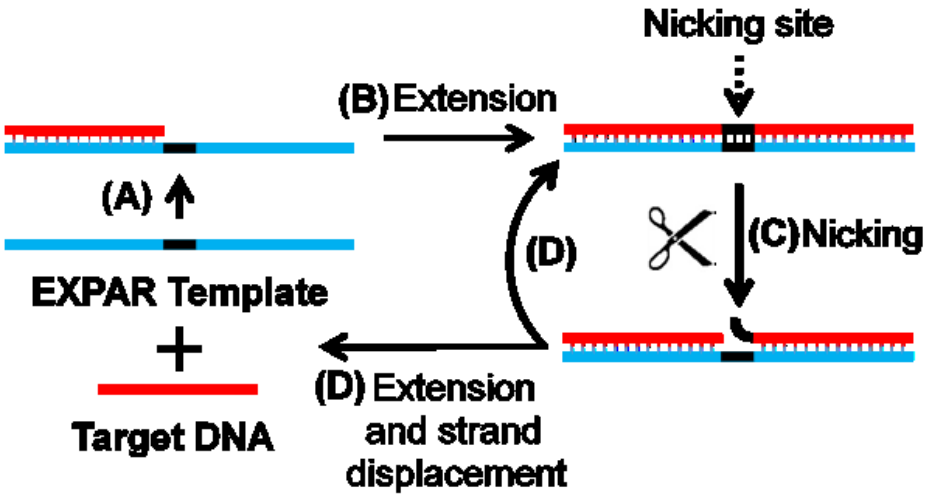

Figure 3.1 Schematic illustration of the EXPAR system. **(A)** Target DNA hybridizes with the EXPAR template. **(B)** DNA polymerase extends the target strand along the EXPAR template, generating the nicking enzyme recognition site. **(C)** Nicking enzyme cleaves the phosphate backbone of the top strand, creating a nicked site in the DNA. **(D)** DNA polymerase extends the 3′-end at the nicked site while simultaneously displacing the previously synthesized DNA strand. The nicking recognition site is regenerated and a new target DNA strand is generated, which can undergo amplification with another EXPAR template.

A major limitation of EXPAR is the presence of nonspecific background amplification.[158] Although background amplification is observed in all EXPAR assays, it is highly variable, resulting in detection limits varying from pM[148] to aM.[142,144] Some variability in background amplification may be attributed to different assay designs and

a user's technical skills, but additional factors must be present to account for the variability of six orders of magnitude. Niemz and coworkers reported that the products of background amplification were specific sequences of the EXPAR template, indicating that the EXPAR template plays a critical role in generating background amplification.[158] The involvement of EXPAR templates in background amplification is supported further by reports that the amount of background amplification varies with different template sequences.[159] Additionally, background amplification is associated with GA-rich regions of the template, which may promote background amplification because of stronger affinity between polymerase and purine oligonucleotides.[159] Due to the X′-X′ sequence of the EXPAR template, once background amplification is triggered, the displaced ssDNA (X) is identical to the target DNA (X) and amplification proceeds as a normal EXPAR amplification reaction. Thus, it is thought that background amplification is generated through nonspecific amplification of the EXPAR template in the absence of the target strand.[149] While the involvement of the EXPAR template in background amplification is well established, the mechanism that triggers background amplification remains unknown. A thorough understanding of what triggers background amplification is required to prevent background amplification and improve the utility of EXPAR.

We hypothesize that EXPAR background amplification is triggered by transient template–template hybridization that results in a 3′-end extension of EXPAR templates by DNA polymerase. Transient interactions capable of generating 3′-end extensions of EXPAR templates are illustrated in Figure 3.2. These include self-priming between two template strands, similar to primer–dimer formation in the polymerase chain reaction

(PCR), or the formation of a hairpin loop within a single template strand. To prevent 3′-end extensions by polymerase, the 3′-ends of EXPAR templates are blocked chemically with phosphate, with a blocking efficiency of ~99%.[160] Although a 99% blocking efficiency is excellent, the remaining 1% of unblocked template is still much higher than the concentration of target that needs to be amplified (typically aM). Because the concentration of the EXPAR template is typically tens to hundreds of nM, 1% of unblocked template DNA strands are approximately 10^9-fold more abundant than the target DNA strands (aM). Thus, only 1 in 10^9 of unblocked templates extended by DNA polymerase would generate a background equivalent to the signal generated by an aM target. Recognizing that chemically blocking the 3′-end nucleotide of templates cannot achieve 100% reaction efficiency, we focused on the transient hybridizations between templates.

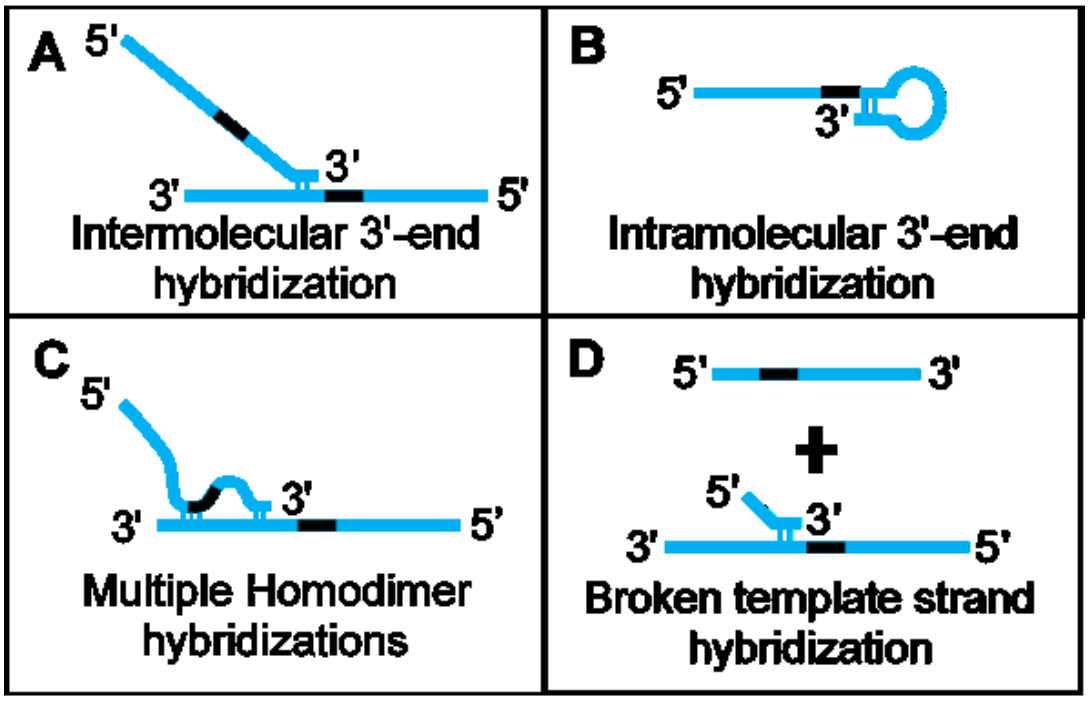

Figure 3.2 Schematic illustration of transient template hybridizations able to be extended by DNA polymerase to trigger background amplification. (A) Hybridization at the 3′-end between two templates. (B) Hairpin formation on the 3′-end of a single template. (C) Transient interactions along the whole template sequence, leading to higher incidences of 3′-end hybridization. (D) Small percentage of hydrolyzed templates resulting in unblocked 3′-ends.

The objectives of this chapter are to (i) examine various intra- and inter- DNA template interactions that result in the generation of EXPAR background, and (ii) minimize the source of background by blocking or weakening these interactions between templates. We investigated template–template hybridization by using several blocking schemes designed to probe each specific template interaction. By comparing blocked and

unblocked EXPAR reactions, we evaluated the contribution of each type of interaction to the overall background. We employed two main blocking strategies: sequence-specific blocking of the 3′-end of templates (Figure 3.3A and B) and sequence-independent blocking of the entire template (Figure 3.3C). Specifically blocking the 3′-end allowed evaluation of the ability of DNA polymerase to extend transient interactions at the 3′-end. Sequence-independent blocking of the entire EXPAR template allowed evaluation of background triggered by interactions along the entire length of the template strand, in addition to the 3′-end specific interactions.

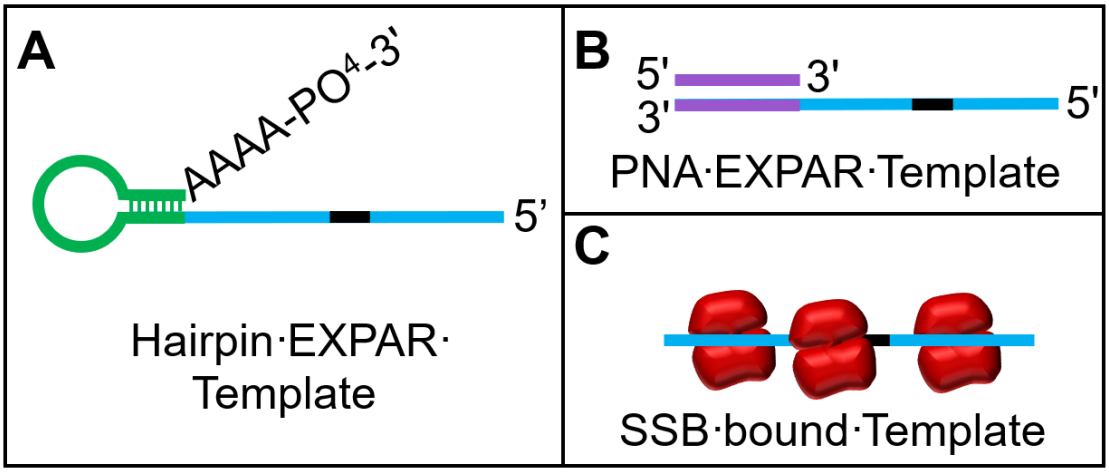

Figure 3.3 Three design approaches to reduce the proposed template interactions that generate background amplification. (A) Hairpin EXPAR template contains a stable 3′-hairpin with a poly-A tail. (B) PNA EXPAR template contains an extended 3′ region to allow PNA binding and blocking of nonspecific 3′-end template hybridizations. (C) SSB binds to single stranded EXPAR templates independent of the sequence to prevent weak template-template hybridizations.

3.2 Experimental

3.2.1 Chemicals and materials

All oligonucleotides were synthesized and HPLC purified by Integrated DNA Technologies Inc. (Coralville, IA). Their sequences and modifications are listed in Table 3.1. *Bst* 2.0 polymerase (8 U/μL) and Nt.BstNBI nicking enzyme (10 U/μL) were both from New England Biolabs (Whitby, ON, Canada). SYBR Green I (10 000X), dNTPs (10 mM mix), and Rox reference dye (Rox) were from Life Technologies (Burlington, ON, Canada). *E. coli* single stranded binding protein (SSB) (59.1 μM), Tris-hydrochloride (Tris-HCl), magnesium chloride ($MgCl_2$), sodium chloride (NaCl), dimethyl sulfoxide (DMSO), glycerol, phosphate buffered saline (PBS, 10X), and bovine serum albumin (BSA, >98%) were from Sigma-Aldrich (Oakville, ON, Canada). The peptide nucleic acid was from PNA Bio (Thousand Oaks, CA). Nanopure H_2O (>18MΩ), purified by an Ultrapure Milli-Q water system, was used for all experiments.

Table 3.1 DNA sequences and modifications for EXPAR

Target DNA	**5′**-T GAG GTA GTA GGT TGT ATA GTT-**3′**
EXPAR Template	**5′**-AAC TAT ACA ACC TAC TAC CTC ATT CAG ACT CAA ACT ATA CAA CCT ACT ACC TCA A-**PO_4-3′**
Hairpin EXPAR Template	5′-AAC TAT ACA ACC TAC TAC CTC ATT CAG ACT CAA ACT ATA CAA CCT ACT ACC TCA AAG CAG CAC CAA AAA GGT GCT GCA AAA-**PO_4**-3′
PNA EXPAR Template	**5′**-AAC TAT ACA ACC TAC TAC CTC ATT CAG ACT CAA ACT ATA CAA CCT ACT ACC TCA TCG ACA GCT ACG GAC TCT-PO_4-**3′**
PNA blocker	**N-Acetyl**-TT A GAG TCC GTA GCT GTC G-**C**
Sequences in blue are complementary to the red target sequence. The underlined sequence is the NEase recognition sequence. The green sequence corresponds to the hairpin loop region. The purple sequence of the PNA EXPAR template is complementary to the purple PNA blocker sequence.	

3.2.2 EXPAR templates

All EXPAR templates were synthesized with phosphate modified 3′-ends. The phosphate at the 3'-end prevents the template from being extended by a DNA polymerase. The standard EXPAR template and target DNA were resuspended in nanopure water and subsequently diluted with 10 mM Tris buffer (pH 7.4) supplemented with 20 mM NaCl and 1 mg/mL BSA. The hairpin EXPAR template, PNA EXPAR template, and PNA were

dissolved in 1X PBS buffer at pH 7.9 and further diluted using 10 mM Tris buffer (pH 7.4 at 25 °C) supplemented with 20 mM NaCl and 1 mg/mL BSA.

The hairpin template was annealed by heating to 95 ºC for 10 min followed by cooling to 25 ºC over 45 min, ensuring that the 3′-end of the template was in a hairpin conformation. Then, the hairpin template was substituted for the standard template in the EXPAR reaction mixture (Mix A).

The PNA blocked template was prepared by mixing PNA and the PNA EXPAR template in varying concentration ratios and annealed by heating to 95 ºC for 10 minutes, followed by cooling to 25 ºC over 45 min. These procedures enabled the PNA to hybridize with the template at the 3′-end. The PNA-template hybrid mixture then replaced the standard template in the EXPAR reaction solution (Mix A).

3.2.3 EXPAR Reaction

Reagents for the EXPAR reaction and detection of products were prepared in two vials, Mix A and Mix B. Mix A consisted of EXPAR template, dNTPs, BSA, blocking reagent (details below), and target. Mix B consisted of *Bst*2.0, Nt.BstNBI, reaction buffer, SYBR Green I, and ROX. Each mixture solution was prepared separately on ice. Enzymes were added to Mix B immediately before combining 10 µL of each mixture on ice. Final reaction conditions were 25 nM EXPAR template, 250 mM dNTPs, 0.5X SYBR Green I, 2.5% ROX, 0.4 Units/µL *Bst2.0*, 0.5 Units/µL Nt.BstNBI, and 1X Tris buffer (55 mM Tris-HCl, 110 mM NaCl, 8 mM $MgCl_2$, 15% glycerol, 0.55 mg/mL BSA, pH = 7.4). The blocking component (PNA, SSB, DMSO, or glycerol) was present in the final reaction mixture at varying concentrations as needed. For isothermal reaction and detection, the

final reaction solution was transferred to an Applied Biosystems StepOnePlus real-time PCR system at 55 ºC, and fluorescence was monitored at 30 s intervals.

SSB was diluted to working concentrations with a 10 mM Tris, 20 mM NaCl, and 1 mg/mL BSA buffer (pH 7.4) before being added to Mix A. This solution was incubated on ice for 15 min before it was combined with Mix B. For comparison, glycerol and DMSO also were used to weaken nonspecific template interactions. They were added directly to Mix A before Mix A and Mix B were combined.

For testing the nicking enzyme storage buffer, an aliquot of stock Nt.BstNBI was heat-inactivated at 90 °C for 30 min. The heat inactivated aliquot of Nt.BstNBI was cooled to room temperature and added to Mix A to account for the effects of Nt.BstNBI storage buffer without increasing the amount of Nt.BstNBI.

3.3 Results and Discussion

3.3.1 Sequence-specific blocking of the template at the 3′-end

We first studied the contribution of the 3′-end template hybridization to triggering background amplification and tested options of blocking multiple nucleotides at the 3′-end of the EXPAR template with complementary nucleic acid strands. We reasoned that hybridization of the blocking complementary nucleic acid strands with the 3′-end of EXPAR templates would weaken the interactions between templates at the 3′-end and reduce the background. Therefore, we designed and tested two approaches, using a 3′-hairpin loop and a peptide nucleic acid (PNA) to block the 3′-end of EXPAR templates. The hairpin loop at the 3′-end of an EXPAR template was designed to block transient duplex formation between two template strands at the 3′-end (Figure 3.3A). The PNA was

designed to hybridize to the 3′-end of EXPAR templates and block the 3′-end duplex interactions as well as 3′-end secondary structures on a single template strand (Figure 3.3B).

The goal of incorporating a DNA hairpin sequence on the 3′-end of the EXPAR template (Figure 3.3A) was to block transient homodimer hybridization between templates. The hairpin has an estimated T_m of 75 °C (IDT OligoAnalyzer 3.1), which is stable under the EXPAR reaction conditions (55 °C.) The hairpin essentially locks the 3′-end onto its own template sequence, limiting intermolecular hybridization with other template molecules in solution. To avoid introducing background, as would occur in the scenario of Figure 3.2B, we incorporated a non-complementary poly-A nucleotide overhang on the 3′-end of the hairpin that cannot pair with the template (Figure 3.3A).

The hairpin template design was compared with the standard template design by performing EXPAR amplification of a 1 pM target and blank. Figure 3.4 shows that there was no difference between the 1 pM target and the blank when the modified hairpin template was used for EXPAR. Incorporating a 3′-hairpin on the template did not decrease the background amplification. Although a poly-A overhang was incorporated after the 3′-hairpin to prevent intramolecular extension, this strategy was unsuccessful in preventing a 3′-extension by DNA polymerase. We reason that the hairpin forced the 3′-poly-A sequence into close proximity with the template, enabling extension by DNA polymerase, which triggered background amplification. Even though the hairpin template was blocked with phosphate at the 3’-end, high background amplification remained.

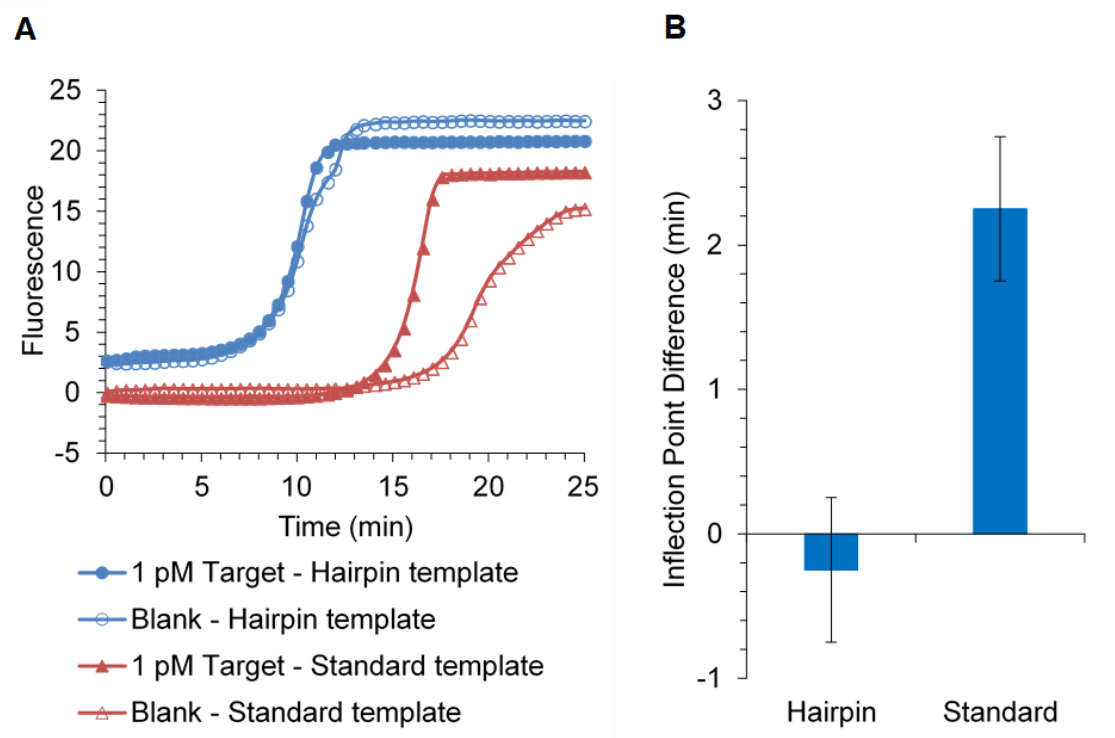

Figure 3.4 Comparison of the signal and background between 1 pM target DNA and blank when a modified hairpin EXPAR template and the standard EXPAR template were used for the EXPAR reaction. (A) Amplification profiles obtained from real-time monitoring of fluorescence. (B) Inflection point difference between the signal (target) and background (blank), calculated from the amplification profile data. The inflection point represents the time when 50% of the maximum fluorescence is reached. Data represent the mean ± the standard deviation.

To test the contribution of 3′-end template interactions in activating EXPAR background further, we designed a PNA strand to hybridize with the 3′-end of an EXPAR template (Figure 3.3B). This strategy blocks both intermolecular and intramolecular interactions at the 3′-end of EXPAR templates. We chose PNAs as the blocking molecules

for their strong hybridization with DNA, high chemical stability, and the inability of DNA polymerase to extend them due to their peptide backbone.[161] A PNA blocker could be designed to hybridize with a standard EXPAR template, but this would also block amplification of the target. Therefore, we extended the 3′-end of the EXPAR template to contain a PNA binding region so that the PNA could block the 3′-end without interfering with amplification of the specific target.

A comparison of the signal (from 1 pM target DNA) and background shows that the presence of the PNA blocker increases the difference between the signal and background (Figure 3.5). We compared various PNA to template ratios to assess the effectiveness of PNA blocking (Figure 3.5B). There is a modest reduction in background as the ratio of PNA to blocker is increased. More complete blocking of the 3′-end of the template occurred when more PNA was used, which reduced the number of templates with free 3′-ends. The reduction of background from blocking the 3′-end indicates that 3′ interactions contribute to the activation of background amplification.

The modified EXPAR template required for the PNA blocker showed high background amplification when no PNA blocker was used, as seen from the 0:1 ratio between PNA and template. This may be due to the longer template that was required, which provided more base pairs for template interactions as well as the potential for increased breakage of the template DNA, resulting in more free or non-blocked 3′-ends to trigger background amplification.

These results demonstrate that limiting interactions at the 3′-end of templates does reduce background amplification. It also shows the ineffectiveness of chemically blocking

the 3′-end to prevent background amplification. Designing strategies that approach 100 % efficiencies should reduce background amplification substantially.

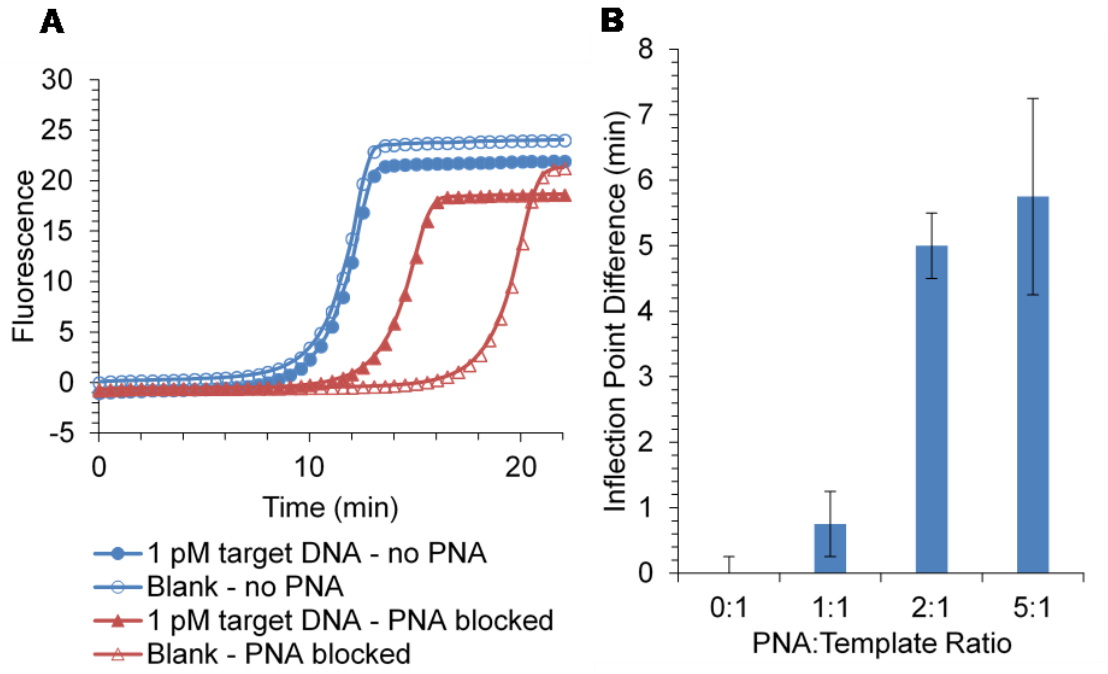

Figure 3.5 Effect of a PNA blocker on the difference between signal (1 pM target DNA) and background (blank). (A) Amplification profiles obtained from real-time monitoring of fluorescence. (B) Inflection point difference between the signal (target) and background (blank), calculated from the amplification profile data.

3.3.2 Sequence-independent blocking of the whole template

To understand background amplification further, we investigated the blocking of the whole template using sequence-independent DNA binding agents to compete with template–template interactions, as depicted in Figure 3.3C. Blocking the 3′-end only prevents hybridization between templates at their 3′-end, but nonspecific hybridization

along the rest of the template sequence remains unhindered. We propose that transient hybridization between templates at positions other than the 3′-end contribute to background. Interactions along the whole template sequence bring the 3′-ends of templates into closer proximity, leading to increased 3′-end extensions by polymerase. *E. coli* single stranded binding protein (SSB) was used to reduce template–template interactions by competitively binding to ssDNA EXPAR templates. DMSO and glycerol were used to weaken nonspecific template interactions.[162–164] Reducing interactions along the whole template sequence allowed assessment of whether non-3′ template interactions contribute to triggering background amplification.

I. Template blocking with single stranded binding protein

SSB was used to test the effect that weak interactions along the EXPAR template have on triggering background amplification. SSB binds to the whole template, independent of the sequence and was used to compete with transient template–template interactions and secondary structures within a single template.[165–170]

The effect of adding SSB to the EXPAR reaction was investigated by testing several concentrations of SSB; Figure 3.6A shows the difference between the signal (from 100 fM of target DNA) and the blank when the EXPAR reactions were performed in the absence or presence of 2 μM SSB. The presence of SSB in the EXPAR reaction solution substantially reduced the background. As the amount of SSB increased, the difference between the signal (100 fM of target DNA) and blank also increased (Figure 3.6B), indicating that SSB reduces background amplification. The reduction of background can be attributed to SSB competitively binding the template to reduce template–template hybridization and secondary structures. These results demonstrate

how limiting interactions along the whole template sequence can decrease background and that all template interactions can contribute to background amplification.

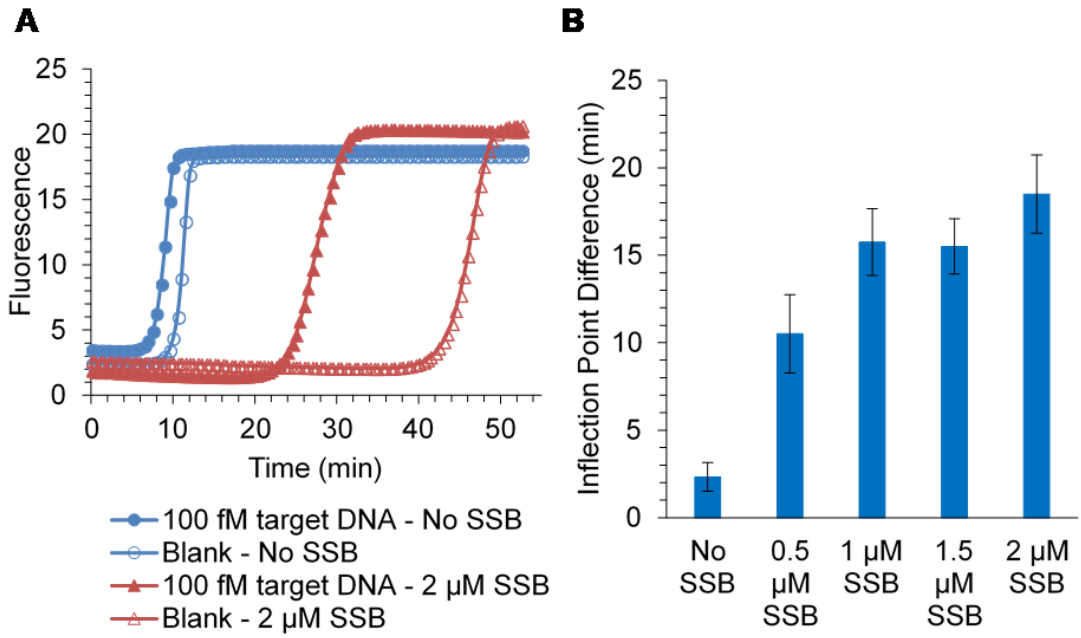

Figure 3.6 Effect of SSB on the difference between the signal (100 fM target DNA) and background (blank). (A) Amplification profiles obtained from real-time monitoring of fluorescence. (B) Inflection point difference between the signal (target) and background (blank), calculated from the amplification profile data. Data represent the mean ± the standard deviation.

The improved performance of EXPAR with the addition of SSB (SSB EXPAR) can be seen by comparing amplification profiles of a standard EXPAR system and the SSB EXPAR system. Figure 3.7A shows the standard EXPAR system and the characteristic high background occurring after 10 min of the EXPAR reactions. With the addition of 2 µM SSB, there is a substantial decrease in the background; significant

background signal is observed only after 40 min of the EXPAR reactions (Figure 3.7B). The lower background resulted in improved limit of detection of EXPAR for the amplification and detection of minute amounts of DNA targets. A log-linear relationship between inflection point time (background corrected) and target DNA concentrations from 10^{-16} M to 10^{-9} M was observed (Figure 3.8). The estimated limit of detection was 37 aM (3.7×10^{-17} M) of target DNA, which represents an improvement of three orders of magnitude vs. the standard EXPAR system. The binding of SSB to all ssDNA in a sample can reduce background amplification by blocking nonspecific interactions between the template and other nucleic acids present in biological samples. In addition, the low detection limit allows for dilution of samples, minimizing potential interference from complicated matrices present in biological samples.

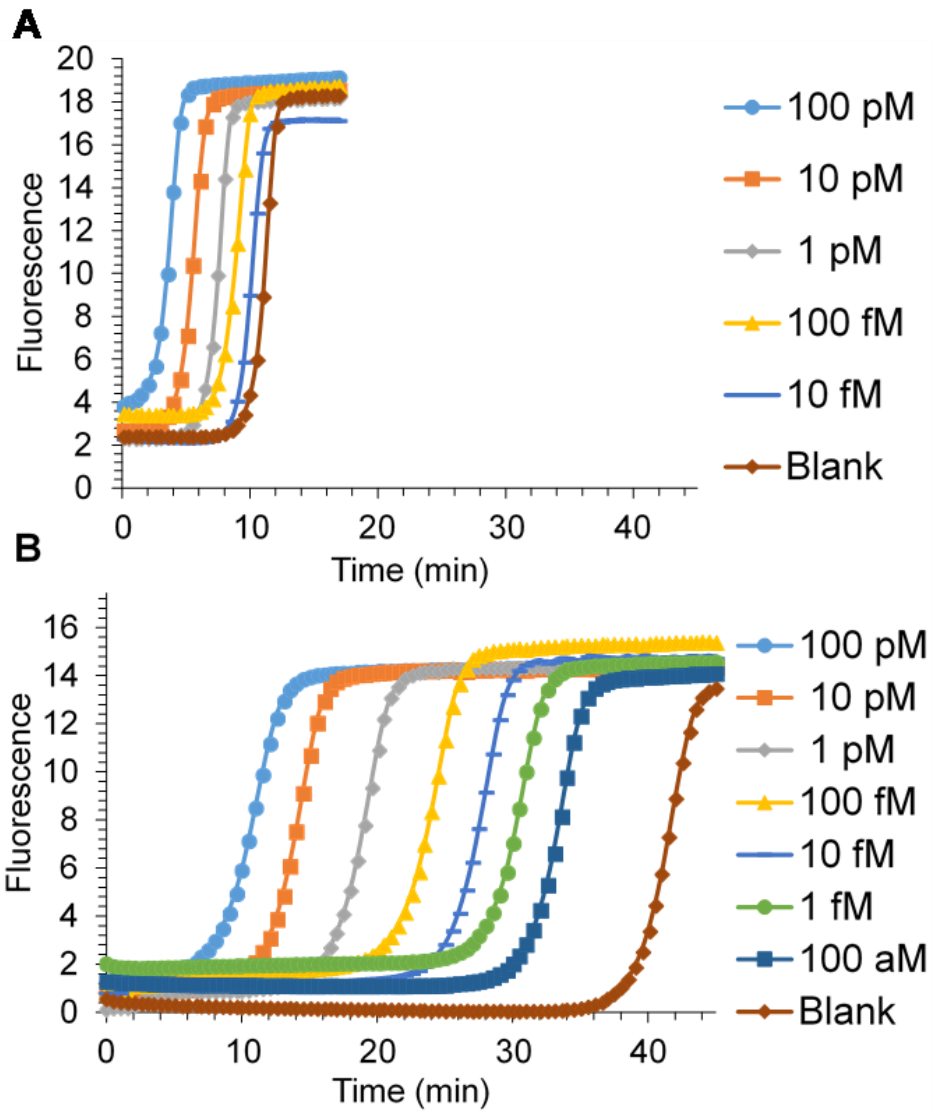

Figure 3.7 Real-time fluorescence monitoring of EXPAR reactions. (A) Varying concentrations of target DNA (10^{-15}–10^{-10}) in a standard EXPAR reaction. (B) Varying concentrations of target DNA (10^{-16}–10^{-10}) in an EXPAR reaction containing 2 µM SSB.

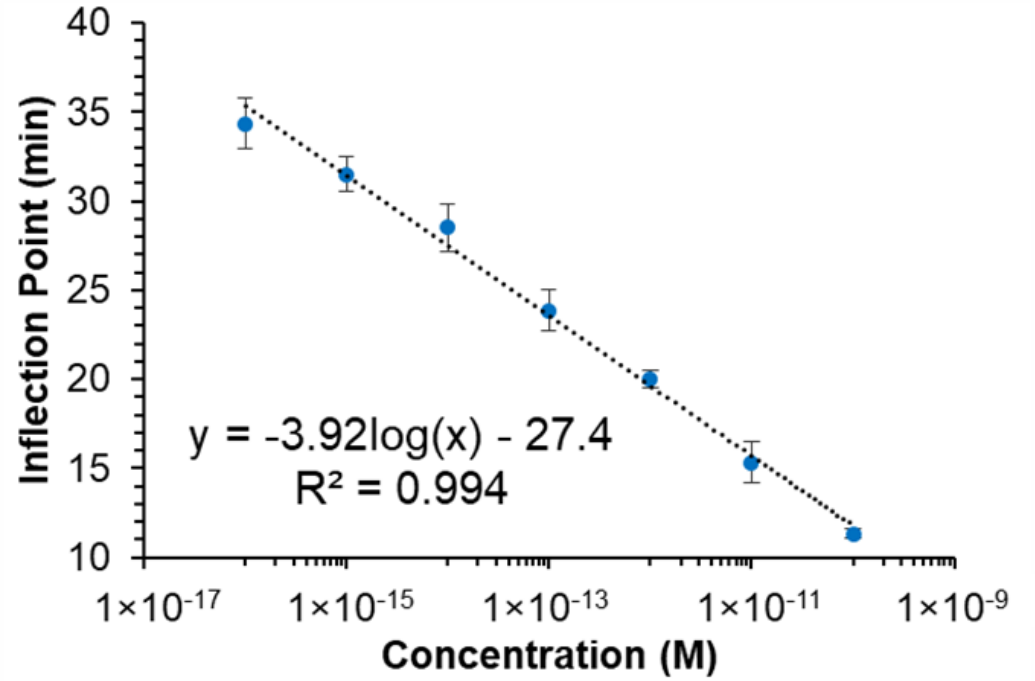

Figure 3.8 Calibration curve from EXPAR amplification and detection of target DNA (10^{-16}–10^{-10}), in the presence of 2 μM SSB. Data represent the mean ± the standard deviation.

II. Reducing template interactions with glycerol

It has been reported previously that increasing the amount of nicking enzyme decreased the reaction kinetics of EXPAR and reduced the background.[158] We also have noticed this unusual result while optimizing the nicking enzyme concentration (Figure 3.9). This finding seemed counter-intuitive at first, because more nicking enzymes should lead to a faster reaction. Our subsequent investigation revealed that glycerol present in the nicking enzyme storage buffer was responsible for the observed slower reaction speed and lower

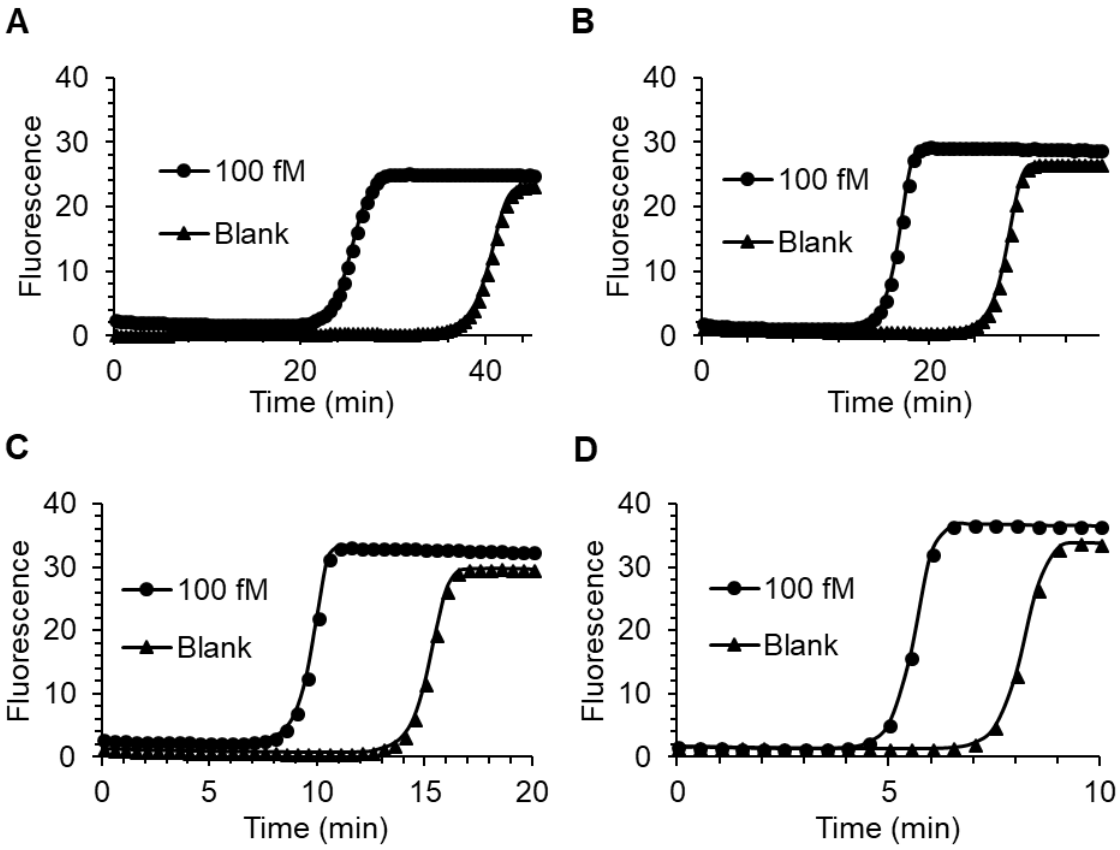

Figure 3.9 Amplification profiles of 2 µM SSB EXPAR with varying nicking enzyme concentrations. (A) 1 U/µL Nt. BstNBI, 7.50 % glycerol. (B) 0.5 U/µL Nt. BstNBI, 5.00 % glycerol. (C) 0.25 U/µL Nt. BstNBI, 3.75 % glycerol. (D) 0.05 U/µL Nt. BstNBI, 2.75 % glycerol. The polymerase and SSB storage buffers contribute 2.5 % of the overall glycerol content in each reaction. The nicking enzyme storage buffer contributions to the final glycerol content are 0.25 % (A), 1.25 % (B), 2.5 % (C), and 5 % (D).

background. The nicking enzyme storage buffer contained 50% glycerol. With increasing amounts of the nicking enzyme from 0.05 U/μL to 1 U/μL, the concentration of glycerol in the final EXPAR reaction solution increased from 2.75% to 7.5%. Figure 3.9 shows lower background and longer reaction time needed for the EXPAR reactions as the amounts of nicking enzyme and glycerol increase. Consistent results also were obtained when additional heat-inactivated nicking enzyme or glycerol were introduced to the reaction mixture (Figure 3.10). We heat-inactivated nicking enzyme to compare directly the effect of its storage buffer on background amplification and the effect of glycerol on background amplification (Figure 3.10B and C). A series of further experiments conducted with a constant nicking enzyme and increasing glycerol (Figure 3.11) further support that the reduction of background is due to glycerol. The beneficial effect of glycerol is probably through its weak adherence to the EXPAR template, thereby weakening nonspecific template interactions.

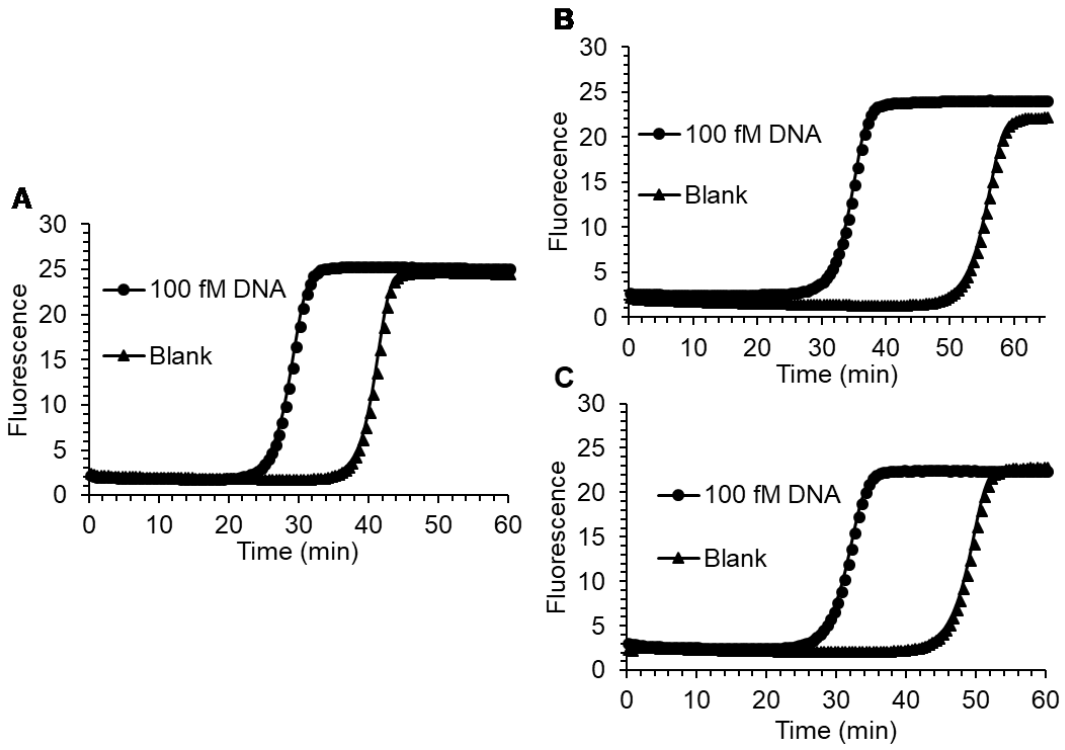

Figure 3.10 Effect of glycerol and NEase buffer on signal (100 fM target DNA) and background (blank) in SSB EXPAR. (A) Standard SSB EXPAR reaction containing a total of 5 % glycerol. (B) SSB EXPAR reaction containing extra nicking enzyme storage buffer for a total of 7.5 % glycerol. The additional 2.5% glycerol, compared to (A), is from extra heat-inactivated stock nicking enzyme. (C) SSB EXPAR with additional glycerol added to the reaction for a total of 7.5 % glycerol.

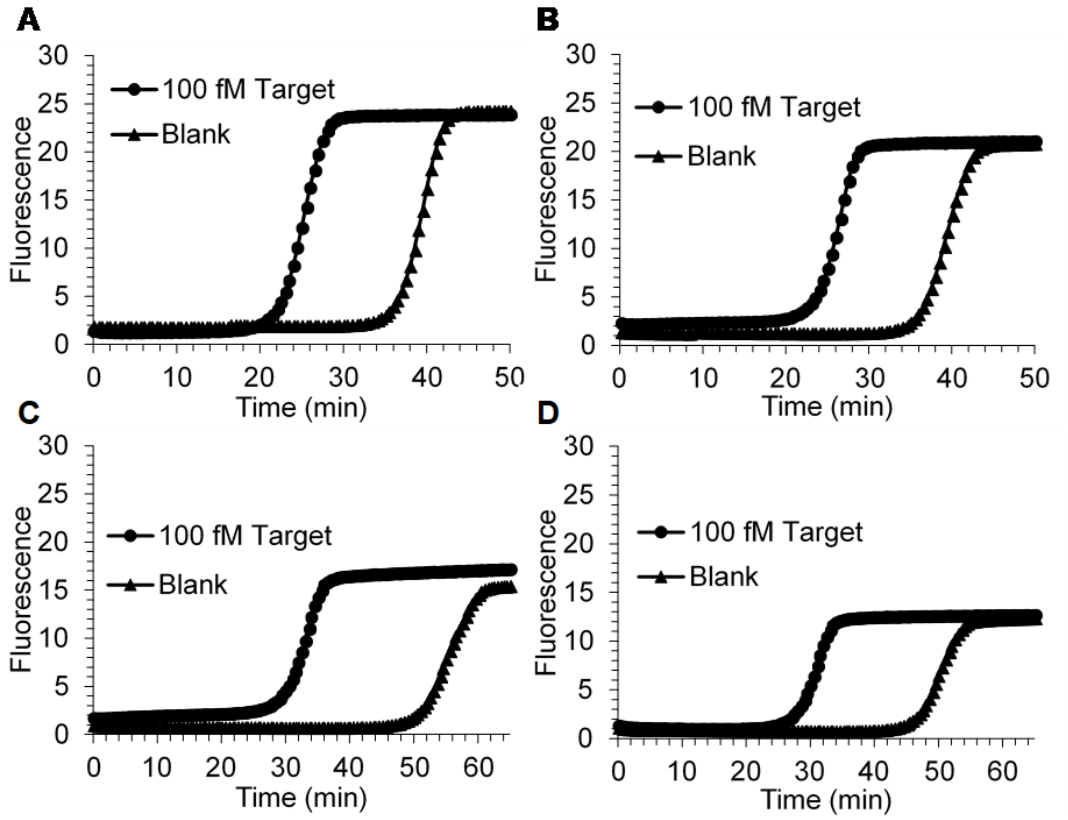

Figure 3.11 Effect of glycerol concentration on the differences between signal (100 fM target DNA) and background (blank) in SSB EXPAR. **(A)** 5 % glycerol. **(B)** 10 % glycerol. **(C)** 15 % glycerol. **(D)** 20 % glycerol.

III. Reducing template interactions with DMSO

DMSO was used to test the effect of template–template interactions on triggering EXPAR background amplification further. DMSO can weaken template interactions and potentially lead to lower background amplification.[171] As the amount of DMSO added to EXPAR increases, background and target specific amplification both decrease (Figure 3.12), leading to no improvement of EXPAR performance. Although no improvement to

EXPAR is observed, the slower reaction with increasing DMSO reinforces the importance of small changes in DNA melting temperature on the performance of EXPAR.

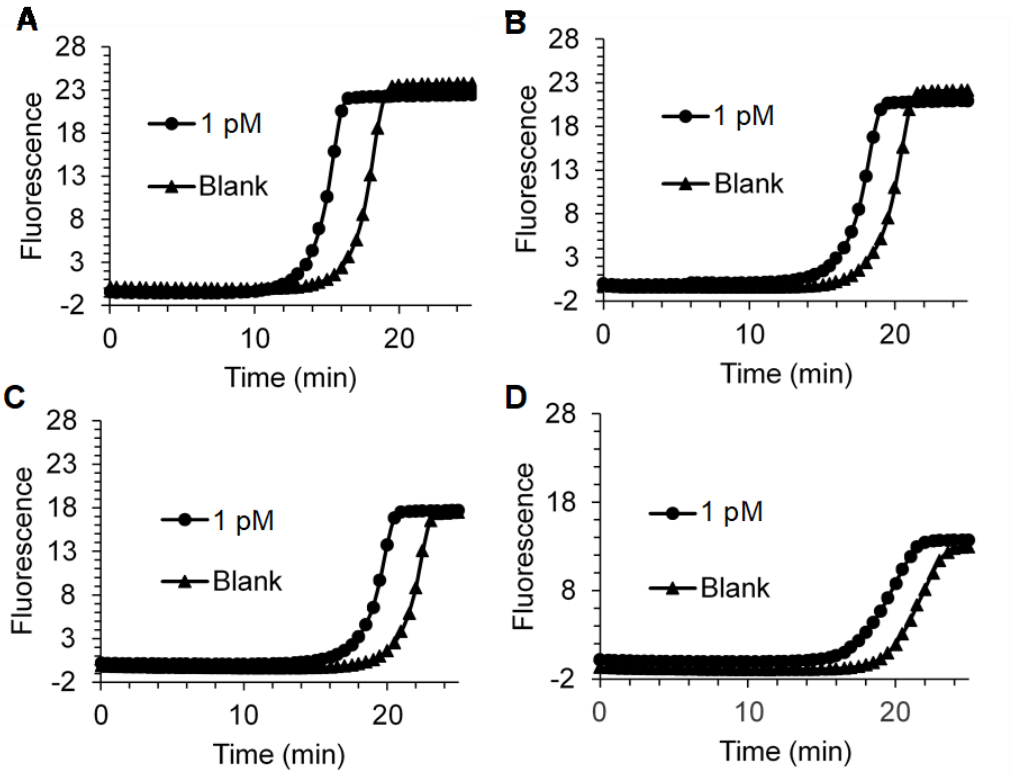

Figure 3.12 EXPAR amplification profiles with increasing amounts of DMSO. (A) no DMSO (B) 1% DMSO (C) 3% DMSO (D) 5% DMSO

3.4 Conclusions

We have performed a systematic investigation of the triggering mechanism of EXPAR background amplification by testing several systems to block template interactions that trigger EXPAR background. Our results indicate that there are two main contributors that trigger background amplification in EXPAR. Firstly, background is initiated by the 3′-end extension of EXPAR templates by DNA polymerase. Extension may occur either through intramolecular hybridization or intermolecular hybridization with another EXPAR template. This extension generates the specific target DNA strand of interest that is amplified further in a normal EXPAR fashion. Secondly, nonspecific hybridization along the whole EXPAR template leads to increased 3′-end extensions, which increases the generation of background amplification.

Both of our specific 3′-end DNA blocking strategies provide evidence that 3′-end extension of templates contributes to background amplification in EXPAR. Incorporating a 3′-hairpin on the EXPAR template showed the ability of DNA polymerase to extend non-complementary 3′-end sequences that are in close proximity. The PNA blocking design demonstrated that more complete blocking of the 3′-end of a template reduces background amplification. These two results suggest that the 3′-end of templates can activate background amplification via polymerase extension.

The sequence-independent blocking strategies showed that reducing template–template interactions along the whole EXPAR template reduces background amplification. Incorporating DMSO or glycerol showed that small decreases in the melting temperature of DNA in EXPAR slows the onset of background, indicating that weak template interactions contribute to the activation of background amplification.

Using SSB to bind the template substantially reduced background by decreasing nonspecific template hybridization, not only at the 3′-end but along the whole EXPAR template.

By focusing on template–template hybridizations in EXPAR, we achieved three orders of magnitude improvement to the LOD in EXPAR when 2 μM SSB was added to the reaction. This work provides valuable insight into the mechanism that triggers EXPAR and gives useful strategies to slow the onset of EXPAR background signal.

Chapter 4: Development of a Binding Induced Loop-Mediated Isothermal Amplification Reaction for Protein Detection

4.1 Introduction

Nucleic acid amplification is an invaluable tool that enables the detection of many biological molecules. There is a high interest in developing methods that harness the signal amplifying power of nucleic acid amplification for the detection of non-nucleic acid targets.[21,22] PCR has been used successfully as a surrogate signal amplifier, but PCR requires thermocycling, which often has longer amplification times and requires thermocycling equipment. Alternatively, isothermal nucleic acid amplification techniques require no thermocycling, and amplification times are typically under 1 h, making these techniques promising for use as signal amplifiers for the detection of non-nucleic acid targets.

LAMP is an isothermal nucleic acid amplification technique capable of detecting <10 copies of DNA in under 1-h amplification time. LAMP has been used extensively for the detection of pathogens,[66,87,172–174] tumors,[175] single nucleotide polymorphisms,[176] organophosphorus pesticides,[177] and embryo sex determination.[178–180] While LAMP shows exceptional performance in the detection of nucleic acids, its complicated design–which uses 4–6 interacting primers and produces several intermediate amplification products–makes it difficult to adapt for signal amplification of non-nucleic acids. Several heterogeneous protein assays have been developed recently that use LAMP for signal amplification. Pourhassan-Moghaddam *et al.* proposed several possible formats for immuno-LAMP techniques, although they have not been validated experimentally.[100] The Kong group recently demonstrated two similar magnetic bead (MB) based immuno-

LAMP techniques. The first assay uses a sandwich format between an antibody labelled MB and an aptamer.[181] Aptamers not linked to the MB through target binding are washed away, and the remaining target bound aptamers are amplified by LAMP. The second assay uses a sandwich technique with antibody labelled MB and antibody labelled liposomes.[99] Liposomes not linked to the MB through target binding are washed away. The remaining liposomes are lysed to release the encapsulated DNA substrate that is amplified and detected via LAMP. While these methods are capable of detecting 1 aM of Mucin 1 and 30 aM of P-glycoprotein, respectively, they involve several washing steps which increases assay time, complexity, and requires trained personnel to perform them. A similar sandwich method also has been developed to detect pathogen-specific IgG antibodies.[182]

The objective of this Chapter is to design and optimize the first homogenous and isothermal assay utilizing LAMP signal amplification for protein detection. I couple LAMP with binding induced DNA assembly for the detection of non-nucleic acid targets (Figure 4.1). The binding induced LAMP (BI-LAMP) procedure is simple, only requiring mixing of reagents in a single tube at room temperature, followed by incubating and monitoring fluorescence at 65 $^{\circ}$C. The assay uses binding induced DNA assembly to trigger the ligation of two target bound probes to generate a new dumbbell structure DNA. The dumbbell DNA is the starting structure required for the cycling phase of LAMP.

This strategy has significant advantages over heterogeneous techniques that require several washing and handling steps to remove unbound probes. The procedure is also simpler than similar techniques, such as *in situ* PLA, which often require washing steps and microscope equipment for detection.[57] While fluorescence microscopes

facilitate low detection limits *in situ* PLA, they require trained personnel, more complicated sample preparation, and are not applicable in a POC setting.

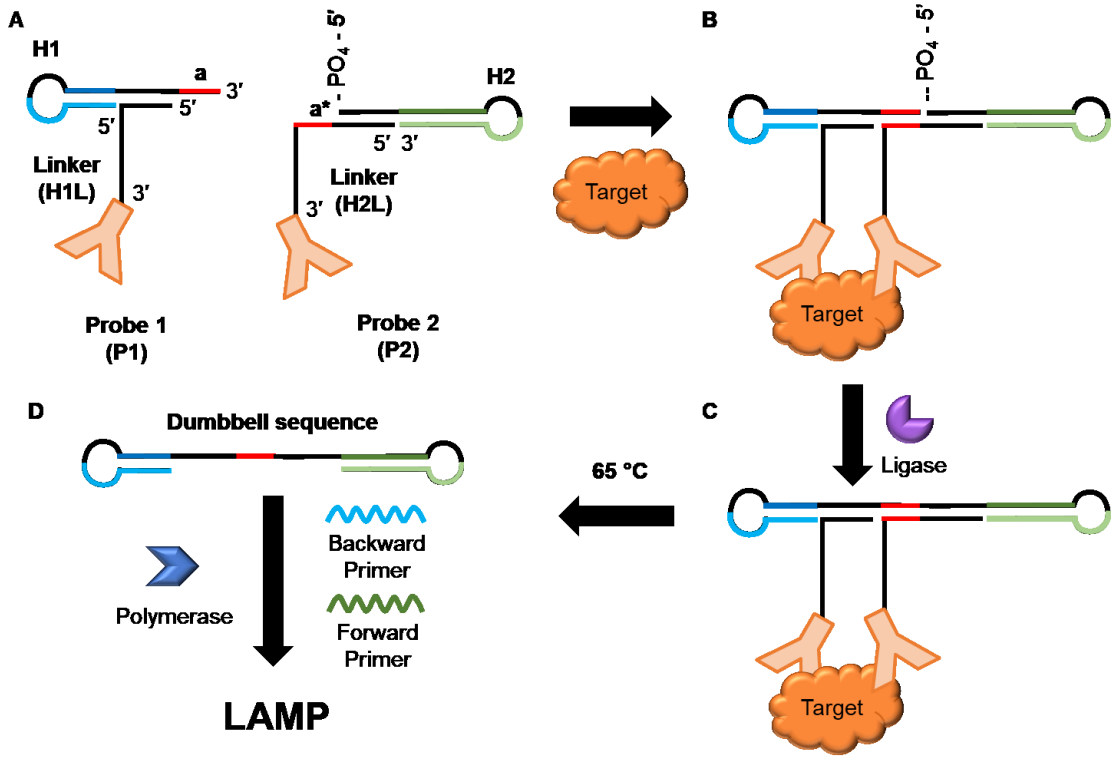

Figure 4.1 Schematic illustration of binding induced loop mediated isothermal amplification (BI-LAMP). (A) The stability between **a** and **a*** is too weak to anneal when probes are free in solution. (B) Upon target binding by P1 and P2, **a** and **a*** anneal to form a stable duplex. The duplex places the 3′-end of H1 next to the 5′ phosphorylated end of H2. (C) Ligase joins the 3′-end of H1 to the 5′-end of H2, which generates a new dumbbell shaped DNA sequence. (D) The reaction is heated to 65 °C and LAMP occurs.

4.2 Experimental

4.2.1 Materials and reagents

All oligonucleotides were synthesized, labelled, and purified by Integrated DNA Technologies (Coralville, IA). All DNA sequences and modification are listed in Table 4.1. Bst 2.0 Warmstart, T4 ligase, Taq ligase, *e.coli* ligase, and their corresponding buffers were from New England Biolabs (Whitby, ON, Canada). SYBR Green I (10 000X), deoxynucleotide triphosphates (10 mM mix), and ROX reference dye were from Thermo Fisher Scientific (Eugene, OR).

Table 4.1 DNA sequences, modifications, and purification for BI-LAMP

DNA	**Synthesis**	**Sequence**
H2	Ultramer	5′-Phosphate - CTC CTA TCA ATC TCC GGC GTT GAT GTA GTC GTA GTG AGA ACA ATA CTG CTC CAC CTC ACT CTA AAC T CAC TAC GAC TAC ATC AAC GCC-3′
H1-5	Ultramer	5′-GGC ACG GAG ACC AGA CGG AGA A GGA GAG CTG ATG AGA TGT G TATA TTC TCC GTC TGG TCT CCG TGC C TTT CCT ACG TGG ACT TCC TTT TCT GC-3′
H1-6	Ultramer	5′-GGC ACG GAG ACC AGA CGG AGA A GGA GAG CTG ATG AGA TGT G TATA TTC TCC GTC TGG TCT CCG TGC C TTT CCT ACG TGG ACT TCC TTT CTC TGC-3′

H1-7	Ultramer	5′-GGC ACG GAG ACC AGA CGG AGA A GGA GAG CTG ATG AGA TGT G TATA TTC TCC GTC TGG TCT CCG TGC C TTT CCT ACG TGG ACT TCC TTT CCT CTG C-3′
H1-8	Ultramer	5′-GGC ACG GAG ACC AGA CGG AGA A GGA GAG CTG ATG AGA TGT G TATA TTC TCC GTC TGG TCT CCG TGC C TTT CCT ACG TGG ACT TCC AAA ACC TCT GC-3′
H2L	Standard desalting	5′-GGA GAT TGA TAG GAG GCA GAG GT AGT CG TTT TTT TTT TTT TTT TTT TTT TTT-Biotin-3′
H1L	Standard desalting	5′-GGA AGt CCA CGT AGG TTT TTT TTT TTT TTT TTT TTT TTT TTT TTT-Biotin-3′
Backwards inner primer (BIP)	HPLC purified	5′-GGC ACG GAG ACC AGA CGG AGA A GG AGA GCT GAT GAG ATG TG-3′
Forward inner primer (FIP)	HPLC purified	5′-GGC GTT GAT GTA GTC GTA GTG AGT TTA GAG TGA GGT GGA GCA G-3′
Blocker-11	Standard desalting	5′-A CTA CCT CTG C-3′
Blocker-10	Standard desalting	5′-CTA CCT CTG C-3′
Blocker-9	Standard desalting	5′-TA CCT CTG C-3′

Positive control linker (PCL)	Standard desalting	5′-GGA GAT TGA TAG GAG GCA GAA AAG GAA GTC CA-3′
Regions in red are the complementary sequences **a** and **a*****. Underlined regions highlight the complementary region between the affinity bound linker strands and the DNA hairpins.		

4.2.2 Preparation of probes for BI-LAMP

All DNA was received lyophilized and subsequently was dissolved in water to 50 µM, and blockers were dissolved to 100 µM. To construct probes to bind to the protein target, the biotinylated linker DNAs were annealed to the hairpin DNAs. **H2**, **H1**, **H2 Linker**, and **H1 Linker** were all diluted to 10 µM using a dilution buffer of 10 mM Tris, 50 mM NaCl, 0.05 % Tween 20, and 4 mM $MgSO_4$ at pH 7.4. To prepare **P2**, 10 µL each of 10 µM **H2** and 10 µM **H2 Linker** were mixed and further diluted to a total volume of 100 µL using the dilution buffer. **P1** was prepared in the same manner using **H1 Linker** and **H1-5**, **H1-6**, **H1-7**, or **H1-8**. The final solutions, each containing 1 µM of H1 or H2 hairpins with their corresponding linker DNA were annealed by heating to 90 °C for 5 min followed by cooling to 20 °C over 1.5 h in a thermocycler. After annealing, each probe was diluted to 100 nM and stored at 4 °C for up to one week.

4.2.3 BI-LAMP procedure

Each reaction was prepared using three parts: the standard solution of streptavidin, a probe mix, and a master mix. The standard solution of streptavidin was diluted to the desired concentration using 10 mM Tris, 50 mM NaCl, and 0.05 % Tween 20 at pH 7.4. Two µL of streptavidin was added to 4 µL of probe mix (6 µL if blocker was used) and incubated

at room temperature for 20 min to allow probe binding and hybridization between probes. Fourteen µL of mastermix, which contained the remaining reaction components, was then added to the probe-streptavidin mixture and further incubated at room temperature for 10 min to allow ligation to occur. After 10 min ligation time, each reaction was transferred to an Applied Biosystems StepOnePlus, and fluorescence was monitored using the SYBR Green channel at 65 °C. The final reaction conditions were 1 µM FIP and BIP, 1X SG, 0.625 µM ROX reference dye, 100 pM **H2** probe, 100 pM **H1** probe, 0.4 U/µL Bst 2.0 Warmstart, 0.4 U/µL T4 ligase, 0.75X isothermal amplification buffer and 0.25X T4 ligase buffer (27.5 mM Tris-HCl, 7.5 mM $(NH_4)_2SO_4$, 37.5 mM KCl, 2.5 mM $MgCl_2$, 1.5 mM $MgSO_4$, 250 µM ATP, 2.5 mM DTT, and 0.075 % Tween 20.

4.2.4 Positive control procedures

Dumbbell positive control sequences were generated by ligating **H1.3** to **H2** at high concentration. Both **H1.3** and **H2** were diluted to 1 µM using 1X T4 buffer, and the ssDNA PC linker (PCL) was diluted to 1 µM in 10 mM Tris, 20 mM NaCl, and 0.05% Tween 20 at pH 7.4. Ten µL each of 1 µM **H1.3**, 1 µM **H2**, 1 µM **PCL**, and 400 U/µL T4 ligase were mixed and diluted to 100 µL using 60 µL of 1X T4 buffer, resulting in 100 nM of **H1.3**¸ **H2**, **PCL**, and 40 U/µL T4 ligase. This reaction mixture was incubated at room temperature for 1 h to allow complete ligation of **H1.3** to **H2**. Then the ligase was inactivated by heating to 90 °C for 10 min. Next, the dumbbell PC was annealed with the temperature program described in Section 4.2.2 to ensure that the DNA formed the proper dumbbell secondary structure. Next, the positive control reaction was performed as in Section 4.2.3, but the ligated dumbbell structure was used in place of **P1** and **P2** and no ligase was present in the reaction.

To test the complete ligation between **H1.3** and **H2**, **PCL** was used as the target molecule. The reaction was performed as described in Section 4.2.3, but **H1.3** and **H2** were used in place of **P1** and **P2**, respectively, and **PCL** was used as the target molecule.

4.3 Results and Discussion

4.3.1 Principle of BI-LAMP

BI-LAMP uses two probes, two primers, ligase, and polymerase to generate an exponentially amplified signal triggered by a protein target. Probe 1 (**P1**) is constructed by annealing H1-Linker (**H1L**) to the H1 hairpin and Probe 2 (**P2**) is constructed by annealing H2-Linker (**H2L**) to the H2 hairpin. Each linker DNA contains an affinity probe to the target molecule. Upon binding of the target from both **P1** and **P2**, assembly occurs between the **a** motif of **P1** and the **a*** motif of **P2**. After assembly of **a** and **a***, T4 ligase ligates the 3′-end of **H1** to the 5′ phosphorylated end of **H2**. The ligation of **H1** to **H2** generates a new sequence with two hairpins in the shape of a dumbbell. This dumbbell structure is the starting sequence required for the cycling amplification phase in LAMP. After a short ligation time at room temperature, the reaction is heated to 65 °C for LAMP to occur. A signal is generated by SG, which has enhanced fluorescence when bound to the double stranded LAMP products

4.3.2 Detection of streptavidin using BI-LAMP

LAMP commonly uses Bst, Bst 2.0, Bst 3.0, or Bst 2.0 Warmstart for amplification. I use Bst 2.0 Warmstart because activity is blocked under 45 °C by a reversibly bound aptamer. This allows ligation of probes at room temperature without polymerase displacing the linking strands from hairpin strands.

The choice of ligase is an important parameter to investigate because different ligase enzymes have different specificities and activities. A ligase with low activity and high fidelity may result in low conversion of the target bound probes to the ligated dumbbell product. A ligase with high activity and low fidelity may result in large amounts of dumbbell structure from a target independent ligation. An ideal ligase produces no target independent ligation but has a high target triggered ligation. Figure 4.2 compares target and blank signals using T4, *E.coli*, and *Taq* ligases. Each reaction system uses 0.5X Bst 2.0 Warmstart buffer and 0.5X the supplied buffer for each specific ligase. The concentration of Mg^{2+} affects DNA hybridization and enzyme activity; therefore, $MgSO_4$ was added to the *E.coli* ligase system so that each reaction contained a final concentration of 4 mM Mg^{2+}. *Taq* ligase showed the slowest background amplification, indicating a low amount of nonspecific ligation of hairpins. However, *Taq* ligase also showed very slow amplification of target, indicating low conversion of target bound probes to the ligated dumbbell product. T4 and *E.coli* ligase both showed fast amplification times of target specific reactions, indicating a high conversion rate of the target bound probes to dumbbell product. However, both ligases showed higher background ligation of free probes compared to *Taq* ligase. T4 ligase was chosen for further experiments. Since the probes are present at several orders of magnitude higher concentration than target concentrations, some nonspecific ligation may be unavoidable.

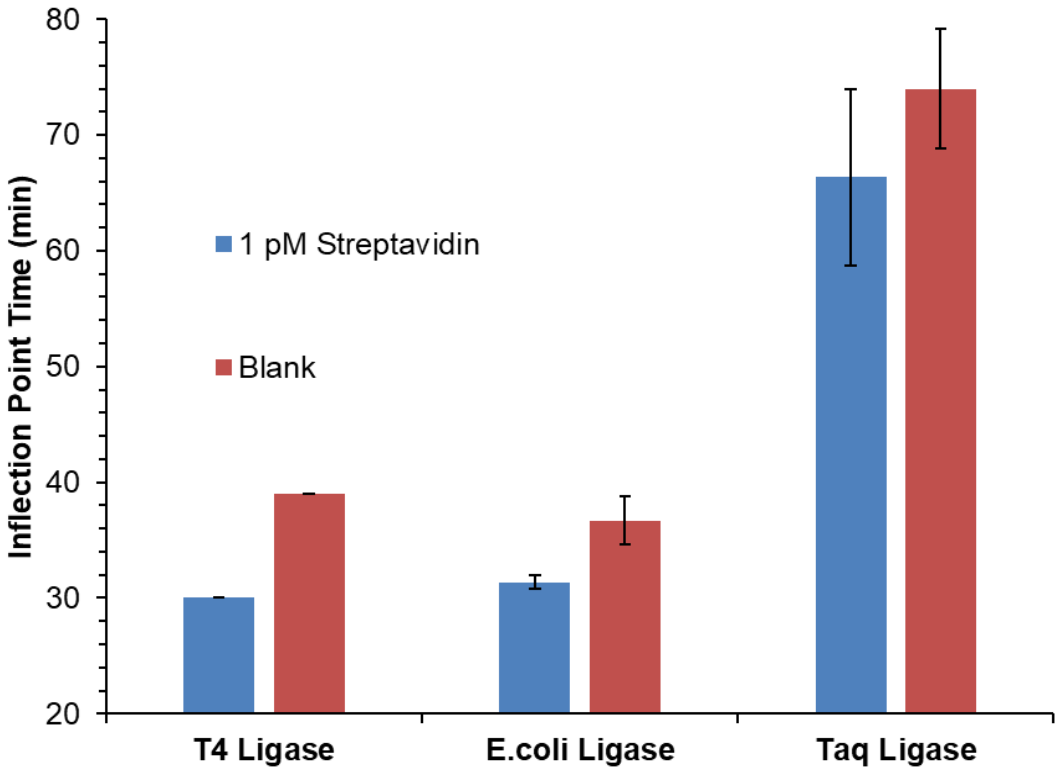

Figure 4.2 Comparison of signal to background amplification using three different ligases in BI-LAMP. Supplied ligase buffers were used for each different ligase and the Mg^{2+} concentration was normalized to ensure consistent hybridization between probes and activity of polymerase. A shorter time to reach the amplification inflection point indicates faster amplification. Data shown is the mean ± standard deviation of triplicate experiments.

Mg^{2+} affects several components in BI-LAMP; therefore, the concentration of Mg^{2+} in the reaction was optimized. Bst 2.0 Warmstart polymerase uses Mg^{2+} as the cofactor and commonly is optimized in LAMP reactions to achieve the fastest amplification without generating background amplification.[183] DNA hybridization also is largely affected by the concentration of Mg^{2+} as it reduces the repulsion between the

negative charges of the phosphate groups on DNA, allowing two DNA strands to have stronger hybridization. The BI-LAMP system has many interacting DNA strands that are affected by Mg^{2+} (stem of hairpins, linker-hairpin hybridization), but the most critical interaction is the complementary region between the hairpin probes. A high Mg^{2+} concentration may promote target independent hybridization, leading to a nonspecific ligation, while a low or no Mg^{2+} will reduce target triggered hybridization and lead to a low conversion of target bound probes to dumbbell structure.

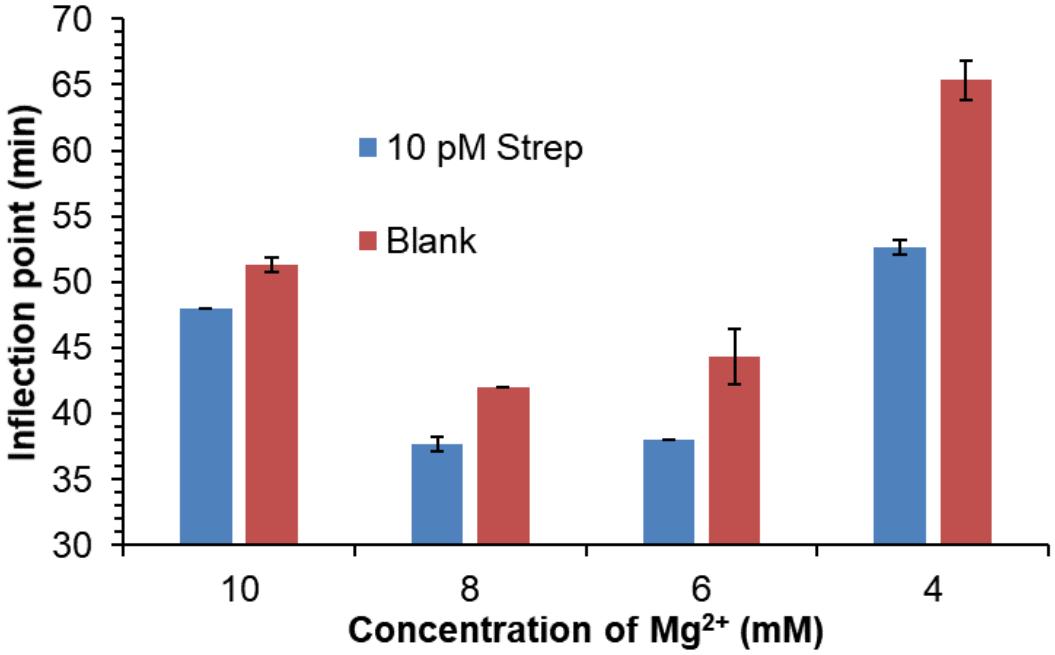

Figure 4.3 Effect of magnesium concentration on BI-LAMP. The magnesium concentration was altered by changing the ratio of Isothermal Amplification Buffer (2 mM Mg^{2+}) and T4 Ligase Buffer (10 mM Mg^{2+}) used in the reaction. A shorter time to reach the amplification inflection point indicates faster amplification. Data shown is the mean ± standard deviation of triplicate experiments.

Figure 4.3 shows that increasing Mg^{2+} from 4 to 8 mM increased the reaction speed of both the target and background signals. Curiously, 10 mM Mg^{2+} showed a slower signal compared to 8 and 6 mM Mg^{2+}; the reason for this is not known. Four mM Mg^{2+} was chosen as the optimum condition because the difference between the target and blank is the largest, even though it shows the slowest amplification speed.

A central design component of BINDA is the concentration of probes used. A high probe concentration leads to a higher incidence of nonspecific hybridization between probes. However, the probes must be present in high enough concentration so that **P1** and **P2** can bind to the same target molecule simultaneously. Figure 4.4 shows faster amplification for both the target and blank reactions as the concentration of probes is increased. Higher than 250 pM probes showed large increases in background amplification, particularly using 1 nM probes where there is little difference between the target and blank amplification. One hundred pM probes were used for further experiments. Although 250 pM probes showed similar amplification times as 100 pM probes, a lower probe concentration, in principle, results in lower hybridization between free probes.

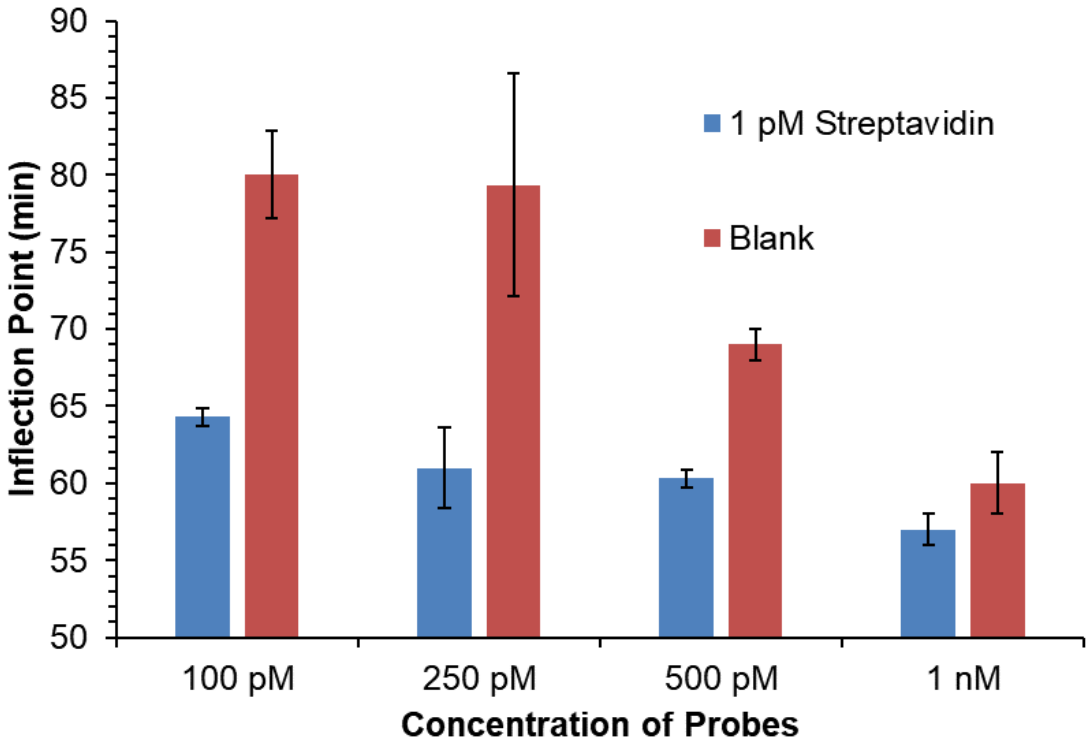

Figure 4.4 Effect of probe concentration on BI-LAMP amplification. A shorter time to reach the amplification inflection point indicates faster amplification. Data shown is the mean ± standard deviation of triplicate experiments.

The most critical component of any BINDA system is the strength of hybridization between the two probes used. The strength of the interaction between **P1** and **P2** (**a**– **a*** region) must be weak enough that unbound probes do not hybridize, yet is strong enough for probes to hybridize readily upon target binding. During the design of **P1** and **P2**, the T_m of the **a**–**a*** region was optimized using IDTs oligoanalyzer tool. However, the strength of hybridization between two DNA strands is affected by many different reaction parameters, therefore, it is important to validate the optimum length and the corresponding strength of **a-a*** hybridization experimentally. The strength of hybridization between two

DNA strands can be altered by changing the percent of G and C bases or by changing the length of the complementary sequence. Here, the length was varied as this provides the most controlled way to test the strength of **a-a*** hybridization. Changing the sequence of **a** and **a*** could introduce nonspecific interactions with other DNA sequences present in the reaction, resulting in data that does not rely solely on the strength of hybridization between **a** and **a***.

As the length of the **a-a*** interaction is increased, the amplification speed from both the target and blank increases (Figure 4.5). A 5-base complementary region was used for further experiments because it showed the lowest background signal and the largest difference between the target and background signal.

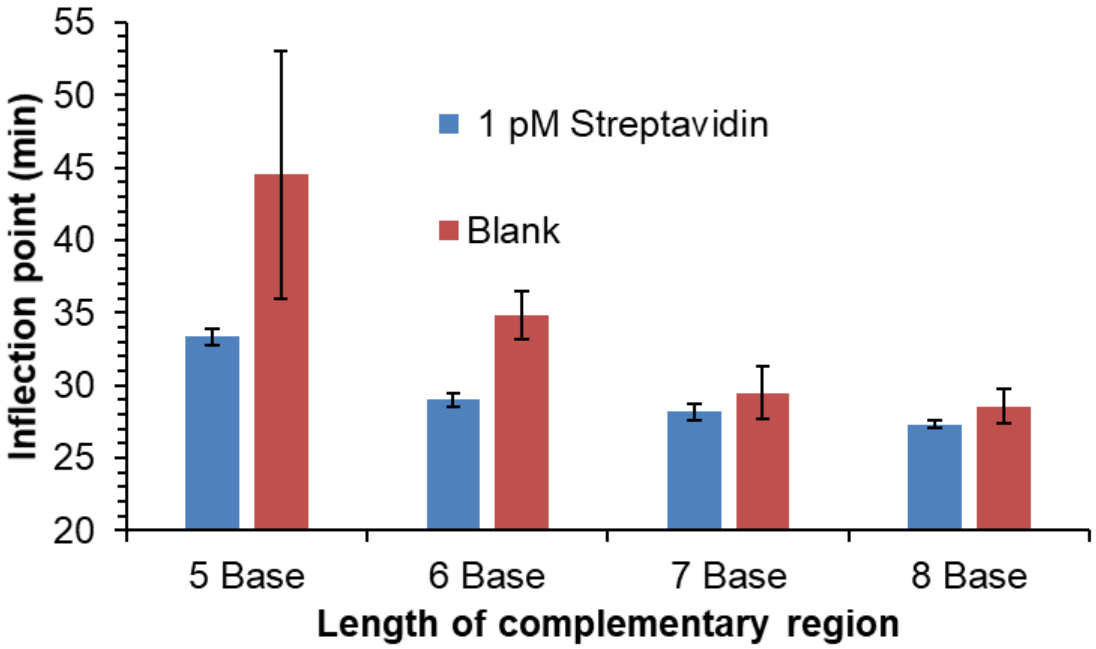

Figure 4.5 Effect of the complementary region length between probes on BI-LAMP amplification. A shorter time to reach the amplification inflection point indicates faster amplification. Data shown is the mean ± standard deviation of triplicate experiments.

Optimizing the concentration of FIP and BIP primers in LAMP will achieve fast target specific amplification while limiting the background. Increasing the concentration of primers increased the reaction speed; however, higher than 1 µM primers showed no increase in target specific amplification (Figure 4.6). Therefore, 1 µM primers were used for further experiments; this is similar to many optimized LAMP reactions.[63,183]

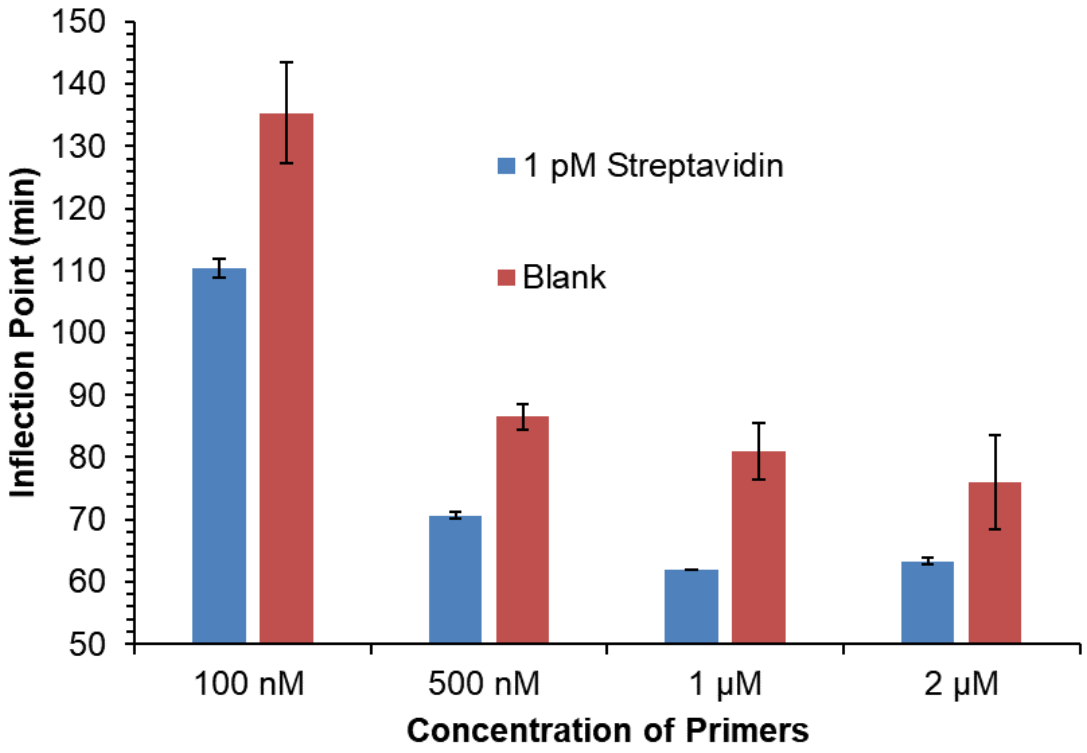

Figure 4.6 Effect of FIP and BIP primer concentration on BI-LAMP amplification. A shorter time to reach the amplification inflection point indicates faster amplification. Data shown is the mean ± standard deviation of triplicate experiments.

Polymerase concentration is optimized commonly in assays that use its DNA replicating activity. Often, polymerase concentrations that are too high will induce nonspecific amplification, while too low a concentration results in a slow amplification.

Increasing Bst 2.0 Warmstart increased the reaction speed of both target and blank (Figure 4.7). The 0.4 U/µL Bst 2.0 Warmstart was chosen for further experiments because it improves the difference between target and blank signals without a large reduction in reaction speed. Using a lower concentration significantly slows the reaction with little improvement to the difference between target and blank amplification speeds.

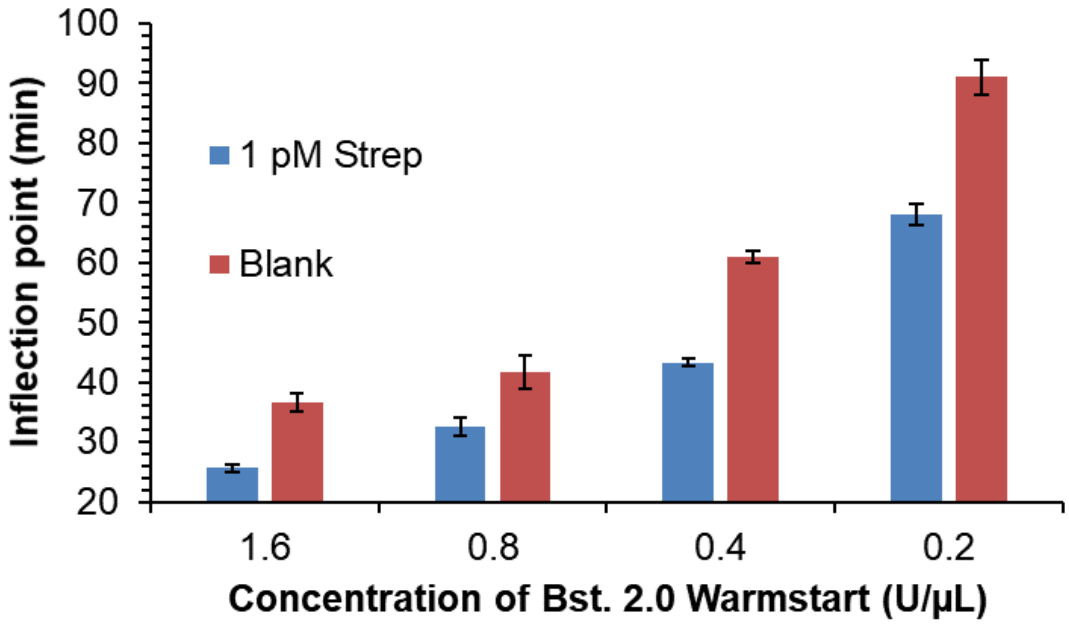

Figure 4.7 Optimization of Bst 2.0 Warmstart in BI-LAMP. A shorter time to reach the amplification inflection point indicates faster amplification. Data shown is the mean ± standard deviation of triplicate experiments.

The amount of ligase used is an important aspect as T4 ligase generates nonspecific ligation products.[184] A low concentration of ligase limits conversion of target bound probes into dumbbell DNA, while a high ligase concentration results in large amounts of ligated dumbbell DNA from a target independent ligation. Changing the

concentration of T4 ligase from 0.05 to 0.4 U/µL T4 showed little effect on the reaction (Figure 4.8). Lower concentrations of T4 ligase showed a small decrease in amplification speed, but no improvement to the difference between the target and blank amplification. 0.4 U/µL was used for further experiments because it showed similar background amplification as lower concentrations, but in theory, results in a more complete ligation of probes, leading to higher target specific amplification.

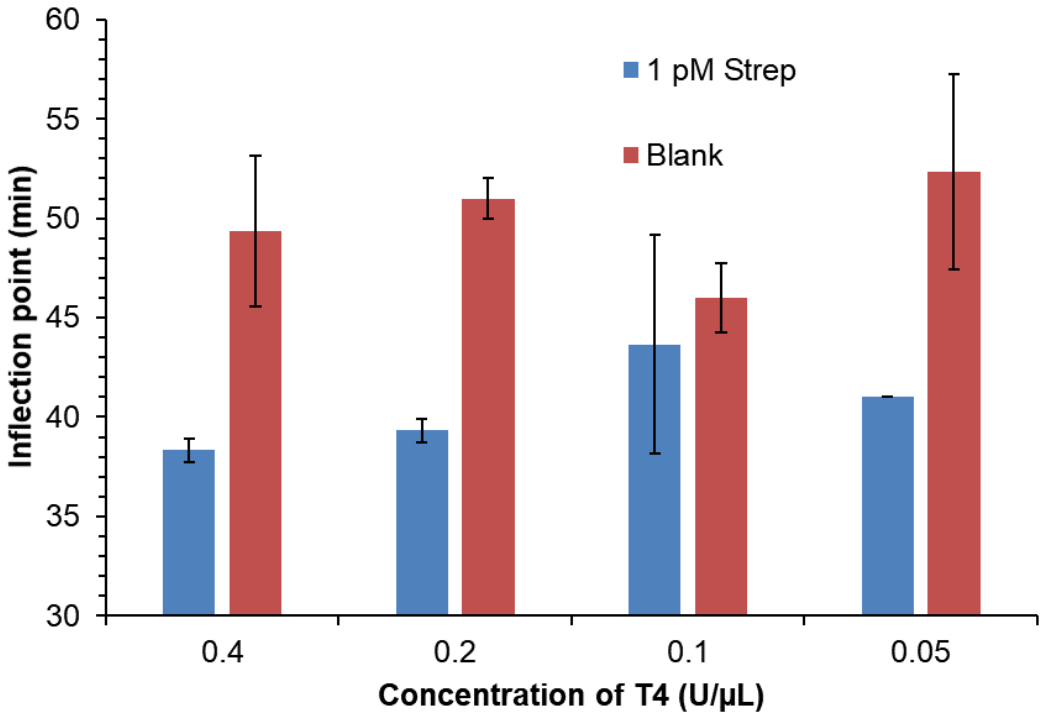

Figure 4.8 Optimization of T4 ligase in BI-LAMP. A shorter time to reach the amplification inflection point indicates faster amplification. Data shown is the mean ± standard deviation of triplicate experiments.

Although several reaction components were investigate and optimized, background amplification was sill present. To prevent background amplification, blocking oligos were designed to prevent nonspecific ligation of probes. The blocking

oligos were designed to compete with the complementary region between probes to prevent nonspecific interaction between **a** and **a*** (Figure 4.9). In the absence of a target, the blocker oligo is ligated to **H2**, preventing nonspecific ligation between **P1** and **P2**. If **P1** and **P2** bind to the same target molecule, then **P1** displaces the blocker oligo and **H1** is ligated to **H2**.

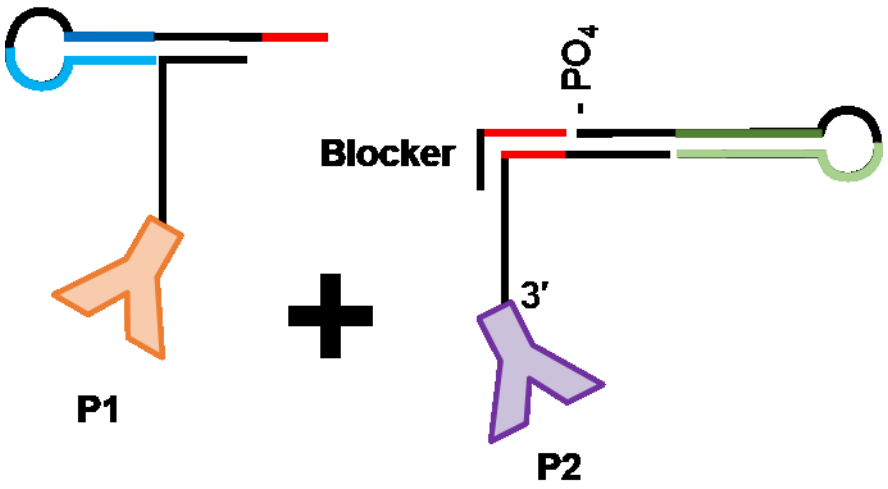

Figure 4.9 Schematic illustration of a blocking oligo in BI-LAMP. The blocker oligo is a short (9-11 nucleotide) DNA oligo that hybridizes with the **a*** region of **P2** to prevent transient interactions between **P1** and **P2**.

The blocking oligo must have a strong enough hybridization with **P2** to block nonspecific ligation between **H1** and **H2**, yet still allow the blocker to be displaced easily by **P1** when the probes are target bound. As the length of the blocker is increased, the background signal is decreased, indicating more complete blocking of nonspecific ligation of probes (Figure 4.10). However, the competitive hybridization introduced by the blocking oligo also decreased target specific ligation as the length of the blocker

increased. To assess the best conditions, the difference of inflection points between the target and blank was used (Table 4.2).

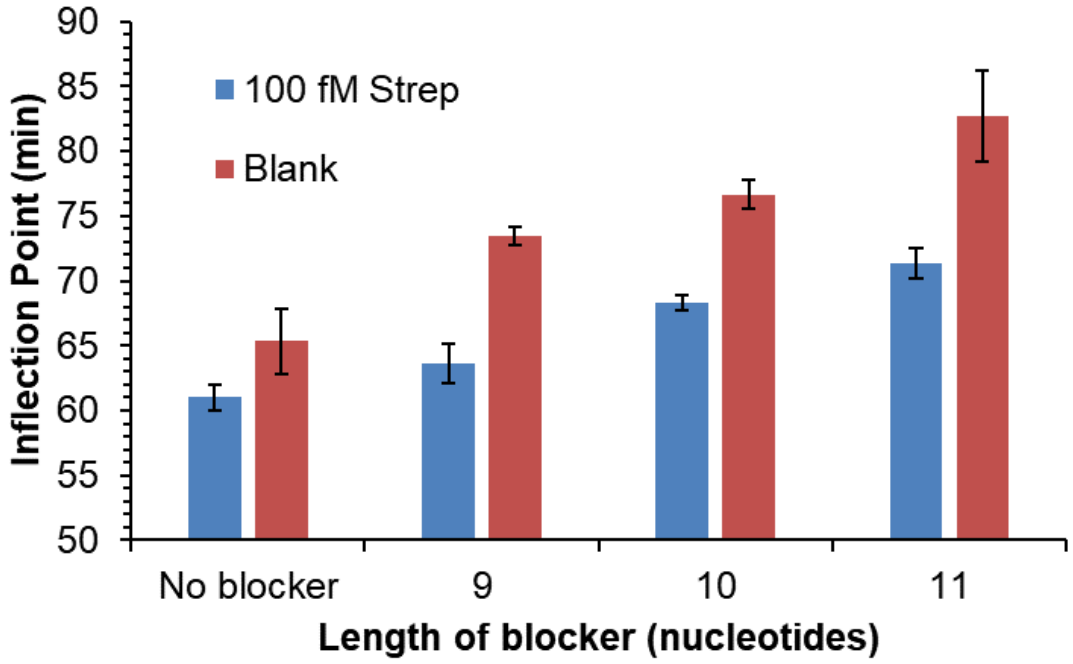

Figure 4.10 Effect of using blockers on BI-LAMP amplification. Blockers were incubated with probes prior to addition of target. The blockers were used at 10 nM (100X the probe concentrations). A shorter time to reach the amplification inflection point indicates faster amplification. Data shown is the mean ± standard deviation of triplicate experiments.

Using a 9-base blocker doubled the difference between the target and blank signals compared to no blocker, while only slowing the target specific signal by 3 min. Using a 10 or 11-base blocker showed no improvement to the target-to-blank signal difference, compared to the 9-base blocker, but it did slow the target specific signal. Therefore, a 9-

base blocker achieves the optimum performance that balances a fast reaction speed and a low background signal. Although the addition of a blocking oligo provided some reduction to background amplification, the reaction still is limited by the presence of background signal.

Table 4.2 Effect of blocker length on the inflection point difference between the target and blank signals

Blocker	**Inflection point difference (min)** (mean ± standard deviation)
No blocker	4 ± 3
9-base blocker	10 ± 2
10-base blocker	8 ± 1
11-base blocker	11 ± 4

There are two ways that background amplification can increase the detection limits of BI-LAMP. The first is from a slow target specific amplification that is unable to overcome a sufficiently slow background signal. The second reason is that the speed of the target specific amplification is adequate, but the background amplification is too fast and, therefore, limits the reaction. These two possibilities offer two different approaches to improve the reaction system: decrease the background amplification or increase the target specific amplification.

4.3.3 BI-LAMP positive controls

To assess the performance systems current conditions, two control reactions were designed. The first control uses a fully ligated dumbbell structure as the target to assess

the efficiency of LAMP amplification. The dumbbell structure was generated using a ssDNA positive control linker strand (**PCL**) to link **H1.3** and **H2** (Figure 4.11). One hundred nM of **H1.3**, **H2**, and **PCL** were used for ligation to ensure a high yield of the fully ligated dumbbell structure. The ligation reaction proceeded for 1 h at room temperature, followed by heat inactivation of ligase. The resulting 100 nM dumbbell was annealed under the same conditions as **P1** and **P2** to insure that the dumbbell secondary structure was formed. Then, the amplification reaction was performed under the same conditions as a standard BI-LAMP reaction in the absence of ligase, probes, and the 10 min ligation time at room temperature.

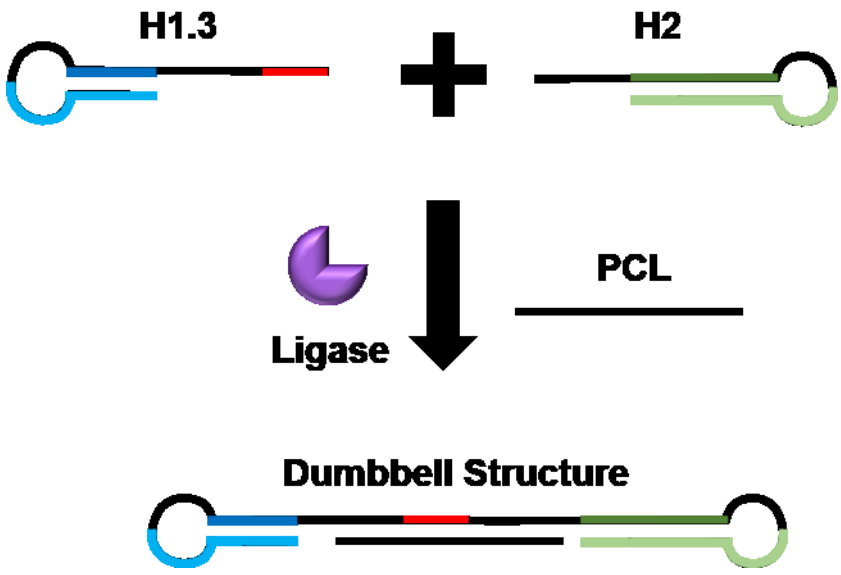

Figure 4.11 Illustration of the positive control linker DNA used to generate the dumbbell structure for LAMP. **PCL** anneals to both hairpins, enabling ligase to join **H1.3** to **H2**, creating the dumbbell structure.

Figure 4.12 shows the amplification profiles and calibration curve of this control reaction. The blank reaction contained FIP and BIP but no hairpins or probes. These results show that no background is generated in the absence of hairpins, indicating that FIP and BIP primers do not generate a primer–dimer like background and that the hairpin structures are required to generate any amplification signal. Further, these results show that as low as 10 aM of the dumbbell structure can be amplified and detected, which is 120 molecules of dumbbell oligo in 20 μL. This value gives a theoretical detection limit of a protein target when 100 % of target molecules are bound by probes and 100 % of target bound probes are ligated without any nonspecific ligation of unbound probes. While this scenario is not possible due to the dynamic and noncovalent nature of affinity binding between probes and target, as well as the dynamic nature of annealing between short complementary DNA, it gives a best-case scenario that additional reaction components can be compared with. Ten aM is 3–4 orders of magnitude lower than the current streptavidin detection, which demonstrates that the amplification efficiency of LAMP is sufficient for ultralow detection limits and does not contribute to the background amplification that limits BI-LAMP.

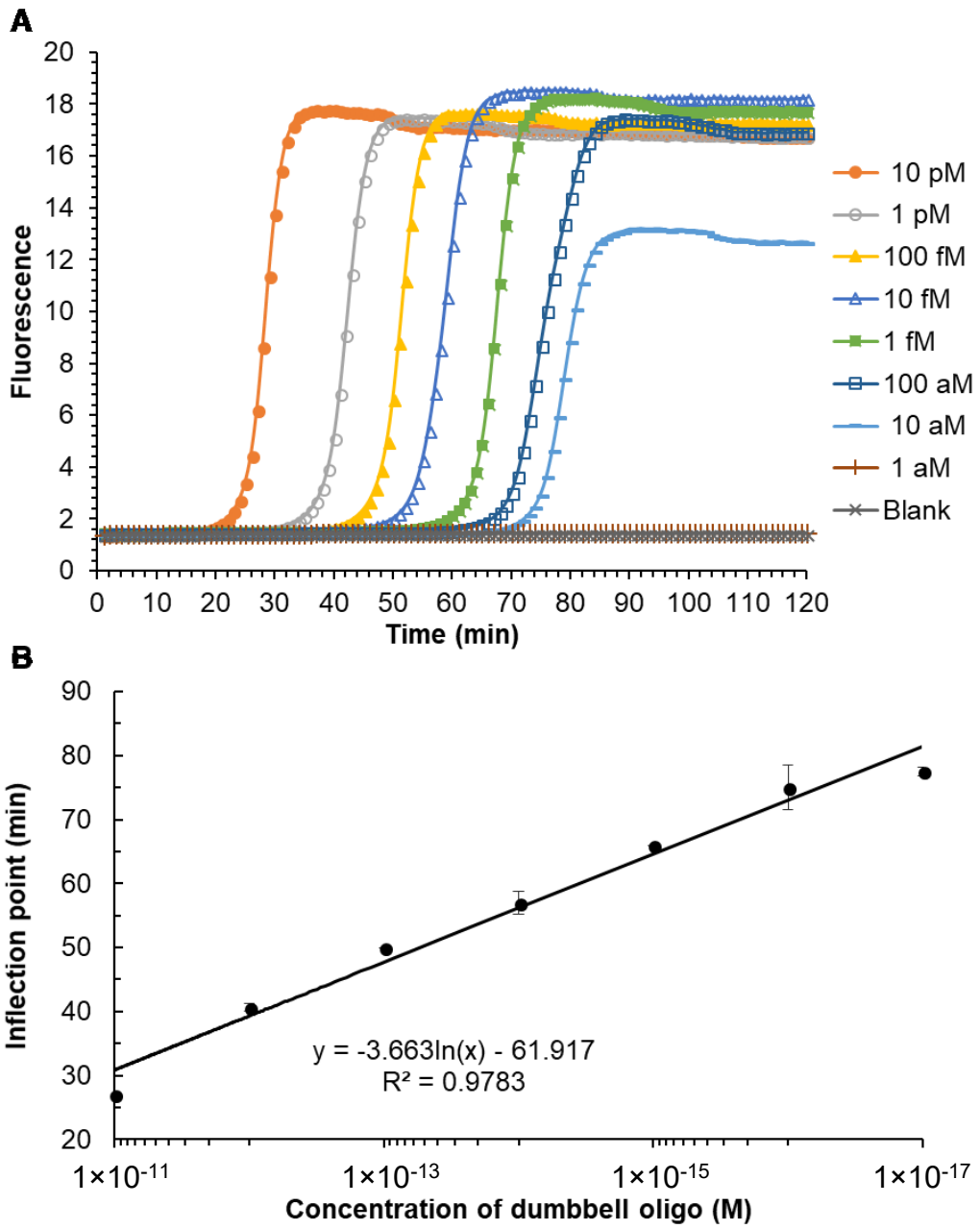

Figure 4.12 Dumbbell positive control to test the efficiency of LAMP amplification. (A) Amplification profiles with various starting concentrations of dumbbell oligo. (B) Calibration curve generated using the inflection point from amplification of varying concentration of dumbbell oligo. Data shown is the mean ± standard deviation of triplicate experiments

The second control reaction incorporates the ligation step of the BI-LAMP system but excludes the BINDA component by using **PCL** to directly link **H1.3** and **H2** for ligation (Figure 4.11). Unlike the first control reaction that used high concentrations and long ligations times, this reaction uses the same ligation time (10 min) and concentrations of hairpins (100 pM) as BI-LAMP. The blank of this reaction contains **H1.3** and **H2**, without **H1L** and **H2L**, and in the absence of **PCL**. Initial experiments showed that the blank of this control system generated a background, indicating that T4 ligase can generate the dumbbell structure nonspecifically by ligating small amounts of the single stranded 3′-end of **H1.3** to the single stranded 5′-end of **H2** in the absence of any linking

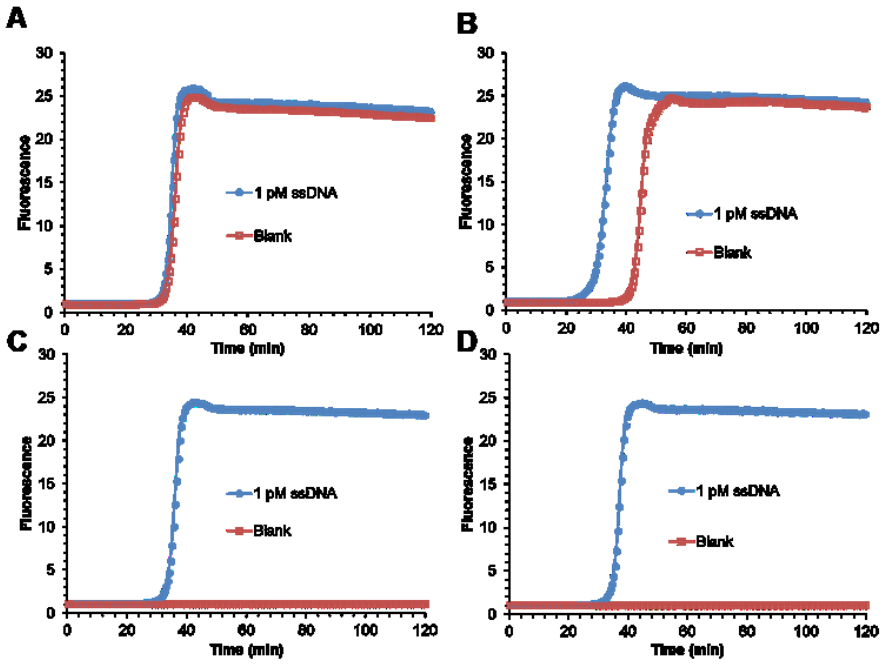

Figure 4.13 Effect of ligase concentration on nonspecific ligation of hairpins. (A) 4 U/µL T4 ligase (B) 0.4 U/µL T4 ligase (C) 0.04 U/µL T4 ligase (D) 0.004 U/µL T4 ligase

oligo. This nonspecific ligation of the two hairpins must be dependent on the amount ligase and the amount of hairpins present in solution. The concentration of hairpins was not investigated because too low a hairpin concentration would limit the dynamic range of the final BI-LAMP system. Figure 4.13 shows that lowering the concentration of ligase can eliminate nonspecific ligation of **H1.3** and **H2**. Using 0.04 U/μL T4 ligase, 1 fM to 10 pM of **PCL** generated amplification, and no background amplification was observed (Figure 4.14). Lower than 1 fM **PCL** showed a sporadic signal, where each replicate showed varied amplification or no amplification. This may be due to incomplete formation of the hybridization between **PCL**, **H1.3**, and **H2** or incomplete ligation at the low concentrations of target and ligase.

Figure 4.14 represents the ideal conditions for the BI-LAMP system, where hybridization between probes is stable when bound to the target but there is no nonspecific hybridization when the target is not present. However, using 0.04 U/μL of T4 ligase with a 5-base complementary region between probes resulted in sporadic signals of 10 fM of streptavidin, similar to the signals from less than 1 fM **PCL**. This may be due to weak duplex formation between **P1** and **P2** when a 5-base complementary region is used. Using IDT OligoAnalyzer 3.1, the estimated hairpin T_m of the 5-base complementary region is 25 °C. Thus, during the ligation phase at room temperature, approximately 50 % of bound probes are in a duplex formation. Since the 5-base complementary region between probes produces a transient duplex, the probes are associating and dissociating continually, which could result in incomplete ligation between **H1** and **H2** on target bound probes. At high concentrations of target (>10 fM)

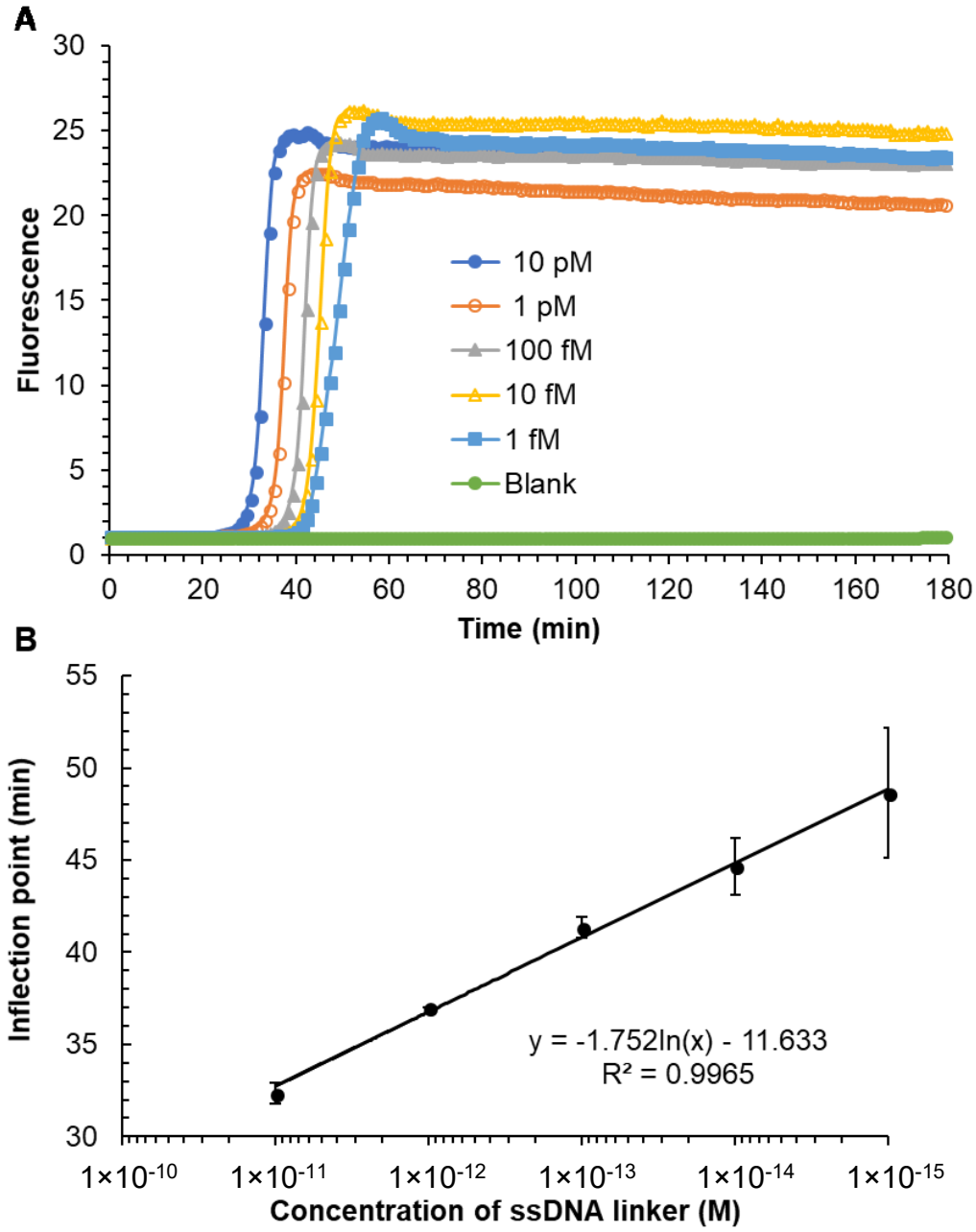

Figure 4.14 Positive control using PCL to link H1.3 and H2 for ligation. (A) Amplification profiles with various starting concentrations of ssDNA linker. (B) Calibration curve generated using the inflection point from amplification of varying concentrations of **PCL**. Data shown is the mean ± standard deviation of triplicate experiments

this is not an issue because there are so many bound probes that even if a small percentage of probes are ligated, they produce enough dumbbell structure to generate amplification. At low concentrations the efficiency of target bound probes being ligated to produce dumbbell structure becomes more critical.

From this observation, using the more stable 6-base complementary region may result in lower detection limits. The estimated T_m of the 6-base hairpin is 38 °C, considerably more stable at room temperature than the 5-base hairpin (25 °C). Although previous results show the 6-base probe resulting in a higher background signal (Figure 4.5), the more stable duplex formation between probes may result in a more efficient ligation of **H1** to **H2**, which becomes more critical when detecting lower concentrations of target. Furthermore, the background generated when using a 6-base complementary region may be lowered, compared to the results in Figure 4.5, if a lower concentrations of T4 ligase is used. If amplification from low concentration targets can be increased, it could improve the detection limits even with a faster background amplification.

Using a more stable interaction between probes also may increase the effectiveness of blockers. Blocker results with the 5-base complementary region showed approximately a 20-min decrease in background amplification using an 11-base blocker. However, the 11-base blocker decreased target specific amplification as well (Figure 4.10). The 5-base complementary region does not displace blocking oligos effectively because the probe duplex is weak, which means that blockers may need to passively dissociate from **P2** before **P1** can hybridize with **P2**. This leads to poor target specific amplification, particularly since blockers hybridized with **P2** can permanently become ligated if not displaced. Using a 6-base complementary region will result in a stable duplex

between target bound probes, which will have a greater ability to displace blockers and will prevent blockers from separating target bound probes that have formed duplexes.

4.4 Conclusions

A novel protein detection method has been developed based on binding induced ligation that triggers amplification via LAMP. This is the first work that takes advantage of LAMPs exceptional DNA amplification capabilities in a homogeneous format. The assay is procedurally simple, only requiring the addition of reagents at room temperature, followed by incubation at 65 °C. Several reaction parameters have been investigated and optimized. Using control reactions, 120 molecules of the ligated dumbbell product can be detected. Nonspecific ligation of probes is the main cause of background amplification and reducing the ligase concentration can decrease nonspecific ligation. Reducing the ligase concentration decreases the target specific ligation at low target concentrations. Further work is required to balance the ligase concentration and the strength of hybridization between probes for the detection of low concentrations of target. Although background amplification is present, this assay is capable of detecting 100 fM streptavidin. The design of the assay is complicated, but it may be adapted easily to detect other targets by simply changing affinity ligands, provided suitable affinity ligands are available.

Chapter 5: Conclusions and Future Works

I have explored the use of isothermal DNA amplification strategies for the development of protein and DNA detection tools. Specifically, I focused on designs with isothermal and homogeneous formats, with the potential to be adapted for point-of-care testing. Chapter 2 focused on using enzymatic nicking and strand displacement of DNA to generate a homogeneous and isothermally amplified signal for protein detection. Chapter 3 investigated the source of the high background amplification observed in EXPAR; several background blocking strategies were designed and tested. Chapter 4 detailed the development of an isothermal and homogeneous assay for proteins that achieves a highly amplified signal through the incorporation of LAMP.

The work performed in Chapter 2 focused on using BINDA to trigger amplification of DNA through enzymatic nicking and strand displacement reactions. Using this strategy I was able to detect 1 pM of streptavidin; this is comparable to a similar technique that uses a switching aptamer to trigger amplification.[152] To demonstrate the capability of this strategy to detect other targets, the target binding probes were modified to detect Her2 protein in buffer. To improve the sensitivity of the assay, EXPAR was incorporated into the reaction system to generate an exponentially amplified signal. After investigating EXPAR reaction parameters, I determined that the introduction of EXPAR into the reaction system generated large amounts of background amplification that limited the detection sensitivity of the system. To minimize the background generated from the EXPAR component of the reaction, the system was modified to have EXPAR occur at 55 °C; a higher temperature reduces nonspecific DNA interactions that could contribute to EXPAR generated background. After testing the reaction at a higher temperature, I

concluded that background amplification from the EXPAR component still limited the sensitivity of the assay.

All three strategies that were developed successfully triggered amplification of DNA from a non-nucleic acid target. Although these designs do not achieve detection limits as low as PLA and BINDA assays, which use PCR for amplification, these designs are advantageous because they do not require thermocycling. Furthermore, detection of protein targets in the low pM concentration range is comparable to ELISA, but these strategies achieve it with much faster (1 h vs. several hours) and simpler procedures.

All three detection systems could be adapted to generate a simple colour change for detection by using gold nanoparticles (AuNP).[147,185] In solution, AuNPs are red in colour, however, if an external stimulus causes the AuNPs to aggregate, they change to a blue/violet colour. Aggregation can be triggered by a linking DNA strand that is complementary to DNA anchored on AuNPs surfaces.[186] DNA functionalized AuNPs could be designed to aggregate in all three detection strategies by functionalizing the AuNPs with complementary sequences to the amplified ssDNA. Coupling AuNP colour change with the protein detection systems developed in Chapter 2 would produce simple visual detection techniques that only require a heating block. A visual detection system is ideal for POC analysis because it does not require instrumentation for detection.

Chapter 3 investigated the background amplification in EXPAR with two goals: firstly, to determine the triggering mechanism of background amplification, and secondly, to rationally design blocking strategies to prevent the triggering of background. Blocking mechanisms either targeted nonspecific 3′-end template interactions or interactions along the whole template sequence. Monitoring the effect of each blocker on target specific

amplification and background amplification allowed evaluation of what types of nonspecific DNA interactions contribute to the triggering of background amplification. Based on observations from only blocking the 3′-end of templates, nonspecific and transient 3′-end DNA interactions between templates trigger background amplification. Nonspecific interactions along the whole template sequence can increase the triggering of background amplification. From these observations, I was able to decrease the limit of detection of an EXPAR system by three orders of magnitude by introducing competitive binding of the whole template sequence. Furthermore, the binding of SSB to all ssDNA in a sample can reduce background amplification by blocking nonspecific interactions between the template and other nucleic acids present in biological samples. In addition, the low detection limit allows for dilution of samples, minimizing potential interference from complicated matrices present in biological samples.

Chapter 3 can be used to guide the design of additional background reduction strategies in EXPAR. Furthermore, the incorporation of single stranded DNA binding protein could be added to any standard EXPAR system to reduce background signal. This is advantageous because it only requires the addition of a single reagent, as opposed to having additional complicated design considerations.

Chapter 4 demonstrated the first system that incorporates the high performance of LAMP for a non-nucleic acid target, without the need for separation steps.Binding induced DNA assembly triggered the ligation of two DNA hairpins. The resulting ligation product was a dumbbell shaped DNA structure, the required starting structure for the cycling phase in LAMP. To estimate the efficiency of the LAMP component, control reactions were used, where only the dumbbell shaped DNA and primers were present in

the reaction mixture. This control showed that the LAMP component is capable of detecting 120 molecules of the dumbbell DNA. A linker DNA was designed to have strong hybridization (15 bases) to both hairpins to trigger the ligation of hairpins. This allowed evaluation of the ligation efficiency in the absence of the streptavidin probes, which could non-specifically hybridize, leading to background ligation. One fM linker DNA was capable of triggering ligation for an amplified signal. This control also revealed that the concentration of ligase used is critical to reduce background ligations. Further work in optimizing reaction parameters is required to achieve this strategy's full potential for ultrasensitive protein detection. Optimizing conditions, such as the strength of hybridization between probes (Mg^{2+} concentration, probe length, probe concentration) and the use of blockers (blocker length, blocker concentration) using low ligase concentrations, may result in improved performance, specifically, decreased background ligation of hairpins and increased target specific ligation of hairpins at ultralow concentrations.

It is possible to detect LAMP products visually by the appearance of a precipitate. Because of the large amount of dsDNA generated by LAMP, there is a large amount of pyrophosphate by-product that can precipitate with metal ions.[183] In this way, the BI-LAMP system could be used to determine the presence or absence of specific target proteins by the appearance of a precipitate. LAMP detection by coupling it with a commercial pregnancy test strip also has been achieved recently; this would result in a simple readout for POC testing.[67]

Each strategy described in this thesis uses isothermal and homogenous amplification; they all have the potential to be applied in a resource limited setting.

Adaptation of bioanalytical detection strategies to POC or field settings requires the long-term storage of reagents away from controlled facilities. In a laboratory setting, many reagents are stored in freezers or fridges to prevent thermal denaturation, oxidation, or hydrolysis; this is not possible in resource limited settings. One possible solution would be to dry all reaction components, by lyophilization, in the bottom of 0.2 mL PCR tubes. To perform the assay, a user would dissolve all reaction components in the tube by adding the sample and water, followed by brief mixing and placing in a handheld fluorometer with a heating block to monitor fluorescence. This could be performed with little instruction and be applied easily in remote or resource limited settings. If colorimetric signals are used, only a heating block would be required as the signal could be detected visually, and an estimated colour intensity could be used for quantitation.

While the drying of reagents in PCR tubes is possible, it only partially addresses the issue of reagent stability. To better address this issue, exciting work into the use of films and tablets for dry storage of reagents is being conducted. Lyophylization can be used to remove the water from reagents for dry storage, however, this process still results in some degradation of reagents. Recently, sugars have been added to stabilize reagents during lyophylization; this results in the production of thin films or tablets that have a glassy matrix.[187–190] These glassy matrices restrict the molecular mobility of reagents, which reduces the thermal instability, and by preventing the interaction of reagents with atmospheric oxygen or water vapour to prevent chemical degradation. Furthermore, glassy matrices have been shown to dissolve rapidly in water and have little or no effect on assay performance. These sugar-glasses increase the stability of enzymes, antibodies,

nucleic acids, polymer microspheres, and reactive organic molecules stored in film or tablet forms.[187–190]

References

(1) Murray, R. K.; Granner, D. C.; Mayes, P. A.; Rodwell, V. W. *Harper's Illustrated Biochemistry*; McGraw-Hill Companies: New York, 2003.

(2) Alberts, B.; Johnson, A.; Lewis, J.; Morgan, D.; Raff, M.; Roberts, K.; Walter, P. *Molecular Biology of the Cell*; Garland Science: New York, 2015.

(3) Trouillon, R.; Passarelli, M. K.; Wang, J.; Kurczy, M. E.; Ewing, A. G. Chemical Analysis of Single Cells. *Anal. Chem.* **2013**, *85*, 522–542.

(4) Chen, X.; Love, J. C.; Navin, N. E.; Pachter, L.; Stubbington, M. J. T.; Svensson, V.; Sweedler, J. V.; Teichmann, S. A. Single-Cell Analysis at the Threshold. *Nat. Biotechnol.* **2016**, *34*, 1111–1118.

(5) Wu, M.; Singh, A. K. Single-Cell Protein Analysis. *Curr. Opin. Biotechnol.* **2012**, *23*, 83–88.

(6) Mannello, F.; Ligi, D.; Magnani, M. Deciphering the Single-Cell Omic: Innovative Applications for Translational Medicine. *Expert Rev. Proteomics* **2012**, *9*, 635–648.

(7) Wills, Q. F.; Higgs, D. R.; Mead, A. J. Studying Epigenomics in Single Cells: What Is Feasible and What Can We Learn? *Epigenomics* **2015**, *7*, 1231–1234.

(8) *General Methods in Biomarker Research and Their Applications*; Preedy, V. R., Patel, V. B., Eds.; Springer: London, 2015.

(9) *Biomarkers in Cancer*; Preedy, V. R., Patel, V. B., Eds.; Springer: London, 2015.

(10) Ludwig, J. A.; Weinstein, J. N. Biomarkers in Cancer Staging, Prognosis and

Treatment Selection. *Nat. Rev. Cancer* **2005**, *5*, 845–856.

(11) Niemz, A.; Ferguson, T. M.; Boyle, D. S. Point-of-Care Nucleic Acid Testing for Infectious Diseases. *Trends Biotechnol.* **2011**, *29*, 240–250.

(12) Gubala, V.; Harris, L. F.; Ricco, A. J.; Tan, M. X.; Williams, D. E. Point of Care Diagnostics: Status and Future. *Anal. Chem.* **2012**, *84*, 487–515.

(13) Craw, P.; Balachandran, W. Isothermal Nucleic Acid Amplification Technologies for Point-of-Care Diagnostics: A Critical Review. *Lab Chip* **2012**, *12*, 2469–2486.

(14) Ahmad, F.; Hashsham, S. a. Miniaturized Nucleic Acid Amplification Systems for Rapid and Point-of-Care Diagnostics: A Review. *Anal. Chim. Acta* **2012**, *733*, 1–15.

(15) McNerney, R.; Daley, P. Towards a Point-of-Care Test for Active Tuberculosis: Obstacles and Opportunities. *Nat. Rev. Microbiol.* **2011**, *9*, 204–213.

(16) Zarei, M. Advances in Point-of-Care Technologies for Molecular Diagnostics. *Biosens. Bioelectron.* **2017**, *98*, 494–506.

(17) Zhang, L.; Ding, B.; Chen, Q.; Feng, Q.; Lin, L.; Sun, J. Point-of-Care-Testing of Nucleic Acids by Microfluidics. *Trends Anal. Chem.* **2017**, *94*, 106–116.

(18) Apweiler, R.; Aslanidis, C.; Deufel, T.; Gerstner, A.; Hansen, J.; Hochstrasser, D.; Kellner, R.; Kubicek, M.; Lottspeich, F.; Maser, E.; et al. Approaching Clinical Proteomics: Current State and Future Fields of Application in Fluid Proteomics. *Clin. Chem. Lab. Med.* **2009**, *47*, 724–744.

(19) Hayes, J.; Peruzzi, P. P.; Lawler, S. MicroRNAs in Cancer: Biomarkers, Functions

and Therapy. *Trends Mol. Med.* **2014**, *20*, 460–469.

(20) Anderson, N. L.; Anderson, N. G. The Human Plasma Proteome. *Mol. Cell. Proteomics* **2002**, *1*, 845–867.

(21) Zhang, H.; Li, F.; Dever, B.; Li, X. F.; Le, X. C. DNA-Mediated Homogeneous Binding Assays for Nucleic Acids and Proteins. *Chem. Rev.* **2013**, *113*, 2812–2841.

(22) Zhao, Y.; Chen, F.; Li, Q.; Wang, L.; Fan, C. Isothermal Amplification of Nucleic Acids. *Chem. Rev.* **2015**, *115*, 12491–12545.

(23) Zhang, D. Y.; Seelig, G. Dynamic DNA Nanotechnology Using Strand-Displacement Reactions. *Nat. Chem.* **2011**, *3*, 103–113.

(24) Watson, J. D.; Crick, Francis, H., D. A Structure for Deoxyribose Nucleic Acid. *Nature* **1953**, *171*, 737–738.

(25) Aldaye, F. A.; Palmer, A. L.; Sleiman, H. F. Assembling Materials with DNA as the Guide. *Science* **2008**, *321*, 1795–1799.

(26) Ellington, A. D.; Szostak, J. W. In Vitro Selection of RNA Molecules That Bind Specific Ligands. *Nature* **1990**, *346*, 818–822.

(27) Bock, L. C.; Griffin, L. C.; Latham, J. A.; Vermaas, E. H.; Toole, J. J. Selection of Single-Stranded DNA Molecules That Bind and Inhibit Human Thrombin. *Nature* **1992**, *355*, 564–566.

(28) Hernandez, L.; Machado, I.; Schafer, T.; Hernandez, F. Aptamers Overview: Selection, Features and Applications. *Curr. Top. Med. Chem.* **2015**, *15*, 1066–1081.

(29) Zhou, J.; Rossi, J. Aptamers as Targeted Therapeutics: Current Potential and Challenges. *Nat. Rev. Drug Discov.* **2017**, *16*, 181–202.

(30) Li, F.; Zhang, H.; Wang, Z.; Newbigging, A. M.; Reid, M. S.; Li, X. F.; Le, X. C. Aptamers Facilitating Amplified Detection of Biomolecules. *Anal. Chem.* **2015**, *87*, 274–292.

(31) Zhang, Y.; Li, Q.; Guo, L.; Huang, Q.; Shi, J.; Yang, Y.; Liu, D.; Fan, C. Ion-Mediated Polymerase Chain Reactions Performed with an Electronically Driven Microfluidic Device. *Angew. Chem. Int. Ed.* **2016**, *55*, 12450–12454.

(32) Wang, X.; Chen, F.; Zhang, D.; Zhao, Y.; Wei, J.; Wang, L.; Song, S.; Fan, C.; Zhao, Y. Single Copy-Sensitive Electrochemical Assay for Circulating Methylated DNA in Clinical Samples with Ultrahigh Specificity Based on a Sequential Discrimination–amplification Strategy. *Chem. Sci.* **2017**, *8*, 4764–4770.

(33) Chen, F.; Wang, X.; Cao, X.; Zhao, Y. Accurate Electrochemistry Analysis of Circulating Methylated DNA from Clinical Plasma Based on Paired-End Tagging and Amplifications. *Anal. Chem.* **2017**, *89*, 10468–10473.

(34) Saiki, R. K.; Scharf, S.; Faloona, F.; Mullis, K. B.; Horn, G. T.; Erlich, H. A.; Arnheim, N. Enzymatic Amplification of B-Globin Genomic Sequences and Restriction Site Analysis for Diagnosis of Sickle Cell Anemia. *Science* **1985**, *230*, 1350–1354.

(35) Asiello, P. J.; Baeumner, A. J. Miniaturized Isothermal Nucleic Acid Amplification, a Review. *Lab Chip* **2011**, *11*, 1420–1430.

(36) Compton, J. Nucleic Acid Sequence-Based Amplification. *Nature* **1991**, *350*, 91–92.

(37) Guatelli, J. C.; Whitfield, K. M.; Kwoh, D. Y.; Barringer, K. J.; Richman, D. D.; Gingeras, T. R. Isothermal, in Vitro Amplification of Nucleic Acids by a Multienzyme Reaction Modeled after Retroviral Replication. *Proc. Natl. Acad. Sci.* **1990**, *87*, 1874–1878.

(38) Gill, P.; Ghaemi, A. Nucleic Acid Isothermal Amplification Technologies: A Review. *Nucleosides. Nucleotides Nucleic Acids* **2008**, *27*, 224–243.

(39) Cook, N. The Use of NASBA for the Detection of Microbial Pathogens in Food and Environmental Samples. *J. Microbiol. Methods* **2003**, *53*, 165–174.

(40) Hønsvall, B. K.; Robertson, L. J. From Research Lab to Standard Environmental Analysis Tool : Will NASBA Make the Leap? *Water Res.* **2017**, *109*, 389–397.

(41) Vincent, M.; Xu, Y.; Kong, H. Helicase-Dependent Isothermal DNA Amplification. *EMBO Rep.* **2004**, *5*, 795–800.

(42) An, L.; Tang, W.; Ranalli, T. A.; Kim, H.; Wytiaz, J.; Kong, H. Characterization of a Thermostable UvrD Helicase and Its Participation in Helicase-Dependent Amplification. *J. Biol. Chem.* **2005**, *280*, 28952–28958.

(43) Motré, A.; Li, Y.; Kong, H. Enhancing Helicase-Dependent Amplification by Fusing the Helicase with the DNA Polymerase. *Gene* **2008**, *420*, 17–22.

(44) Jeong, Y. J.; Park, K.; Kim, D. E. Isothermal DNA Amplification in Vitro: The Helicase-Dependent Amplification System. *Cell. Mol. Life Sci.* **2009**, *66*, 3325–

3336.

(45) Piepenburg, O.; Williams, C. H.; Stemple, D. L.; Armes, N. A. DNA Detection Using Recombination Proteins. *PLoS Biol.* **2006**, *4*, 1115–1121.

(46) Lutz, S.; Weber, P.; Focke, M.; Faltin, B.; Hoffmann, J.; Claas, M.; Mark, D.; Munday, P.; Armes, N.; Piepenburg, O.; et al. Microfluidic Lab-on-a-Foil for Nucleic Acid Analysis Based on Isothermal Recombinase Polymerase Amplification (RPA). *Lab Chip* **2010**, *10*, 887–893.

(47) Shen, F.; Davydova, E. K.; Du, W.; Kreutz, J. E.; Piepenburg, O.; Ismagilov, R. F. Digital Isothermal Quantification of Nucleic Acids via Simultaneous Chemical Initiation of Recombinase Polymerase Amplification. *Anal. Chem.* **2011**, *83*, 3533–3540.

(48) Rohrman, B. A.; Richards-Kortum, R. R. A Paper and Plastic Device for Performing Recombinase Polymerase Amplification of HIV DNA. *Lab Chip* **2012**, *12*, 3082–3088.

(49) Daher, R. K.; Stewart, G.; Boissinot, M.; Boudreau, D. K.; Bergeron, M. G. Influence of Sequence Mismatches on the Specificity of Recombinase Polymerase Amplification Technology. *Mol. Cell. Probes* **2015**, *29*, 116–121.

(50) Daher, R. K.; Stewart, G.; Boissinot, M.; Bergeron, M. G. Recombinase Polymerase Amplification for Diagnostic Applications. *Clin. Chem.* **2016**, *62*, 947–958.

(51) Lillis, L.; Siverson, J.; Lee, A.; Cantera, J.; Parker, M.; Piepenburg, O.; Lehman,

D. A.; Boyle, D. S. Factors Influencing Recombinase Polymerase Amplification (RPA) Assay Outcomes at Point of Care. *Mol. Cell. Probes* **2016**, *30*, 74–78.

(52) Walker, G. T.; Little, M. C.; Nadeau, J. G.; Shank, D. D. Isothermal in Vitro Amplification of DNA by a Restriction Enzyme/DNA Polymerase System. *Proc. Natl. Acad. Sci. U. S. A.* **1992**, *89*, 392–396.

(53) Walker, G. T.; Fraiser, M. S.; Schram, J. L.; Little, M. C.; Nadeau, J. G.; Malinowski, D. P. Strand Displacement Amplification--an Isothermal, in Vitro DNA Amplification Technique. *Nucleic Acids Res.* **1992**, *20*, 1691–1696.

(54) Shi, C.; Liu, Q.; Zhong, W. Exponential Strand-Displacement Amplification for Detection of MicroRNAs. *Anal. Chem.* **2014**, *86*, 336–339.

(55) Lizardi, P. M.; Huang, X.; Zhu, Z.; Bray-Ward, P.; Thomas, D. C.; Ward, D. C. Mutation Detection and Single-Molecule Counting Using Isothermal Rolling-Circle Amplification. *Nat. Genet.* **1998**, *19*, 225–232.

(56) Murakami, T.; Sumaoka, J.; Komiyama, M. Sensitive Isothermal Detection of Nucleic-Acid Sequence by Primer Generation–rolling Circle Amplification. *Nucleic Acids Res.* **2009**, *37*, e19.

(57) Söderberg, O.; Gullberg, M.; Jarvius, M.; Ridderstrale, K.; Leuchowius, K.-J.; Jarvius, J.; Wester, K.; Hydbring, P.; Bahram, F.; Larsson, L.-G.; et al. Direct Observation of Individual Endogenous Protein Complexes in Situ by Proximity Ligation. *Nat. Methods* **2006**, *3*, 995–1000.

(58) Ali, M. M.; Li, F.; Zhang, Z.; Zhang, K.; Kang, D.-K.; Ankrum, J. A.; Le, X. C.;

Zhao, W. Rolling Circle Amplification: A Versatile Tool for Chemical Biology, Materials Science and Medicine. *Chem. Soc. Rev.* **2014**, *43*, 3324–3341.

(59) Zhao, W.; Ali, M. M.; Brook, M. A.; Li, Y. Rolling Circle Amplification: Applications in Nanotechnology and Biodetection with Functional Nucleic Acids. *Angew. Chem. Int. Ed.* **2008**, *47*, 6330–6337.

(60) Van Ness, J.; Van Ness, L. K.; Galas, D. J. Isothermal Reactions for the Amplification of Oligonucleotides. *Proc. Natl. Acad. Sci. U. S. A.* **2003**, *100*, 4504–4509.

(61) Mori, Y.; Kanda, H.; Notomi, T. Loop-Mediated Isothermal Amplification (LAMP): Recent Progress in Research and Development. *J. Infect. Chemother.* **2013**, *19*, 404–411.

(62) Notomi, T.; Mori, Y.; Tomita, N.; Kanda, H. Loop-Mediated Isothermal Amplification (LAMP): Principle, Features, and Future Prospects. *J. Microbiol.* **2015**, *53*, 1–5.

(63) Notomi, T.; Okayama, H.; Masubuchi, H.; Yonekawa, T.; Watanabe, K.; Amino, N.; Hase, T. Loop-Mediated Isothermal Amplification of DNA. *Nucleic Acids Res.* **2000**, *28*, e63.

(64) Mori, Y.; Nagamine, K.; Tomita, N.; Notomi, T. Detection of Loop-Mediated Isothermal Amplification Reaction by Turbidity Derived from Magnesium Pyrophosphate Formation. *Biochem. Biophys. Res. Commun.* **2001**, *289*, 150–154.

(65) Nagamine, K.; Hase, T.; Notomi, T. Accelerated Reaction by Loop-Mediated

Isothermal Amplification Using Loop Primers. *Mol. Cell. Probes* **2002**, *16*, 223–229.

(66) Fang, X.; Liu, Y.; Kong, J.; Jiang, X. Loop-Mediated Isothermal Amplification Integrated on Microfluidic Chips for Point-of-Care Quantitative Detection of Pathogens. *Anal. Chem.* **2010**, *82*, 3002–3006.

(67) Du, Y.; Pothukuchy, A.; Gollihar, J. D.; Nourani, A.; Li, B.; Ellington, A. D. Coupling Sensitive Nucleic Acid Amplification with Commercial Pregnancy Test Strips. *Angew. Chem. Int. Ed.* **2017**, *56*, 992–996.

(68) Hsieh, K.; Patterson, A. S.; Ferguson, B. S.; Plaxco, K. W.; Soh, H. T. Rapid, Sensitive, and Quantitative Detection of Pathogenic DNA at the Point of Care through Microfluidic Electrochemical Quantitative Loop-Mediated Isothermal Amplification. *Angew. Chem. Int. Ed.* **2012**, *51*, 4896–4900.

(69) Zhao, Y. Y.; Chen, F.; Qin, J.; Wei, J.; Wu, W.; Zhao, Y. Y. Engineered Janus Probes Modulate Nucleic Acid Amplification to Expand the Dynamic Range for Direct Detection of Viral Genomes in One Microliter Crude Serum Samples. *Chem. Sci.* **2018**, *9*, 392–397.

(70) Burchill, S.; Perebolte, L.; Johnston, C.; Top, B.; Selby, P. Comparison of the RNA-Amplification Based Methods RT–PCR and NASBA for the Detection of Circulating Tumour Cells. *Br. J. Cancer* **2002**, *86*, 102–109.

(71) Gracias, K. S.; McKillip, J. L. Nucleic Acid Sequence-Based Amplification (NASBA) in Molecular Bacteriology: A Procedural Guide. *J. Rapid Methods Autom. Microbiol.* **2007**, *15*, 295–309.

(72) Hill, C. S. Molecular Diagnostic Testing for Infectious Diseases Using TMA Technology. *Expert Rev. Mol. Diagn.* **2001**, *1*, 445–455.

(73) Li, J.; Macdonald, J. Advances in Isothermal Amplification: Novel Strategies Inspired by Biological Processes. *Biosens. Bioelectron.* **2014**, *64*, 196–211.

(74) Li, Y.; Jortani, S. A.; Ramey-Hartung, B.; Hudson, E.; Lemieux, B.; Kong, H. Genotyping Three SNPs Affecting Warfarin Drug Response by Isothermal Real-Time HDA Assays. *Clin. Chim. Acta* **2011**, *412*, 79–85.

(75) Chen, F.; Zhao, Y.; Fan, C.; Zhao, Y. Mismatch Extension of DNA Polymerases and High-Accuracy Single Nucleotide Polymorphism Diagnostics by Gold Nanoparticle-Improved Isothermal Amplification. *Anal. Chem.* **2015**, *87*, 8718–8723.

(76) Crannell, Z. A.; Rohrman, B.; Richards-Kortum, R. Quantification of HIV-1 DNA Using Real-Time Recombinase Polymerase Amplification. *Anal. Chem.* **2014**, *86*, 5615–5619.

(77) Rohrman, B.; Richards-Kortum, R. Inhibition of Recombinase Polymerase Amplification by Background Dna: A Lateral Flow-Based Method for Enriching Target DNA. *Anal. Chem.* **2015**, *87*, 1963–1967.

(78) Hellyer, T. J.; Nadeau, J. G. Strand Displacement Amplification: A Versatile Tool for Molecular Diagnostics. *Expert Rev. Mol. Diagn.* **2004**, *4*, 251–261.

(79) Van der Pol, B.; Ferrero, D. V.; Buck-Barrington, L.; Hook, E.; Lenderman, C.; Quinn, T.; Gaydos, C. A.; Lovchik, J.; Schachter, J.; Moncada, J.; et al. Multicenter

Evaluation of the BDProbeTec ET System for Detection of Chlamydia Trachomatis and Neisseria Gonorrhoeae in Urine Specimens, Female Endocervical Swabs, and Male Urethral Swabs. *J. Clin. Microbiol.* **2001**, *39*, 1008–1016.

(80) Chan, E. L.; Brandt, K.; Olienus, K.; Antonishyn, N.; Horsman, G. B. Performance Characteristics of the Becton Dickinson ProbeTec System for Direct Detection of Chlamydia Trachomatis and Neisseria Gonorrhoeae in Male and Female Urine Specimens in Comparison with Roche Cobas Systems. *Arch. Pathol. Lab. Med.* **2000**, *124*, 1649–1652.

(81) Cosentino, L. A.; Landers, D. V; Hillier, S. L. Detection of Chlamydia Trachomatis and Neisseria Gonorrhoeae by Strand Displacement Amplification and Relevance of the Amplification Control for Use with Vaginal Swab Specimens. *J. Clin. Microbiol.* **2003**, *41*, 3592–3596.

(82) Little, M. C.; Andrews, J.; Moore, R.; Bustos, S.; Jones, L.; Embres, C.; Durmowicz, G.; Harris, J.; Berger, D.; Yanson, K.; et al. Strand Displacement Amplification and Homogenous Real-Time Detection Incorporated into a Second-Generation DNA Probe System, BDProbeTecET. *Mol. Diagnostics Genet.* **1999**, *45*, 777–784.

(83) Liu, D.; Daubendiek, S. L.; Zillman, M. A.; Ryan, K.; Kool, E. T. Rolling Circle DNA Synthesis: Small Circular Oligonucleotides as Afficient Templates for DNA Polymerases. *J. Am. Chem. Soc.* **1996**, *118*, 1587–1594.

(84) Daubendiek, S. L.; Ryan, K.; Kool, E. T. Rolling-Circle RNA Synthesis: Circular Oligonucleotides as Efficient Substrates for T7 RNA Polymerase. *J. Am. Chem.*

Soc. **1995**, *117*, 7818–7819.

(85) Fire, A.; Xu, S. Q. Rolling Replication of Short DNA Circles. *Proc. Natl. Acad. Sci.* **1995**, *92*, 4641–4645.

(86) Parida, M.; Sannarangaiah, S.; Dash, P. K.; Rao, P. V. L.; Morita, K. Loop Mediated Isothermal Amplification (LAMP): A New Generation of Innovative Gene Amplification Technique; Perspectives in Clinical Diagnosis of Infectious Diseases. *Rev. Med. Virol.* **2008**, *18*, 407–421.

(87) Li, Y.; Fan, P.; Zhou, S.; Zhang, L. Loop-Mediated Isothermal Amplification (LAMP): A Novel Rapid Detection Platform for Pathogens. *Microb. Pathog.* **2017**, *107*, 54–61.

(88) Tien, D.; Nam, L.; Vu, T. Progress of Loop-Mediated Isothermal Amplification Technique in Molecular Diagnosis of Plant Diseases. *Appl. Biol. Chem.* **2017**, *60*, 169–180.

(89) Engvall, E.; Perlmann, P. Enzyme-Linked Immunosorbent Assay (ELISA) Quantitative Assay of Immunoglobulin G. *Immunochemistry* **1971**, *8*, 871–874.

(90) Engvall, E.; Perlmann, P. Enzyme-Linked Immunosorbent Assay, Elisa: III. Quantitation of Specific Antibodies by Anti-Immunoglobulin in Antigen-Coated Tubes. *J. Immunol.* **1972**, *109*, 129–135.

(91) Voller, A.; Bartlett, A.; Bidwell, D. E. Enzyme Immunoassays with Special Reference to ELISA Techniques. *J. Clin. Pathol.* **1978**, *31*, 507–520.

(92) Tighe, P. J.; Ryder, R. R.; Todd, I.; Fairclough, L. C. ELISA in the Multiplex Era:

Potentials and Pitfalls. *Proteomics Clin. Appl.* **2015**, *9*, 406–422.

(93) Belanger, L.; Sylvestre, C.; Dufour, D. Enzyme-Linked Immunoassay for Alpha-Fetoprotein by Competitive and Sandwich Procedures. *Clin. Chim. Acta* **1973**, *48*, 15–18.

(94) Sano, T.; Smith, C.; Cantor, C. Immuno-PCR: Very Sensitive Antigen Detection by Means of Specific Antibody-DNA Conjugates. *Science* **1992**, *258*, 120–122.

(95) Niemeyer, C. M.; Adler, M.; Wacker, R. Immuno-PCR: High Sensitivity Detection of Proteins by Nucleic Acid Amplification. *Trends Biotechnol.* **2005**, *23*, 208–216.

(96) Schweitzer, B.; Wiltshire, S.; Lambert, J.; O'Malley, S.; Kukanskis, K.; Zhu, Z.; Kingsmore, S. F.; Lizardi, P. M.; Ward, D. C. Immunoassays with Rolling Circle DNA Amplification: A Versatile Platform for Ultrasensitive Antigen Detection. *Proc. Natl. Acad. Sci.* **2000**, *97*, 10113–10119.

(97) Gusev, Y.; Sparkowski, J.; Raghunathan, A.; Ferguson, H.; Montano, J.; Bogdan, N.; Schweitzer, B.; Wiltshire, S.; Kingsmore, S. F.; Maltzman, W.; et al. Rolling Circle Amplification: A New Approach to Increase Sensitivity for Immunohistochemistry and Flow Cytometry. *Am. J. Pathol.* **2001**, *159*, 63–69.

(98) Zhao, X.; Dong, T.; Yang, Z.; Pires, N.; Høivik, N. Compatible Immuno-NASBA LOC Device for Quantitative Detection of Waterborne Pathogens: Design and Validation. *Lab Chip* **2012**, *12*, 602–612.

(99) Cao, H.; Fang, X.; Liu, P.; Li, H.; Chen, W.; Liu, B.; Kong, J. Magnetic-Immuno-Loop-Mediated Isothermal Amplification Based on DNA Encapsulating Liposome

for the Ultrasensitive Detection of P-Glycoprotein. *Sci. Rep.* **2017**, *7*, 1–7.

(100) Pourhassan-Moghaddam, M.; Rahmati-Yamchi, M.; Akbarzadeh, A.; Daraee, H.; Nejati-Koshki, K.; Hanifehpour, Y.; Joo, S. W. Protein Detection through Different Platforms of Immuno-Loop-Mediated Isothermal Amplification. *Nanoscale Res. Lett.* **2013**, *8*, 485–495.

(101) Zhang, H.; Li, X.; Le, X. C. Binding-Induced DNA Assembly and Its Application to Yoctomole Detection of Proteins. *Anal. Chem.* **2012**, *84*, 877–884.

(102) Zhang, H.; Li, F.; Dever, B.; Wang, C.; Li, X. F.; Le, X. C. Assembling DNA through Affinity Binding to Achieve Ultrasensitive Protein Detection. *Angew. Chem. Int. Ed.* **2013**, *52*, 10698–10705.

(103) Li, F.; Zhang, H.; Lai, C.; Li, X. F.; Le, X. C. A Molecular Translator That Acts by Binding-Induced DNA Strand Displacement for a Homogeneous Protein Assay. *Angew. Chem. Int. Ed.* **2012**, *51*, 9317–9320.

(104) Li, F.; Lin, Y.; Le, X. C. Binding-Induced Formation of DNA Three-Way Junctions and Its Application to Protein Detection and DNA Strand Displacement. *Anal. Chem.* **2013**, *85*, 10835–10841.

(105) Zhang, H.; Lai, M.; Zuehlke, A.; Peng, H.; Li, X. F.; Le, X. C. Binding-Induced DNA Nanomachines Triggered by Proteins and Nucleic Acids. *Angew. Chem. Int. Ed.* **2015**, *54*, 1426–14330.

(106) Li, F.; Zhang, H.; Wang, Z.; Li, X.; Li, X.; Le, X. C. Dynamic DNA Assemblies Mediated by Binding-Induced DNA Strand Displacement. *J. Am. Chem. Soc.* **2013**,

135, 2443–2446.

(107) Chen, J.; Zuehlke, A.; Deng, B.; Peng, H.; Hou, X.; Zhang, H. A Target-Triggered DNAzyme Motor Enabling Homogeneous, Amplified Detection of Proteins. *Anal. Chem.* **2017**, *89*, 12888–12895.

(108) Li, J.; Zhong, X.; Zhang, H.; Le, X. C.; Zhu, J. J. Binding-Induced Fluorescence Turn-on Assay Using Aptamer-Functionalized Silver Nanocluster DNA Probes. *Anal. Chem.* **2012**, *84*, 5170–5174.

(109) Hu, J.; Wang, T.; Kim, J.; Shannon, C.; Easley, C. J. Quantitation of Femtomolar Protein Levels via Direct Readout with the Electrochemical Proximity Assay. *J. Am. Chem. Soc.* **2012**, *134*, 7066–7072.

(110) Heyduk, E.; Heyduk, T. Nucleic Acid-Based Fluorescence Sensors for Detecting Proteins. *Anal. Chem.* **2005**, *77*, 1147–1156.

(111) Heyduk, E.; Dummit, B.; Chang, Y.-H.; Heyduk, T. Molecular Pincers: Antibody-Based Homogenous Protein Sensors. *Anal. Chem.* **2008**, *80*, 5152–5159.

(112) Tian, L.; Heyduk, T. Antigen Peptide-Based Immunosensors for Rapid Detection of Antibodies and Antigens. *Anal. Chem.* **2009**, *81*, 5218–5225.

(113) Lass-Napiorkowska, A.; Heyduk, E.; Tian, L.; Heyduk, T. Detection Methodology Based on Target Molecule-Induced Sequence-Specific Binding to a Single-Stranded Oligonucleotide. *Anal. Chem.* **2012**, *84*, 3382–3389.

(114) Heyduk, E.; Moxley, M. M.; Salvatori, A.; Corbett, J. A.; Heyduk, T. Homogeneous Insulin and C-Peptide Sensors for Rapid Assessment of Insulin and

C-Peptide Secretion by the Islets. *Diabetes* **2010**, *59*, 2360–2365.

(115) Tang, Y.; Wang, Z.; Yang, X.; Chen, J.; Liu, L.; Zhao, W.; Le, X. C.; Li, F. Constructing Real-Time, Wash-Free, and Reiterative Sensors for Cell Surface Proteins Using Binding-Induced Dynamic DNA Assembly. *Chem. Sci.* **2015**, *6*, 5729–5733.

(116) Fredriksson, S.; Gullberg, M.; Jarvius, J.; Olsson, C.; Pietras, K.; Gústafsdóttir, S. M.; Östman, A.; Landegren, U. Protein Detection Using Proximity-Dependent DNA Ligation Assays. *Nat. Biotechnol.* **2002**, *20*, 473–477.

(117) Schallmeiner, E.; Oksanen, E.; Ericsson, O.; Spangberg, L.; Eriksson, S.; Stenman, U.-H.; Pettersson, K.; Landegren, U. Sensitive Protein Detection via Triple-Binder Proximity Ligation Assays. *Nat. Methods* **2007**, *4*, 135–137.

(118) Kim, J.; Hu, J.; Sollie, R. S.; Easley, C. J. Improvement of Sensitivity and Dynamic Range in Proximity Ligation Assays by Asymmetric Connector Hybridization. *Anal. Chem.* **2010**, *82*, 6976–6982.

(119) Gullberg, M.; Fredriksson, S.; Taussig, M.; Jarvius, J.; Gustafsdottir, S.; Landegren, U. A Sense of Closeness: Protein Detection by Proximity Ligation. *Curr. Opin. Biotechnol.* **2003**, *14*, 82–86.

(120) Gustafsdottir, S. M.; Nordengrahn, A.; Fredriksson, S.; Wallgren, P.; Rivera, E.; Schallmeiner, E.; Merza, M.; Landegren, U. Detection of Individual Microbial Pathogens by Proximity Ligation. *Clin. Chem.* **2006**, *52*, 1152–1160.

(121) Fredriksson, S.; Horecka, J.; Brustugun, O. T.; Schlingemann, J.; Koong, A. C.;

Tibshirani, R.; Davis, R. W. Multiplexed Proximity Ligation Assays to Profile Putative Plasma Biomarkers Relevant to Pancreatic and Ovarian Cancer. *Clin. Chem.* **2008**, *54*, 582–589.

(122) Liu, B.; Zhang, B.; Chen, G.; Yang, H.; Tang, D. Proximity Ligation Assay with Three-Way Junction-Induced Rolling Circle Amplification for Ultrasensitive Electronic Monitoring of Concanavalin A. *Anal. Chem.* **2014**, *86*, 7773–7781.

(123) Gajadhar, A.; Guha, A. A Proximity Ligation Assay Using Transiently Transfected, Epitope-Tagged Proteins: Application for in Situ Detection of Dimerized Receptor Tyrosine Kinases. *Biotechniques* **2010**, *48*, 145–152.

(124) Zieba, A.; Wählby, C.; Hjelm, F.; Jordan, L.; Berg, J.; Landegren, U.; Pardali, K. Bright-Field Microscopy Visualization of Proteins and Protein Complexes by in Situ Proximity Ligation with Peroxidase Detection. *Clin. Chem.* **2010**, *56*, 99–110.

(125) Leuchowius, K.-J.; Jarvius, M.; Wickström, M.; Rickardson, L.; Landegren, U.; Larsson, R.; Söderberg, O.; Fryknäs, M.; Jarvius, J. High Content Screening for Inhibitors of Protein Interactions and Post-Translational Modifications in Primary Cells by Proximity Ligation. *Mol. Cell. Proteomics* **2010**, *9*, 178–183.

(126) Aubele, M.; Spears, M.; Ludyga, N.; Braselmann, H.; Feuchtinger, A.; Taylor, K. J.; Lindner, K.; Auer, G.; Stering, K.; Höfler, H.; et al. In Situ Quantification of HER2-Protein Tyrosine Kinase 6 (PTK6) Protein-Protein Complexes in Paraffin Sections from Breast Cancer Tissues. *Br. J. Cancer* **2010**, *103*, 663–667.

(127) Darmanis, S.; Nong, R. Y.; Vänelid, J.; Siegbahn, A.; Ericsson, O.; Fredriksson, S.; Bäcklin, C.; Gut, M.; Heath, S.; Gut, I. G.; et al. ProteinSeq: High-Performance

Proteomic Analyses by Proximity Ligation and next Generation Sequencing. *PLoS One* **2011**, *6*, e25583.

(128) Ghanipour, L.; Darmanis, S.; Landegren, U.; Glimelius, B.; Påhlman, L.; Birgisson, H. Detection of Biomarkers with Solid-Phase Proximity Ligation Assay in Patients with Colorectal Cancer. *Transl. Oncol.* **2016**, *9*, 251–255.

(129) Blokzijl, A.; Nong, R.; Darmanis, S.; Hertz, E.; Landegren, U.; Kamali-Moghaddam, M. Protein Biomarker Validation via Proximity Ligation Assays. *Biochim. Biophys. Acta* **2014**, *1844*, 933–939.

(130) Giusto, D. A. Di; Wlassoff, W. A.; Gooding, J. J.; Messerle, B. A.; King, G. C. Proximity Extension of Circular DNA Aptamers with Real-Time Protein Detection. *Nucleic Acids Res.* **2005**, *33*, e64.

(131) Avin, A.; Levy, M.; Porat, Z.; Abramson, J. Quantitative Analysis of Protein-Protein Interactions and Post-Translational Modifications in Rare Immune Populations. *Nat. Commun.* **2017**, *8*, 1524–1533.

(132) Zhang, Z. Z.; Zhang, C. Y. Highly Sensitive Detection of Protein with Aptamer-Based Target-Triggering Two-Stage Amplification. *Anal. Chem.* **2012**, *84*, 1623–1629.

(133) Zipper, H.; Brunner, H.; Bernhagen, J.; Vitzthum, F. Investigations on DNA Intercalation and Surface Binding by SYBR Green I, Its Structure Determination and Methodological Implications. *Nucleic Acids Res.* **2004**, *32*, e103.

(134) Deng, H.; Gao, Z. Bioanalytical Applications of Isothermal Nucleic Acid

Amplification Techniques. *Anal. Chim. Acta* **2015**, *853*, 30–45.

(135) Reid, M. S.; Le, X. C.; Zhang, H. Exponential Isothermal Amplification of Nucleic Acids and Amplified Assays for Proteins, Cells, and Enzyme Activities. *Angew. Chem. Int. Ed.* **2018**, DOI:10.1002/anie.201712217.

(136) Shen, Y.; Tian, F.; Chen, Z.; Li, R.; Ge, Q.; Lu, Z. Amplification-Based Method for MicroRNA Detection. *Biosens. Bioelectron.* **2015**, *71*, 322–331.

(137) Graybill, R. M.; Bailey, R. C. Emerging Biosensing Approaches for MicroRNA Analysis. *Anal. Chem.* **2016**, *88*, 431–450.

(138) Yu, Y.; Chen, Z.; Shi, L.; Yang, F.; Pan, J.; Zhang, B.; Sun, D. Ultrasensitive Electrochemical Detection of MicroRNA Based on an Arched Probe Mediated Isothermal Exponential Amplification. *Anal. Chem.* **2014**, *86*, 8200–8205.

(139) Yan, Y.; Zhao, D.; Yuan, T.; Hu, J.; Zhang, D.; Cheng, W.; Zhang, W.; Ding, S. A Simple and Highly Sensitive Electrochemical Biosensor for MicroRNA Detection Using Target-Assisted Isothermal Exponential Amplification Reaction. *Electroanalysis* **2013**, *25*, 2354–2359.

(140) Ye, L.-P.; Hu, J.; Liang, L.; Zhang, C. Surface-Enhanced Raman Spectroscopy for Simultaneous Sensitive Detection of Multiple MicroRNAs in Lung Cancer Cells. *Chem. Comm.* **2014**, *50*, 11883–11886.

(141) Zhang, Y.; Hu, J.; Zhang, C. Sensitive Detection of Transcription Factors by Isothermal Exponential Amplification-Based Colorimetric Assay. *Anal. Chem.* **2012**, *84*, 9544–9549.

(142) Wang, K.; Zhang, K.; Lv, Z.; Zhu, X.; Zhu, L.; Zhou, F. Ultrasensitive Detection of MicroRNA with Isothermal Amplification and a Time-Resolved Fluorescence Sensor. *Biosens. Bioelectron.* **2014**, *57*, 91–95.

(143) Wang, G.; Zhang, C. Sensitive Detection of MicroRNAs with Hairpin Probe-Based Circular Exponential Amplification Assay. *Anal. Chem.* **2012**, *84*, 7037–7042.

(144) Zhang, X.; Liu, C.; Sun, L.; Duan, X.; Li, Z. Lab on a Single Microbead: An Ultrasensitive Detection Strategy Enabling MicroRNA Analysis at the Single-Molecule Level. *Chem. Sci.* **2015**, *6*, 6213–6218.

(145) Liu, Y.; Zhang, M.; Yin, B.; Ye, B. Attomolar Ultrasensitive MicroRNA Detection by DNA-Scaffolded Silver-Nanocluster Probe Based on Isothermal Amplification. *Anal. Chem.* **2012**, *84*, 5165–5169.

(146) Chen, J.; Zhou, X.; Ma, Y.; Lin, X.; Dai, Z.; Zou, X. Asymmetric Exponential Amplification Reaction on a Toehold/Biotin Featured Template: An Ultrasensitive and Specific Strategy for Isothermal MicroRNAs Analysis. *Nucleic Acids Res.* **2016**, *44*, e130.

(147) Tan, E.; Wong, J.; Nguyen, D.; Zhang, Y. Y. Y.; Erwin, B.; Van Ness, L. K.; Baker, S. M.; Galas, D. J.; Niemz, A. Isothermal DNA Amplification Coupled with DNA Nanosphere-Based Colorimetric Detection. *Anal. Chem.* **2005**, *77*, 7984–7992.

(148) Nie, J.; Zhang, D.-W. W.; Tie, C.; Zhou, Y.-L. L.; Zhang, X.-X. X. G-Quadruplex Based Two-Stage Isothermal Exponential Amplification Reaction for Label-Free DNA Colorimetric Detection. *Biosens. Bioelectron.* **2014**, *56*, 237–242.

(149) Wang, J.; Zou, B.; Rui, J.; Song, Q.; Kajiyama, T.; Kambara, H.; Zhou, G. Exponential Amplification of DNA with Very Low Background Using Graphene Oxide and Single-Stranded Binding Protein to Suppress Non-Specific Amplification. *Microchim. Acta* **2015**, *182*, 1095–1101.

(150) Yu, Y.; Chen, Z.; Jian, W.; Sun, D.; Zhang, B.; Li, X.; Yao, M. Ultrasensitive Electrochemical Detection of Avian Influenza A (H7N9) Virus DNA Based on Isothermal Exponential Amplification Coupled with Hybridization Chain Reaction of DNAzyme Nanowires. *Biosens. Bioelectron.* **2015**, *64*, 566–571.

(151) Xie, S.; Chai, Y.; Yuan, Y.; Bai, L.; Yuan, R. A Novel Electrochemical Aptasensor for Highly Sensitive Detection of Thrombin Based on the Autonomous Assembly of Hemin/G-Quadruplex Horseradish Peroxidase-Mimicking DNAzyme Nanowires. *Anal. Chim. Acta* **2014**, *832*, 51–57.

(152) Zhang, Z. Z.; Zhang, C. Y. Highly Sensitive Detection of Protein with Aptamer-Based Target-Triggering Two-Stage Amplification. *Anal. Chem.* **2012**, *84*, 1623–1629.

(153) Wang, L.; Zhang, Y.; Zhang, C. A Target-Triggered Exponential Amplification-Based DNAzyme Biosensor for Ultrasensitive Detection of Folate Receptors. *Chem. Comm.* **2014**, *50*, 15393–15396.

(154) He, P.; Zhang, Y.; Liu, L.; Qiao, W.; Zhang, S. Ultrasensitive SERS Detection of Lysozyme by a Target-Triggering Multiple Cycle Amplification Strategy Based on a Gold Substrate. *Chem. Eur. J.* **2013**, *19*, 7452–7460.

(155) Ma, F.; Yang, Y.; Zhang, C. Ultrasensitive Detection of Transcription Factors

Using Transcription-Mediated Isothermally Exponential Amplification-Induced Chemiluminescence. *Anal. Chem.* **2014**, *86*, 6006–6011.

(156) Wang, L.; Zhang, Y.; Zhang, C. Ultrasensitive Detection of Telomerase Activity at the Single-Cell Level. *Anal. Chem.* **2013**, *85*, 11509–11517.

(157) Jia, H.; Wang, Z.; Wang, C.; Chang, L.; Li, Z. Real-Time Fluorescence Detection of Hg2+ Ions with High Sensitivity by Exponentially Isothermal Oligonucleotide Amplification. *RSC Adv.* **2014**, *4*, 9439–9444.

(158) Tan, E.; Erwin, B.; Dames, S.; Ferguson, T.; Buechel, M.; Irvine, B.; Voelkerding, K.; Niemz, A. Specific versus Nonspecific Isothermal DNA Amplification through Thermophilic Polymerase and Nicking Enzyme Activities. *Biochemistry* **2008**, *47*, 9987–9999.

(159) Qian, J.; Ferguson, T. M.; Shinde, D. N.; Ramírez-Borrero, A. J.; Hintze, A.; Adami, C.; Niemz, A. Sequence Dependence of Isothermal DNA Amplification via EXPAR. *Nucleic Acids Res.* **2012**, *40*, e87.

(160) Dames, S.; Margraf, R. L.; Pattison, D. C.; Wittwer, C. T.; Voelkerding, K. V. Characterization of Aberrant Melting Peaks in Unlabeled Probe Assays. *J. Mol. Diagn.* **2007**, *9*, 290–296.

(161) Sen, A.; Nielsen, P. E. On the Stability of Peptide Nucleic Acid Duplexes in the Presence of Organic Solvents. *Nucleic Acids Res.* **2007**, *35*, 3367–3374.

(162) Chester, N.; Marshak, D. R. Dimethyl Sulfoxide-Mediated Primer Tm Reduction-A Method for Analyzing the Role of Renaturation Temperature in the Polymerase

Chain Reaction. *Anal. Biochem.* **1993**, *209*, 284–290.

(163) Sorokin, V. A.; Gladchenko, G. O.; Valeev, V. A.; Sysa, I. V.; Petrova, L. G.; Blagoi, Y. P. Effect of Salt and Organic Solvents on DNA Thermal Stability and Structure. *J. Mol. Struct.* **1997**, *408/409*, 237–240.

(164) Wang, C.; Altieri, F.; Ferraro, A.; Giartosio, A.; Turano, C. The Effect of Polyols on the Stability of Duplex DNA. *Physiol. Chem. Phys. Med. NMR* **1993**, *25*, 273–280.

(165) Sigal, N.; Delius, H.; Kornberg, T.; Gefter, M. L.; Alberts, B. A DNA-Unwinding Protein Isolated from Escherichia Coli: Its Interaction with DNA and with DNA Polymerases. *Proc. Natl. Acad. Sci. U. S. A.* **1972**, *69*, 3537–3541.

(166) Meyer, R. R.; Laine, P. S. The Single-Stranded DNA-Binding Protein of Escherichia Coli. *Microbiol. Rev.* **1990**, *54*, 342–380.

(167) Raghunathan, S.; Kozlov, A. G.; Lohman, T. M.; Waksman, G. Structure of the DNA Binding Domain of E. Coli SSB Bound to SsDNA. *Nat. Struct. Biol.* **2000**, *7*, 648–652.

(168) Kozlov, A. G.; Lohman, T. M. E. Coli SSB Tetramer Binds the First and Second Molecules of (DT) 35 with Heat Capacities of Opposite Sign. *Biophys. Chem.* **2011**, *159*, 48–57.

(169) Maffeo, C.; Aksimentiev, A. Molecular Mechanism of DNA Association with Single-Stranded DNA Binding Protein. *Nucleic Acids Res.* **2017**, *45*, 12125–12139.

(170) Hamon, L.; Pastré, D.; Dupaigne, P.; Le Breton, C.; Le Cam, E.; Piétrement, O.;

Breton, C. Le; Cam, E. Le; Pie, O.; Inserm, U. High-Resolution AFM Imaging of Single-Stranded DNA-Binding (SSB) Protein - DNA Complexes. *Nucleic Acids Res.* **2007**, *35*, e58.

(171) Cullen, B. R.; Bick, M. D. Thermal Denaturation of DNA from Bromodeoxyuridine Substituted Cells. *Nucleic Acids Res.* **1976**, *3*, 49–62.

(172) Liu, C.; Geva, E.; Mauk, M.; Qiu, X.; Abrams, W. R.; Malamud, D.; Curtis, K.; Owen, S. M.; Bau, H. H. An Isothermal Amplification Reactor with an Integrated Isolation Membrane for Point-of-Care Detection of Infectious Diseases. *Analyst* **2011**, *136*, 2069.

(173) Jung, J. H.; Park, B. H.; Oh, S. J.; Choi, G.; Seo, T. S. Integrated Centrifugal Reverse Transcriptase Loop-Mediated Isothermal Amplification Microdevice for Influenza A Virus Detection. *Biosens. Bioelectron.* **2015**, *68*, 218–224.

(174) Niessen, L.; Vogel, R. F. Detection of Fusarium Graminearum DNA Using a Loop-Mediated Isothermal Amplification (LAMP) Assay. *Int. J. Food Microbiol.* **2010**, *140*, 183–191.

(175) Yoneda, A.; Taniguchi, K.; Torashima, Y.; Susumu, S.; Kanetaka, K.; Kuroki, T.; Eguchi, S. The Detection of Gastric Cancer Cells in Intraoperative Peritoneal Lavage Using the Reverse Transcription-Loop-Mediated Isothermal Amplification Method. *J. Surg. Res.* **2014**, *187*, e1–e6.

(176) Nakamura, N.; Ito, K.; Takahashi, M.; Hashimoto, K.; Kawamoto, M.; Yamanaka, M.; Taniguchi, A.; Kamatani, N.; Gemma, N. Detection of Six Single-Nucleotide Polymorphisms Associated with Rheumatoid Arthritis by a Loop-Mediated

Isothermal Amplification Method and an Electrochemical DNA Chip. *Anal. Chem.* **2007**, *79*, 9484–9493.

(177) Hua, X.; Yin, W.; Shi, H.; Li, M.; Wang, Y.; Wang, H.; Ye, Y.; Kim, H. J.; Gee, S. J.; Wang, M.; et al. Development of Phage Immuno-Loop-Mediated Isothermal Amplification Assays for Organophosphorus Pesticides in Agro-Products. *Anal. Chem.* **2014**, *86*, 8441–8447.

(178) Hirayama, H.; Kageyama, S.; Takahashi, Y.; Moriyasu, S.; Sawai, K.; Onoe, S.; Watanabe, K.; Kojiya, S.; Notomi, T.; Minamihashi, A. Rapid Sexing of Water Buffalo (Bubalus Bubalis) Embryos Using Loop-Mediated Isothermal Amplification. *Theriogenology* **2006**, *66*, 1249–1256.

(179) Hirayama, H.; Kageyama, S.; Moriyasu, S.; Sawai, K.; Onoe, S.; Takahashi, Y.; Katagiri, S.; Toen, K.; Watanabe, K.; Notomi, T.; et al. Rapid Sexing of Bovine Preimplantation Embryos Using Loop-Mediated Isothermal Amplification. *Theriogenology* **2004**, *62*, 887–896.

(180) Almasi, M. A.; Almasi, G. Loop Mediated Isothermal Amplification (LAMP) for Embryo Sex Determination in Pregnant Women at Eight Weeks of Pregnancy. *J. Reprod. Infertil.* **2017**, *18*, 197–204.

(181) Cao, H.; Fang, X.; Li, H.; Li, H.; Kong, J. Ultrasensitive Detection of Mucin 1 Biomarker by Immuno-Loop-Mediated Isothermal Amplification. *Talanta* **2017**, *164*, 588–592.

(182) Burbulis, I. E.; Yamaguchi, K.; Nikolskaia, O. V.; Prigge, S. T.; Magez, S.; Bisser, S.; Reller, M. E.; Grab, D. J. Detection of Pathogen-Specific Antibodies by Loop-

Mediated Isothermal Amplification. *Clin. Vaccine Immunol.* **2015**, *22*, 374–380.

(183) Tomita, N.; Mori, Y.; Kanda, H.; Notomi, T. Loop-Mediated Isothermal Amplification (LAMP) of Gene Sequences and Simple Visual Detection of Products. *Nat. Protoc.* **2008**, *3*, 877–882.

(184) Kuhn, H.; Frank-kamenetskii, M. D. Template-Independent Ligation of Single-Stranded DNA by T4 DNA Ligase. *FEBS J.* **2005**, *272*, 5991–6000.

(185) Tan, E.; Erwin, B.; Dames, S.; Voelkerding, K.; Niemz, A. Isothermal DNA Amplification with Gold Nanosphere- Based Visual Colorimetric Readout for Herpes Simplex Virus Detection. *Clin. Chem.* **2007**, *53*, 2017–2020.

(186) Mirkin, C. A.; Letsinger, R. L.; Mucic, R. C.; Storhoff, J. J. A DNA-Based Method for Rationally Assembling Nanoparticles into Macroscopic Materials. *Nature* **1996**, *382*, 607–609.

(187) Jahanshahi-Anbuhi, S.; Pennings, K.; Leung, V.; Liu, M.; Carrasquilla, C.; Kannan, B.; Li, Y.; Pelton, R.; Brennan, J. D.; Filipe, C. D. M. Pullulan Encapsulation of Labile Biomolecules to Give Stable Bioassay Tablets. *Angew. Chem. Int. Ed.* **2014**, *53*, 6155–6158.

(188) Jahanshahi-Anbuhi, S.; Kannan, B.; Leung, V.; Pennings, K.; Liu, M.; Carrasquilla, C.; White, D.; Li, Y.; Pelton, R. H.; Brennan, J. D.; et al. Simple and Ultrastable All-Inclusive Pullulan Tablets for Challenging Bioassays. *Chem. Sci.* **2016**, *7*, 2342–2346.

(189) Udugama, B.; Kadhiresan, P.; Samarakoon, A.; Chan, W. C. W. Simplifying

Assays by Tableting Reagents. *J. Am. Chem. Soc.* **2017**, *139*, 17341–17349.

(190) Stidham, S. E.; Chin, S. L.; Dane, E. L.; Grinstaff, M. W. Carboxylated Glucuronic Poly-Amido-Saccharides as Protein Stabilizing Agents. *J. Am. Chem. Soc.* **2014**, *136*, 9544–9547.

Appendix A: List of publications from the PhD program

5. **Reid, M.S.**; Paliwoda, R.E.; Zhang, H., Le, X.C. Reduction of background generated from template-template hybridizations in the Exponential Amplification Reaction, Submitted to Analytical Chemistry (Manuscript ID: ac-2018-02788w).

4. **Reid, M. S.**; Le, X.C.; Zhang, H Exponential isothermal amplification of nucleic acids and assays for proteins, cells, small molecules, and enzyme activities, Angewandte Chemie International Edition. DOI 10.1002/ange.201712217

3. Peng, H.; **Reid, M. S.**; Le, X. C. Consumption of Rice and Fish in an Electronic Waste Recycling Area Contributes Significantly to Total Daily Intake of Mercury, Journal of Environmental Sciences. 2015, 38, 83–86.

2. Li, F.; Zhang, H.; Wang, Z.; Newbigging, A.M.; **Reid, M.S.**; Le, X.C. Aptamers Facilitating Amplified Detection of Biomolecules, Analytical Chemistry. 2015, 87, 274–292.

1. Paliwoda, R.; Li, F.; **Reid, M.S.**; Lin, Y.; Le, X.C. Sequential Strand Displacement Beacon for Detection of DNA Coverage on Functionalized Gold Nanoparticles, Analytical Chemistry. 2014, 86, 6138–6143.